Sr/Ca $\delta^{88/86}$Sr and $\delta^{44/40}$Ca as a Tool to Study Corals' Calcification Mechanisms

Noa Fruchter

Dissertation
Submitted to the Christian Albrechts University
for the degree of
Dr. rer. nat.
at the faculty of Mathematics and Natural Sciences

May 2014

First referee: Prof. Dr. Anton Eisenhauer
Second referee: Prof. Dr. Thor Hansteen

Date of the oral examination: July 07, 2014
Approved for publication:

The Dean

I hereby declare that I wrote the present doctorate thesis independently and without the use of unauthorized aid. Neither this thesis nor a similar work has been submitted to any other examination board. Further, I declare that I have carried out my scientific work according to the principles of good scientific practice of the German research community.

Noa Fruchter

TABLE OF CONTENTS

LIST OF FIGURES

LIST OF TABLES

ABSTARCT

Over the last few decades corals have received a special focus in scientific research. The global climate changes and their effect on the marine environment raised the concern on the resistance of the marine fauna, including corals, to these changes. Even before the increasing interest on the effect of ocean acidification and temperature rise, studies already used the skeleton of stony corals as a tool to reconstruct paleo-environmental conditions such as marine temperature and pH. Variations in elemental and isotopic composition of the skeleton are used to determine environmental parameters of the corals surrounding habitat. The use of corals for paleo-environmental purposes and ecological studies requires understanding of the biological processes including the skeletogenesis (the process of skeleton formation). Nevertheless, the knowledge on corals calcification, and the biological effect on geochemical elements incorporation in the skeleton is still limited.

In this thesis Sr and Ca isotopes incorporation was studied in corals compared to their incorporation in inorganic aragonite. Ca is the major cation in the aragonite crystal, and Sr is the most abundant trace element that incorporates in inorganic and corals aragonite. These two elements are used as a paleo-temperature proxy as Sr/Ca ratio in corals even though their incorporation mechanism and deviation from the thermodynamic equilibrium is not fully understood.

Elemental mapping conducted in this study for Sr/Ca of *Acropora* sp. skeletons on electron microprobe and micro-SXRF showed a patchy growth pattern on the pre-existing skeleton walls. *Acropora* sp. growth pattern is not restricted to axial and radial growth but also exist in older parts of the skeleton. Hence, these results suggest that *Acropora* sp. corals may not be suitable as a paleo-proxy recorder.

Analyses results of geochemical isotopes show a strong kinetic effect of Ca isotopes incorporation in aragonite. Corals that calcify at higher rates display lower fractionation than inorganic aragonite. This observation implies a direct control of coral physiology on the rate of skeleton growth, and as a consequence on the Ca isotopes fractionation. On the contrary, Sr isotopes fractionation is not influenced by rate and do not show any variation between inorganic and corals aragonite. The similarity in Sr isotope fractionation between inorganic and corals

aragonite rules out the Rayleigh Based multi element model to explain corals calcification process.

KURZZUSAMMENFASSUNG

In den letzten Jahrzehnten haben Korallen einen besonderen Schwerpunkt in der wissenschaftlichen Forschung erhalten. Die globalen Klimaveränderungen und ihre Auswirkungen auf die Meeresumwelt gaben Anlass zur Sorge wie es um die Widerstandsfähigkeit der Meeresfauna, einschließlich der Korallen, bestellt ist und wie diese auf Veränderungen reagieren. Bereits vor dem steigenden Interesse an den Auswirkungen der Ozeanversauerung und des Temperaturanstiegs, wurde in wissenschaftlichen Studien bereits das Skelett von Steinkorallen als Instrument zur Rekonstruktion von Paläo-Umweltbedingungen wie Meerestemperatur und –pH-Wert verwendet. Variationen in Element-und Isotopenzusammensetzung des Skeletts werden verwendet um Umweltparameter, des die Korallen umgebenden Lebensraums, zu bestimmen. Die Verwendung von Korallen für Paläo-Umweltzwecke und ökologische Studien erfordert ein Verständnis der biologischen Prozesse, einschließlich der Skeletogenese (Prozess der Skelettbildung). Dennoch ist das Wissen über Korallenskeletbildung und die biologische Wirkung auf den Einbau geochemischer Elemente in das Skelett noch begrenzt.

In dieser Arbeit wurde der Einbau von Sr- und Ca-Isotopen in Korallen im Vergleich zu ihrem Einbau in anorganischem Aragonit untersucht. Ca ist das häufigste Kation im Aragonitkristall und Sr ist das häufigste Spurenelement das in anorganischem und Korallenaragonit enthalten ist. Diese beiden Elemente werden als Paläotemperaturproxy als Sr/ Ca-Verhältnis in Korallen benutzt obwohl ihr Einbaumechanismus und ihre Abweichung vom thermodynamischen Gleichgewicht nicht vollständig verstanden werden.

Die in dieser Studie durchgeführten Elementkartierungen der Sr/Ca-Raten an *Acropora* sp. Skeletten wurden mittels Elektronenmikrosonde und Mikro-SXRF durchgeführt und zeigten ein ungleichmäßiges Wachstumsmuster auf den bereits bestehenden Skelettwänden. Das Wachstumsmuster von *Acropora* sp. ist nicht auf axiales und radiales Wachstum beschränkt, sondern auch in den älteren Teilen des Skeletts vorhanden. Somit legen diese Ergebnisse nahe, dass *Acropora* sp. nicht als Paläoproxyrecorder geeignet sein dürfte.

Analysenergebnisse der geochemischen Isotope zeigen eine starke kinetische Wirkung auf den Ca-Isotopeneinbau in Aragonit. Korallen, die bei höheren Raten calcifizieren, zeigen geringere

Fraktionierung als anorganischer Aragonit. Diese Beobachtung impliziert eine direkte Steuerung der Korallenphysiologie auf die Rate des Skelettwachstums und als Folge davon auf die Ca-Isotopenfraktionierung. Im Gegensatz dazu, ist die Sr-Isotopenfraktionierung nicht durch die Rate beeinflusst und zeigt keine Variation zwischen anorganischem und Korallenaragonit. Durch die Ähnlichkeit in der Sr-Isotopenfraktionierung zwischen anorganischem und Korallenaragonit, kann das rayleighbasierte Multi-Element-Model als Erklärung für den Korallencalcifizierungsprozess ausgeschlossen werden.

CHAPTER I. INTRODUCTION

Stony corals, which are termed scleractinians, are a crucial organism in the existence of the marine ecosystem (Smith, 1978). They form thriving reefs in continental shelves of oligotrophic zones and enable the subsistence of many of the marine fauna (Hallock and Schlager, 1986; Stanley, 2006). In addition, they have an important role in the global carbon cycle as about 50% of the $CaCO_3$ production in the ocean is made in the reef areas (Smith, 1978; Milliman, 1993). Over the last decades scleractinians have been widely applied as proxies for paleo-climate reconstructions. The scleractinians are considered to have many advantages as paleo-climate proxies for their prolonging life over centuries and for their unique skeleton composition and structure. The scleractinians' skeleton contains a continuous record of the environmental conditions prevailed during their growth. In most of the scleractinians the skeleton consists of seasonal banding that enables to determine the growth period of the skeleton. In many cases fossil corals are well preserved and can be used to reconstruct paleo-climate proxies together with an accurate dating of the skeleton.

The use of geochemical elements and isotopes in corals' skeletons for climate parameters reconstruction purposes is dependent on understanding the calcification mechanisms. Similarly, the effect of the atmospheric CO_2 increase on corals calcification process can be comprehended better if the mechanism of calcification was understood. Many attempts are made to decipher the calcification mechanism in corals (e.g. Allemand et al., 2004; Gaetani and Cohen, 2006; Holcomb et al., 2009; Tambutté et al., 2011). Despite these efforts, there is still a poor knowledge of the mechanism of corals' skeleton formation. In my work I will try to shed some light on the geochemical perspective of corals' calcification process by comparing elemental ratio and isotopes (Sr/Ca, $^{88}Sr/^{86}Sr$ and $^{44}Ca/^{40}Ca$) incorporation in inorganic aragonite and in corals' skeletons.

Scleractinian Physiology

The Polyp

Scleractinians are mostly colonial and hermatypic (contains symbiotic photosynthetic algae), and therefore are restricted to warm (above 18°C) and shallow water in the tropics and

subtropics. The coral's organism is called polyp, and is situated on top of its skeleton. The polyp is a sac with a single mouth surrounded by tentacles. It is comprised of two double tissue layers (Allemand et al., 2004), the oral layer close to the mouth and the ab-oral layer closer to the coral's skeleton. Each of the layers is composed of two tissues layers, the ectoderm and the endoderm. The unicellular symbiotic algae, zooxanthellae, are present in hermatipic corals at the oral endoderm. The coelenteron cavity or gastrovascular cavity, where digestion takes place, is located between the ab-oral endoderm and the oral endoderm tissues. This is also where the skeleton's constructing ions pass through on the way to the calcification site (Al-Horani et al., 2003). Calcification occurs on the calicoblastic epithelium, which is situated at the innermost margin of the ab-oral ectoderm (Figure I.1).

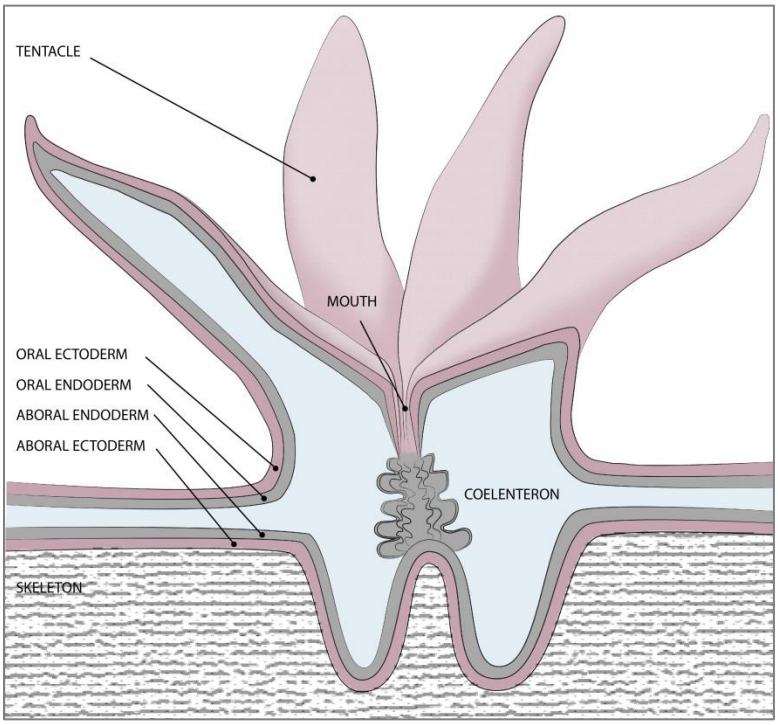

Figure I.1 A cross section sketch of a coral's polyp. The polyp is a sac-like structure with two double tissue layers. A coelenteron cavity is present between the two endoderm layers. Seawater enters the coelenteron cavity through the polyp mouth. The skeleton of the coral is underneath the innermost tissue layer, the aboral ectoderm

The Skeleton

The scleractinian skeleton is composed of aragonite, a calcium carbonate polymorph. Scleractinian uses the skeleton to acquire physical stability on the sediment or rocky surface on

which they live. Aragonite calcification is a hundred times faster than inorganic aragonite precipitation (Cohen and McConnaughey, 2003). The high calcification rates enable corals to cope with the dissolution and erosion processes, and to expand their colonies (Cohen and McConnaughey, 2003).

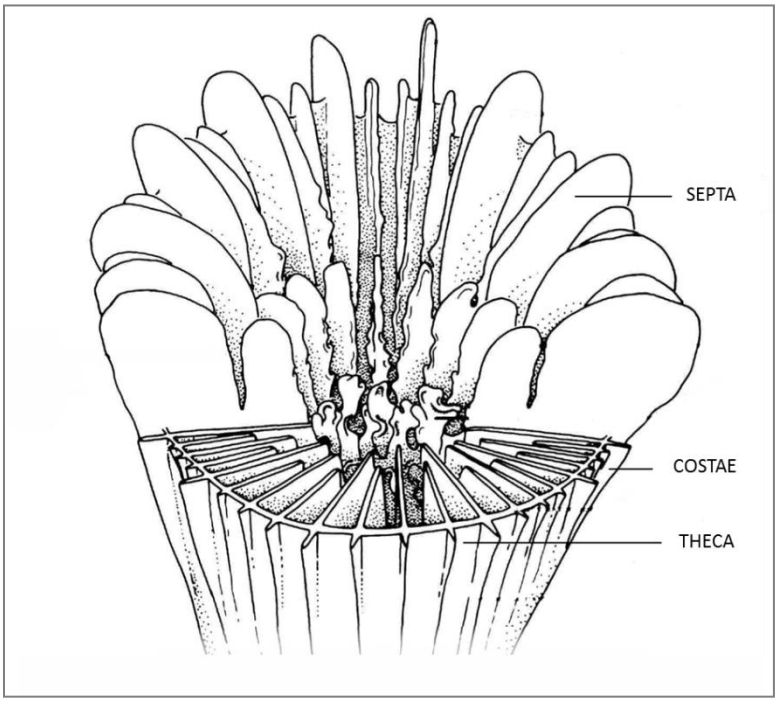

Figure I.2 A sketch of a coral's single polyp skeleton, which is termed corallite. The tube like structure is supported by the theca (the structure walls). The vertical plates that radiate from the theca toward the center of the tube are the septa. The extensions of the septa outside the theca are called costae. Figure from Cairns (1994).

Calcification takes place in the margin between the tissue and the skeleton. Generally there are two forms of aragonite in the skeleton, granular crystals and fibers. These two forms are the basic building blocks of the skeleton, and are called sclerodermites (Wells 1956). The granular crystals are submicron in size and are traditionally considered as the centers of calcification (COC) (Gladfelter, 1983; Le Tissier, 1988; Cohen et al., 2001). The COC are related to slow calcification and their formation alters the fibers formation in diurnal cycles (Gladfelter, 1983; Cohen et al., 2001). It is claimed that the centers of calcification serves as nucleation sites for the growth of fibers (Gladfelter, 1983; Le Tissier, 1988; Cohen et al., 2001). Groups of thin aragonite fibers radiate from the centers of calcification, and form the complex structure of the coral's skeleton. There is a customary nomenclature for the different parts of the corals' skeleton.

The skeleton of each polyp in the colony is termed corallite (Figure I.2). Each corallite is connected to adjacent corallites by the coenostea. The corallite itself is a tube shape with walls that are termed theca. From the theca toward the center of the corallite radiate vertical plates that are called septa, the extensions of the septa outside the theca are costae. Only the few upper millimeters of the corallite is the active skeleton that is directly connected to the polyp's tissue. As the colony grows, the polyps are being pushed higher leaving the old skeleton surface inactive. This growth upwards creates the axial growth and the growth bands that are visible in most scleractinians.

Calcification Process Models

The high rates of calcification and the complex skeleton structure together with the non-equilibrium state of the isotopic composition (McConnaughey, 1989; Adkins et al., 2003) intrigued scientists to understand the mechanism of corals' calcification. The differences between coral calcification and inorganic aragonite precipitation are controlled by the organism's biology, and were termed 'the vital effect'(Weber and Woodhead, 1972). Coral's skeleton is precipitated extracellularly in the calicoblastic fluid (ECF) at the interface between the aboral ectoderm and the existing skeleton (Clode and Marshall, 2002a; Allemand et al., 2004; Tambutté et al., 2007). There are generally two theories that approach the transport pathways to the calcifying fluid. Some studies claim that ions are transported in transcellular pathway (Krishnaveni et al., 1989; Tambutté et al., 1996), while other studies support a passive paracellular transport (Erez and Braun, 2007; Gagnon et al., 2012; Tambutté et al., 2012). The transcellular pathway is an active transport, in which ions are carried through the cells using designated enzymes. The enzyme that is responsible for Ca transport is called Ca^{2+}-ATPase. The activity of this enzyme is detected in eukaryotic cells (Strehler and Zacharias, 2001) including corals. Al-Horani et al. (2003) proposed a mechanism that correlates the enzyme activity to calcification process. According to them, Ca^{2+} is transported from the cells to the ECF, and in exchange H^{+} is transported out of the calciblastic fluid. In this manner, Ca^{2+} concentration increases in the ECF and the pH increases causing inorganic carbon system to shift toward increasing concentration of the CO_3^{2-} species. According to this model an additional amount of carbon diffuses to the ECF as CO_2 from respiration and is converted to CO_3^{2-} due to the high pH conditions (Goreau, 1977; Erez, 1978; Furla et al., 2000). The supporting observations for this

model include pH and Ca^{2+} concentration measurements of the ECF (Al-Horani et al., 2003), as well as the use of Ca^{2+}-ATPase and ruthenium red inhibitors that cause a significant decrease in corals calcification (Krishnaveni et al., 1989; Marshall, 1996; Allison et al., 2011). While the transcellular pathway model is supported by several observations and experiments, other studies supply supporting observations for paracellular pathway mechanism. Erez and Braun (2007) and Tambutté et al. (2012) provided a supporting evidence for paracellular transport using Calcein and FITC-Dextran dyes. These dyes molecules that are used to label calcification have a large diameter that cannot pass through cells in transcellular pathway, and therefore, can pass only between the cells. Gagnon et al. (2012) observe synchronous incorporation of Ca, Sr, Ba and Tb in the coral's skeleton and assume that it is more likely to indicate a paracellular transport rather than different pathways that acts similarly on different elements.

Trace elements and Isotopes Incorporation in the Coral's Skeleton

The deviation of trace elements and isotopes incorporation in corals compared to their incorporation in inorganic aragonite is an obstacle for paleo-climate reconstruction but can be a useful tool for studying the mechanism of corals' calcification. Several hypotheses were proposed for calcification mechanism to explain the elements incorporation differences between corals and inorganic aragonite. Disequilibrium precipitation of carbonate in marine organisms was first detected on $\delta^{13}C$ and $\delta^{18}O$ (Urey, 1947). Also the Ca uptake in corals was investigated and isotopic disequilibrium was found when ^{45}Ca was added to the corals' experimental environment (Goreau and Bowen, 1955; Goreau and Goreau, 1960; Erez, 1978). Over the years $\delta^{18}O$ and Sr/Ca became important paleo-temperature proxies in corals (e.g. Weber and Woodhead, 1972; Beck et al., 1992). Yet, the explanation for the disequilibrium effect was not found, and at the same time that these proxies are used to reconstruct paleo-temperature other researches try to model their incorporation mechanism. For example, in carbon incorporation it is hypothesized that photosynthesis and respiration alters the isotopic composition of C in corals (Goreau, 1959; Erez, 1978; McConnaughey, 1989). Erez (1978) and Adkins et al. (2003) suggested that C composition in corals is a result of a mixture of a metabolic source with isotopically lighter composition and an equilibrium seawater source.

Ca is a major component in $CaCO_3$ crystal as it comprises ~40% of the crystal's molar mass. Sr is a trace element that incorporates into the $CaCO_3$ crystal. The element binds to the CO_3^{2-} ion

and substitutes the Ca. The incorporation of Sr into inorganic aragonite and corals' aragonite is about 1% of the crystal's molar mass. The Sr/Ca ratios in corals and marine inorganic aragonite are close to seawater composition, meaning that the partitioning coefficient of Sr ($K_{DSr,a}$) is close to unity. Sr/Ca ratio in corals is temperature dependent, but displays significantly different Sr/Ca- temperature slopes between inorganic aragonite and corals (Dietzel et al., 2004). The different partitioning coefficients of Mg/Ca and Sr/Ca in corals compared to inorganic aragonite are claimed to occur due to Rayleigh distillation effect (Gaetani and Cohen, 2006; Gaetani et al., 2011). According to this proposed model, seawater enters the site of calcification in a passive paracellular pathway, but is slightly modified by active enzyme pumps and ion transport channels. After entering the calcification site the precipitation takes place as an inorganic process from a renewable finite solution. Gagnon et al., (2007) offered an explanation for calcification process in the COC's. While they agree that the growth of the fiber aragonite crystals in the coral is a result of a Rayleigh effect, they claim that the COC's are formed in a different process that induces higher Mg/Ca ratios. They proposed that either biomolecules or organic matrix are involved in calcification of the COC's or that high rate precipitation following the inorganic surface entrapment model (Watson, 2004) is responsible for the calcification. Despite these many efforts, there is no satisfactory explanation for the mechanism of trace elements and isotopes incorporation in corals' skeletons.

Sr and Ca Isotopes Incorporation in $CaCO_3$

Recent advances in the analytical abilities and development of new analytical methods such as the double spike method enabled investigating small variations in isotopic ratios that could not be detected till then. Two of such isotopic systems are $^{44}Ca/^{40}Ca$ and $^{88}Sr/^{86}Sr$. The use of the double spike method is possible for elements that have at least four stable isotopes. Two of these isotopes are added as a double spike with a known isotopic ratio, and other two isotopes are measured as the sample's analyte. Both Ca isotopes and Sr isotopes are reported in the δ notation normalized to the element's standard (NIST SRM915a and SRM NBS987, respectively).

$$\delta^{44/40}Ca = \left(\frac{^{44}Ca/^{40}Ca}{^{44}Ca/^{40}Ca_{SRM\ 915a}} - 1\right) \times 1000 \quad \text{Eq. I.1}$$

$$\delta^{88/86}Sr = \left(\frac{^{88}Sr/^{86}Sr}{^{88}Sr/^{86}Sr_{NBS987}} - 1\right) \times 1000 \quad \text{Eq. I.2}$$

Sr Isotopes

$^{88}Sr/^{86}Sr$ ratios were used until recently only as a constant value ($^{88}Sr/^{86}Sr$=8.375209, which is the accepted value of the Sr standard SRM987) to correct the well-established sediment origin reconstruction method of $^{87}Sr/^{86}Sr$ (e.g. Dasch, 1969) and the dating method of $^{87}Rb/^{86}Sr$. Even before applying the double spike technique, significant variations in $^{88}Sr/^{86}Sr$ ratios were detected in both marine and terrestrial environments (Fietzke and Eisenhauer, 2006; Halicz et al., 2008). It was discovered that $^{88}Sr/^{86}Sr$ in marine carbonates and corals in particular is significantly lighter than seawater, meaning that the carbonates tend to favor incorporation of the light isotope. Few early researches found correlation between $^{88}Sr/^{86}Sr$ isotopes and temperature in corals (Fietzke and Eisenhauer, 2006; Rüggeberg et al., 2008). These studies used the bracketing method on MC-ICP-MS. However, later studies could not repeat this observation (Halicz et al., 2008; Raddatz et al., 2013). The double spike method in Sr isotopes was developed to correct for the fractionation occurring during sample preparation and analytical measurement (Krabbenhöft et al., 2009). The double spike solution is a mixture of ^{87}Sr and ^{84}Sr with a known and calibrated ratio value, and is added to the sample solution before the sample preparation process. Even though introducing the double spike method on Sr isotopes measurements (Krabbenhöft et al., 2009) improved significantly the analytical error by a factor of 2-3, a temperature relation to $^{88}Sr/^{86}Sr$ in *L. pertusa*, could not be reproduced (Raddatz et al., 2013).

Ca Isotopes

Ca isotopes were used from the 1950's as a tool to investigate the Ca uptake in corals (Goreau and Bowen, 1955; Goreau and Goreau, 1960; Erez, 1978). The synthetic and radioactive ^{45}Ca was added to the bulk solution, and the ^{45}Ca uptake by the polyp was counted using G-M tubes (Geiger-Müller Tube). Measuring small variations in stable Ca isotopes became possible with the analytical improvements of the Thermal Ionization Mass Spectrometry (TIMS) and the Inductively Coupled Plasma Mass Spectrometry (ICP-MS). The double spike method, using $^{43}Ca/^{48}Ca$ ratios, was applied for Ca measurements on the multi collector TIMS (Heuser et al., 2002), even though other double spikes were tested and are being used as well (($^{42}Ca/^{48}Ca$ (Russell and Papanastassiou, 1978; Zhu and Macdougall, 1998) and $^{42}Ca/^{43}Ca$ (Gopalan et al., 2006)). Similar to Sr isotopes fractionation, marine carbonates tend to be significantly lighter in

Ca isotopes than the bulk seawater from which they precipitate. Several studies reported a temperature dependence on Ca isotopes fractionation in inorganic aragonite (Gussone et al., 2003; Niedermayr, 2011), inorganic calcite (Marriott et al., 2004; Tang et al., 2008), foraminifera (Zhu and Macdougall, 1998; Nägler et al., 2000; Gussone et al., 2003), and even in corals (Böhm et al., 2006). The Ca isotopes-temperature correlation is positive, meaning that as temperature increases the isotopic composition of the carbonate becomes heavier and less fractionated.

A special focus on Ca isotopes is attained in studies of mechanism of inorganic calcite precipitation. Many studies try to understand the process of crystallization in the interface between the existing crystal and the solution, and Ca isotopes are used to test these models. The surface entrapment model, SEMO (Watson, 2004), claims that the trace elements concentration in the new growth of the calcite crystal is a result of a competition between the growth rate and the elements' diffusivity from the crystal. The model was tested and verified on Ca isotopes in inorganic calcite (Tang et al., 2008). According to the SEMO model, the surface of the calcite crystal entraps the light ^{40}Ca isotope and discriminate the heavy ^{44}Ca isotope. This kinetically controlled process is balanced by a re-equilibration process of solid state diffusion of ^{44}Ca into the surface layer, which is strongly dependent on the rate of precipitation. DePaolo (2011) proposes the surface reaction model and criticized the SEMO model. He claims that the solid state diffusion in moderate temperatures is too slow to be considered as competitive with the precipitation rate. The surface reaction model is proposing a balance between forward (attachment) and backward reactions (detachment), each with different fractionations. Both of the described models are explaining the general negative correlation between the rate of calcite formation and $^{44}Ca/^{40}Ca$ ratio in the calcite. However, one obtained a positive $^{44}Ca/^{40}Ca$ - precipitation rate correlation in inorganic calcite (Lemarchand et al., 2004). The positive correlation was later explained as precipitation from highly oversaturated solutions, where calcite grows by the formation of amorphous calcium carbonate (ACC) (Nielsen et al., 2012). Data of Ca isotopes in inorganic aragonite show a positive $^{44}Ca/^{40}Ca$ - precipitation rate correlation, which is opposite to the two described models (Gussone et al., 2005; Niedermayr, 2011). The difference in the behavior of Ca isotopes incorporation in inorganic aragonite and calcite can be used to explain the corals' biological calcification mechanism when compared to corals Ca isotopes data.

In conclusion, Sr and Ca isotopes measurements in corals can provide another perspective on the incorporation mechanism of one of the most important marine paleo-proxy, Sr/Ca. Through these isotopes and their different incorporation properties we can learn about the mechanism of calcification in corals as compared to inorganic precipitation.

Thesis Structure

In this thesis I provide a geochemical perspective on the process of corals calcification using Sr and Ca isotopes and Sr/Ca ratios. The thesis is divided into chapters, which are manuscripts intended to be sent to scientific journals in the next few months.

Chapter II – Sr/Ca distribution in Acropora sp. coral as observed in elemental mapping using Electron Microprobe and Synchrotron X-ray fluorescence micro analyses. A significantly different Sr/Ca ratio in the bulk solution of the pre-experiement and the experiment conditions, resulted in two distinctive Sr/Ca ratios in the corals' skeletons. The results show a patchy calcification pattern. Calcification that is not restricted only to the normal axial and radial growth known in other coral genus (e.g. *Porites* spp., *Pocillopora* spp.), but is present also in contact of old skeleton that is no longer active.

Chapter III – $\delta^{88/86}$Sr results in inorganic aragonite and various coral species show high fractionation from the bulk seawater. The corals and the inorganic aragonite incorporate at the same extent in which the light, ^{86}Sr, isotope is preferred over the heavy, ^{88}Sr, isotope. As opposed to previous studies on $\delta^{88/86}$Sr in corals, we observe no correlation between $\delta^{88/86}$Sr and temperature. In addition, the previously proposed Rayleigh based model for mechanism of coral calcification is applied on Sr isotopes. Despite the promising results in trace elements, the model cannot predict the ^{88}Sr/^{86}Sr incorporation in corals.

Chapter IV –$\delta^{44/40}$Ca was measured on *Acropora* sp. corals and inorganic aragonite that was precipitated from natural seawater. The inorganic and corals were precipitated at different temperatures and different saturation states of the solutions. Comparison of the inorganic aragonite results with previous studies indicates no effect of ionic strength and salinity on the aragonite $\delta^{44/40}$Ca. In addition, a strong kinetic effect was observed in $\delta^{44/40}$Ca in inorganic aragonite. The significant lighter ^{44}Ca/^{40}Ca ratio in corals is interpreted here as a kinetic effect of very high rates of aragonite formation.

References

Adkins J. F., Boyle E. A., Curry W. B. and Lutringer A. (2003) Stable isotopes in deep-sea corals and a new mechanism for "vital effects". *Geochim. Cosmochim. Acta* **67**, 1129–1143.

Al-Horani F. A., Al-Moghrabi S. M. and De Beer D. (2003) The mechanism of calcification and its relation to photosynthesis and respiration in the scleractinian coral Galaxea fascicularis. *Mar. Biol.* **142**, 419–426.

Allemand D., Ferrier-Pagès C., Furla P., Houlbrèque F., Puverel S., Reynaud S., Tambutté É., Tambutté S. and Zoccola D. (2004) Biomineralisation in reef-building corals: from molecular mechanisms to environmental control. *Comptes Rendus Palevol* **3**, 453–467.

Allison N., Cohen I., Finch A. A. and Erez J. (2011) Controls on Sr/Ca and Mg/Ca in scleractinian corals: The effects of Ca-ATPase and transcellular Ca channels on skeletal chemistry. *Geochim. Cosmochim. Acta* **75**, 6350–6360.

Beck J. W., Edwards R. L., Ito E., Taylor F. W., Recy J., Rougerie F., Joannot P. and Henin C. (1992) Sea-surface temperature from coral skeletal strontium/calcium ratios. *Science (80-.).* **257**, 644–7.

Böhm F., Gussone N., Eisenhauer A., Dullo W. C., Reynaud S. and Paytan A. (2006) Calcium isotope fractionation in modern scleractinian corals. *Geochim. Cosmochim. Acta* **70**, 4452–4462.

Clode P. L. and Marshall A. T. (2002) Low temperature FESEM of the calcifying interface of a scleractinian coral. *Tissue Cell* **34**, 187–198.

Cohen A. L., Layne G. D., Hart S. R. and Lobel P. S. (2001) Kinetic control of skeletal Sr/Ca in a symbiotic coral: Implications for the paleotemperature proxy. *Paleoceanography* **16**, 20–26.

Cohen A. L. and McConnaughey T. A. (2003) Geochemical perspectives on coral mineralization. *Rev. Mineral. Geochemistry* **54**, 151–187.

Dasch E. J. (1969) Strontium isotopes in weathering profiles, deep-sea sediments, and sedimentary rocks. *Geochim. Cosmochim. Acta* **33**, 1521–1552.

DePaolo D. J. (2011) Surface kinetic model for isotopic and trace element fractionation during precipitation of calcite from aqueous solutions. *Geochim. Cosmochim. Acta* **75**, 1039–1056.

Dietzel M., Gussone N. and Eisenhauer A. (2004) Co-precipitation of Sr^{2+} and Ba^{2+} with aragonite by membrane diffusion of CO_2 between 10 and 50°C. *Chem. Geol.* **203**, 139–151.

Erez J. (1978) Vital effect on stable-isotope composition seen in foraminifera and coral skeletons. *Nature* **273**, 199–202.

Erez J. and Braun A. (2007) Calcification in hermatypic corals is based on direct seawater supply to the biomineralization site. *Geochim. Cosmochim. Acta* **71**, SA260.

Fietzke J. and Eisenhauer A. (2006) Determination of temperature-dependent stable strontium isotope ($^{88}Sr/^{86}Sr$) fractionation via bracketing standard MC-ICP-MS. *Geochemistry Geophys. Geosystems* **7**.

Furla P., Galgani I., Durand I. and Allemand D. (2000) Sources and mechanisms of inorganic carbon transport for coral calcification and photosynthesis. *J. Exp. Biol.* **203**, 3445–57.

Gaetani G. A. and Cohen A. L. (2006) Element partitioning during precipitation of aragonite from seawater: A framework for understanding paleoproxies. *Geochim. Cosmochim. Acta* **70**, 4617–4634.

Gaetani G. A., Cohen A. L., Wang Z. and Crusius J. (2011) Rayleigh-based, multi-element coral thermometry: A biomineralization approach to developing climate proxies. *Geochim. Cosmochim. Acta* **75**, 1920–1932.

Gagnon A. C., Adkins J. F. and Erez J. (2012) Seawater transport during coral biomineralization. *Earth Planet. Sci. Lett.* **329-330**, 150–161.

Gagnon A. C., Adkins J. F., Fernandez D. and Robinson L. (2007) Sr/Ca and Mg/Ca vital effects correlated with skeletal architecture in a scleractinian deep-sea coral and the role of Rayleigh fractionation. *Earth Planet. Sci. Lett.* **261**, 280–295.

Gladfelter E. H. (1983) Skeletal development in Acropora cervicornis. II. Diel patterns of calcium carbonate accretion. *Coral Reefs* **2**, 91–100.

Gopalan K., Macdougall J. D. and Macisaac C. (2006) Evaluation of a 42Ca –43Ca double-spike for high precision Ca isotope analysis. *Int. J. Mass Spectrom.* **248**, 9–16.

Goreau T. F. (1959) The physiology of skeleton formation in corals. I. A method for measuring the rate of calcium deposition by corals under different conditions. *Biol. Bull* **116**, 59–75.

Goreau T. F. and Bowen V. T. (1955) Calcium uptake by a coral. *Science (80-.).* **122**, 1188–1189.

Goreau T. F. and Goreau N. I. (1960) physiology of skeleton formation in corals. IV. On isotopic equilibrium exchanges of calcium between corallum and environment in living and dead reef-building corals. *Biol. Bull.* 416–427.

Goreau T. J. (1977) Coral skeletal chemistry: physiological and environmental regulation of stable isotopes and trace metals in Montastrea annularis. *Proc. R. Soc. London. Ser. B* **196**, 291–315.

Gussone N., Böhm F., Eisenhauer A., Dietzel M., Heuser A., Teichert B. M. A., Reitner J. and Dullo W. C. (2005) Calcium isotope fractionation in calcite and aragonite. *Geochim. Cosmochim. Acta* **69**, 4485– 4494.

Gussone N., Eisenhauer A., Heuser A., Dietzel M., Bock B., Böhm F., Spero H. J., Lea D. W., Bijma J. and Nägler T. F. (2003) Model for kineticeffects on calciumisotopefractionation (δ^{44}Ca) in inorganic aragonite and cultured planktonic foraminifera. *Geochim. Cosmochim. Acta* **67**, 1375–1382.

Halicz L., Segal I., Fruchter N., Stein M. and Lazar B. (2008) Strontium stable isotopes fractionate in the soil environments? *Earth Planet. Sci. Lett.* **272**, 406–411.

Hallock P. T. and Schlager W. (1986) Nutrient Excess and the Demise of Coral Reefs and Carbonate Platforms. *Palaios* **1**, 389.

Heuser A., Eisenhauer A., Gussone N., Bock B., Hansen B. T. and Nägler T. F. (2002) Measurement of calcium isotopes (δ^{44}Ca) using a multicollector TIMS technique. *Int. J. Mass Spectrom.* **220**, 385–397.

Holcomb M., Cohen A. L., Gabitov R. I. and Hutter J. L. (2009) Compositional and morphological features of aragonite precipitated experimentally from seawater and biogenically by corals. *Geochim. Cosmochim. Acta* **73**, 4166–4179.

Krabbenhöft A., Fietzke J., Eisenhauer A., Liebetrau V., Böhm F. and Vollstaedt H. (2009) Determination of radiogenic and stable strontium isotope ratios (^{87}Sr/^{86}Sr; $\delta^{88/86}$Sr) by thermal ionization mass spectrometry applying an ^{87}Sr/^{84}Sr double spike. *J. Anal. At. Spectrom.* **24**, 1267.

Krishnaveni P., Chou L. and Ip Y. K. (1989) Deposition of calcium ($^{45}Ca^{2+}$) in the coral, Galaxea fascicularis. *Comp. Biochem. Physiol. Part A Physiol.* **94**, 509–513.

Lemarchand D., Wasserburg G. J. and Papanastassiou D. A. (2004) Rate-controlled calcium isotope fractionation in synthetic calcite. *Geochim. Cosmochim. Acta* **68**, 4665–4678.

Marriott C. S., Henderson G. M., Belshaw N. S. and Tudhope A. W. (2004) Temperature dependence of δ^{7}Li, δ^{44}Ca and Li/Ca during growth of calcium carbonate. *Earth Planet. Sci. Lett.* **222**, 615–624.

Marshall A. T. (1996) Calcification in Hermatypic and Ahermatypic Corals. *Science (80-.).* **271**, 637–639.

McConnaughey T. A. (1989) 13C and 18O isotopic disequilibrium in biological carbonates: I. Patterns. *Geochim. Cosmochim. Acta* **53**, 151–162.

Milliman J. D. (1993) Production and accumulation of calcium carbonate in the ocean: Budget of a nonsteady state. *Global Biogeochem. Cycles* **7**, 927–957.

Nägler T. F., Eisenhauer A., Müller A., Hemleben C. and Kramers J. (2000) The δ^{44}Ca-temperature calibration on fossil and cultured Globigerinoides sacculifer : New tool for reconstruction of past sea surface temperatures. *Geochemistry Geophys. Geosystems* **1**.

Niedermayr A. (2011) Effects of magnesium , polyaspartic acid , carbonate accumulation rate and temperature on the crystallization , morphology , elemental incorporation and isotopic fractionation of calcium carbonate phases.

Nielsen L. C., DePaolo D. J. and De Yoreo J. J. (2012) Self-consistent ion-by-ion growth model for kinetic isotopic fractionation during calcite precipitation. *Geochim. Cosmochim. Acta* **86**, 166–181.

Raddatz J., Liebetrau V., Rüggeberg A., Hathorne E. C., Krabbenhöft A., Eisenhauer A., Böhm F., Vollstaedt H., Fietzke J., López Correa M., Freiwald A. and Dullo W.-C. (2013) Stable Sr-isotope, Sr/Ca, Mg/Ca, Li/Ca and Mg/Li ratios in the scleractinian cold-water coral Lophelia pertusa. *Chem. Geol.* **352**, 143–152.

Rüggeberg A., Fietzke J., Liebetrau V., Eisenhauer A., Dullo W. C. and Freiwald A. (2008) Stable strontium isotopes (δ88/86Sr) in cold-water corals — A new proxy for reconstruction of intermediate ocean water temperatures. *Earth Planet. Sci. Lett.* **269**, 570–575.

Russell W. A. and Papanastassiou D. A. (1978) Calcium isotope fractionation in ion-exchange chromatography. *Anal. Chem.*

Smith S. V. (1978) Coral-reef area and the contributions of reefs to processes and resources of the world's oceans. *Nature* **273**, 225–226.

Stanley G. D. (2006) Photosymbiosis and the Evolution of Modern Coral Reefs Auxin Transport , but. *Science (80-.).* **312**.

Strehler E. E. and Zacharias D. a (2001) Role of alternative splicing in generating isoform diversity among plasma membrane calcium pumps. *Physiol. Rev.* **81**, 21–50.

Tambutté É., Allemand D., Müller E. and Juabert J. (1996) A compartmental approach to the mechanism of calcification in hermatypic corals. *J. Exp. Biol.* **1041**, 1029–1041.

Tambutté É., Allemand D., Zoccola D., Meibom A., Lotto S., Caminiti N. and Bénazet-Tambutté S. (2007) Observations of the tissue-skeleton interface in the scleractinian coral Stylophora pistillata. *Coral Reefs* **26**, 517–529.

Tambutté É., Tambutté S., Segonds N., Zoccola D., Venn A., Erez J. and Allemand D. (2012) Calcein labelling and electrophysiology: insights on coral tissue permeability and calcification. *Proc. R. Soc. B Biol. Sci.* **279**, 19–27.

Tambutté S., Holcomb M., Ferrier-Pagès C., Reynaud S., Tambutté É., Zoccola D. and Allemand D. (2011) Coral biomineralization: From the gene to the environment. *J. Exp. Mar. Bio. Ecol.* **408**, 58–78.

Tang J., Dietzel M., Böhm F., Köhler S. J. and Eisenhauer A. (2008) Sr^{2+}/Ca^{2+} and $^{44}Ca/^{40}Ca$ fractionation during inorganic calcite formation: II. Ca isotopes. *Geochim. Cosmochim. Acta* **72**, 3733–3745.

Le Tissier M. A. A. (1988) Patterns of formation and the ultrastructure of the larval skeleton of Pocillopora damicornis. *Mar. Biol.* **98**, 493–501.

Urey H. C. (1947) The thermodynamic properties of isotopic substances. *J. Chem. Soc.* 561–581.

Watson E. B. (2004) A conceptual model for near-surface kinetic controls on the trace-element and stable isotope composition of abiogenic calcite crystals1. *Geochim. Cosmochim. Acta* **68**, 1473–1488.

Weber J. N. and Woodhead P. M. J. (1972) Temperature dependence of oxygen-18 concentration in reef coral carbonates. *J. Geophys. Res.* **77**, 463.

Zhu P. and Macdougall J. D. (1998) Calcium isotopes in the marine environment and the oceanic calcium cycle. *Geochim. Cosmochim. Acta* **62**, 1691–1698.

CHAPTER II. PATCHY CALCIFICATION PATTERN IN *ACROPORA* SP. DETERMINED BY ELECTRON MICROPROBE AND MICRO-SXRF ELEMENT MAPPINGS USING TWO DISTINCT Sr ELEMENT CONCENTRATIONS

Noa Fruchter[1*], Anton Eisenhauer[1], Thor Hansteen[1], Jan Fietzke[1], Florian Böhm[1], Karen Appel[2], Jonathan Erez[3]

[1] *GEOMAR, Helmholtz-Zentrum für Ozeanforschung Kiel, Wischhofstr. 1-3, 24148 Kiel, Germany*

[2] *Deutsches Elektronen-Synchrotron Notkestraße 85, D-22607 Hamburg, Germany*

[3] *The Hebrew University, The Edmond J. safra Campus Givat Ram Jerusalem, Israel*

[*] *Present address: Geological Survey of Israel, Malkhei Israel 30 Jerusalem, Israel*

In preparation, to be submitted to *Coral Reef*

Abstract

Electron microprobe and synchrotron X-ray fluorescence micro-analyses were used to study the calcification pattern of *Acropora* sp.. Specimens of *Acropora* sp. were cultured in two stages at two distinct Sr concentrations in the bulk solutions, where the low concentrations represent the pre-experiment and the high concentrations represent the conditions during the experiments. The experimental, high concentrations, Sr comprise both patches on the pre-existing skeleton walls and growth extensions of the skeleton. We show a clear visualization of the patchy calcification pattern in *Acropora*. We assume that the precipitation in older parts of the skeleton is biogenically controlled. That secondary infilling calcification reduces the porosity and increases the stability of the skeleton.

Introduction

Scleractinia (stony corals) have a broad application in geochemistry as paleo-proxy recorder. Their aragonite skeleton records the marine conditions through changes in trace elements (e.g. Sr, Ba, etc.) and isotopes composition (e.g. $^{87}Sr/^{86}Sr$ $\delta^{18}O$, $\delta^{11}B$ etc), and can provide valuable information on past climate and the marine environment. Corals exhibit an approximate linear growth pattern with maximum extension in the growth axis. The rate of extension is controlled by environmental parameters such as light intensities and temperature (de Villiers et al., 1995). In many corals, seasonal growth bands can be detected and can be used as a timescale.

Acropora corals are among the fastest growing corals as their mean extension rates can exceed 10 cm per year (Huston, 1985). This allows gaining high resolution records of environmental changes through geochemical proxies. However, several studies have raised the question of the enigmatic growth pattern of this genus. Gladfelter (1982); Oliver et al. (1983) and others observed an axial gradient in the *Acropora* skeleton density as a function of age. In addition to the observation of no distinct growth bands and a deep gastrovascular system, researchers suggested that *Acropora* show secondary infilling of skeletal pores in older portions of the colony (Gladfelter, 1982; Oliver et al., 1983; Roche et al., 2011). Shirai et al. 2008 observed (using NanoSIMS and EPMA) inhomogeneous element distribution on the micro-scale level of *Acropora nobilis*. They attributed this heterogeneity to secondary infilling. As opposed to the

current study, where we have two distinct Sr concentrations that represent two different stages of growth, Shirai et al., (2008) show inhomogeneity that does not necessarily indicate secondary infilling. Despite this infilling theory, *Acropora* is being used for calibrating proxies and for reconstructing paleo-environmental conditions (e.g. Juillet-Leclerc at al., 1997; Reynaud et al., 2004; Rollion-Bard et al., 2009).

Methods

Micro colonies of *Acropora* sp. were cultured for several weeks in different temperatures (19°C, 22°C, 25°C, 28°C). The micro colonies were collected from the same mother colony that was held in a depleted Sr concentration aquarium (i.e. holding aquarium) in the coral laboratory of Prof. Jonathan Erez at the Hebrew University, Jerusalem Israel. Each of the micro colonies was attached to stable surface using underwater epoxy putty (AquaStik, Aquasonic, Ingleburn, New South Wales, Australia) and was left in the holding aquarium for recovery of five weeks. In the experiment we used natural seawater from the Gulf of Aqaba (at the pier of the Interuniversity Institute for Marine Sciences in Eilat (IUI)), which was then diluted to 37 $g \cdot kg^{-1}$. The experiments took place in a flow through system with water residence time of 12 hours, while Sr and Ca concentrations in the seawater solution remained stable throughout the experiment. Total alkalinity measurements were performed weekly on the reservoir seawater solution and on the collected outflow seawater solution. Total alkalinity was determined by Gran titration using a Metrohm DMS Titrino. The amount of calcification was determined using the alkalinity anomaly technique (Smith and Kinsey, 1978; Chisholm and Gattuso, 1991), and was divided by the final weight of the skeleton to obtain percent of growth. After seven weeks the experiment was terminated. The corals' tissue was removed by high air pressure and was then rinsed with deionized water to remove tissue and seawater remaining. Bleaching (1% NaClO) and ultrasonic treatment were done in addition to each branch that was used for mapping analyses. Skeleton powder were collected from the specimens' epoxy surfaces, dissolved in 2% HNO_3 and measured on Agilent 7500 Quadrupole ICP-MS at GEOMAR, Kiel. Water samples from the pre-experimental and experimental water were measured on Varian 720-ES ICP-OES at GEOMAR, Kiel. The Sr/Ca ratio of the experimental water (8.5±0.1 $mmol \cdot mol^{-1}$) is approximately 2 times higher than the ratio in the pre-experimental water (~3.7 $mmol \cdot mol^{-1}$). The rough estimation of Sr/Ca in the pre-experimental water is based on a single water sampling

(3.7±0.1 mmol·mol^{-1}). Due to the addition of Ca to the pre-experimental solution to compensate for the consumption by calcification, Sr/Ca was variable in the pre-experimental phase, and therefore the single Sr/Ca measurement is considered as an approximation only.

A branch from each coral specimen was used for Sr Ca and S elemental mapping using an electron microprobe (JEOL JXA 8200 super probe) at GEOMAR, Kiel. The branches were embedded into resin, polished, and carbon coated. For the measurements we used an acceleration voltage of 15.0 kV, a beam current of 0.04 μA, a beam diameter of 10 μm, a dwell time of 20 msec, and 10 accumulations for each image. Calibration of Sr and Ca concentrations were done using four standards with known average concentrations (VG-2 (Jarosewich et al., 1980), KAN-1 (Reay et al., 1993), Strontionite (Jarosewich and White, 1987) and Calcite (Jarosewich and MacIntyre, 1983)). For the calibration we used only 1 accumulation and dwell time of 50 msec on an area of 10 pixels by 10 pixels.

Two branches from the 19°C and 25°C experiments were measured using synchrotron X-ray fluorescence micro-analysis (μ-SXRF) at beamline L of HASYLAB (Hamburger Synchrotronstrahlungs-Labor) which is located at DESY (Deutsches Elektronen-Synchrotron) in Hamburg, Germany. The synchrotron radiation at the second-generation electron/positron storage ring DORIS III originates from positrons with 4.5 GeV at a bending magnet with 12.12 m radius, and is emitted in a tangential direction into the beam pipe (Janssens et al., 2004). At beamline L, the complete SXRF set-up can be adjusted in the vertical and horizontal directions by stepper motors. The photon beam reaches the sample surface at a 45° angle, and can both be collimated and focused. In order to enable a tomographic imaging of the carbonate samples, we used a confocal glass capillary designed to concentrate more than 95% of the incoming energy of the white X-Ray beam within a pre-defined volume of 20 x 20 x 20 micrometers. Characteristic X-Rays emitted from each such 3D-pixel was detected with a SiLi EDS-detector, and corrected off-line for the attenuation arising from the overlying pixels (i.e. those pixels between the measured pixel and the detector). We measured Ca and Sr in both branches. Thus in contrast to the EMPA, μ-SXRF can be used to obtain a three dimensional micro-chemical map of a given sample. This is due to the high penetration of the hard X-rays used for the investigation.

Data processing and calculations were done in Matlab R2011a software (MathWorks®).

Results and discussion

Aragoite infilling in Acropora sp.

Both the Electron microprobe (EMPA) and the μ-SXRF mapping results indicate two distinctive Sr/Ca ratios (3.0±1.0 mmol·mol^{-1}, 8.5±1.5 mmol·mol^{-1}), which roughly correlate to the average Sr/Ca ratios measurements of the pre-experiment skeleton and the experiment's skeleton, respectively (3.0±0.1 mmol·mol^{-1}; 9.4±0.1 mmol·mol^{-1}). The large difference in Sr/Ca thus represents two periods in the corals' skeleton growth, which enables us to observe the unique growth pattern of *Acropora* sp. skeleton.

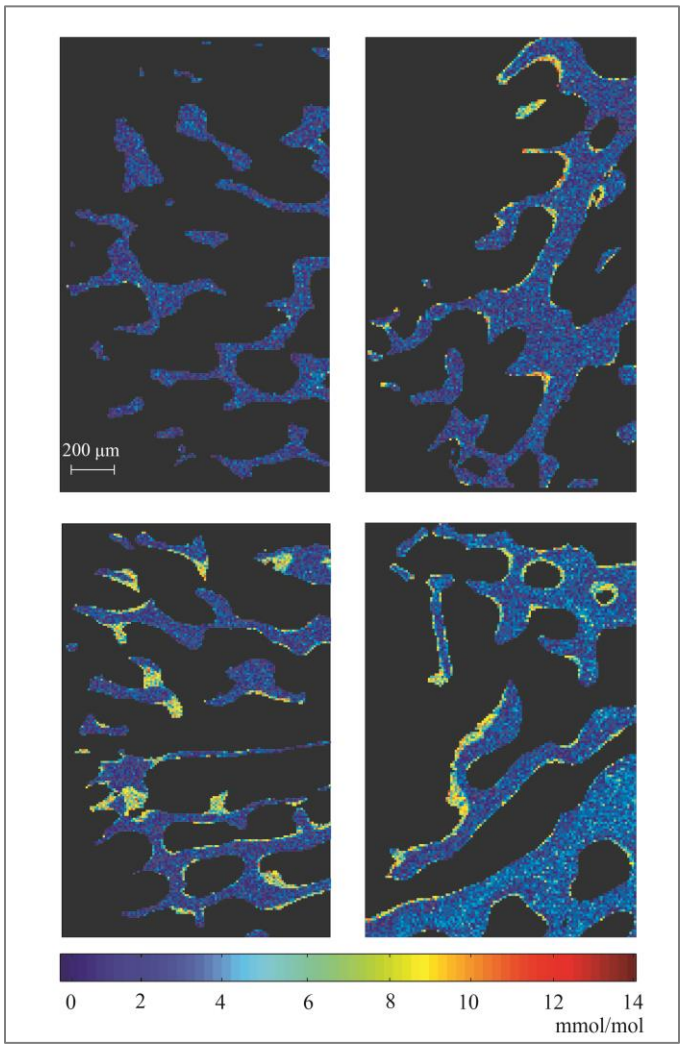

Figure II.1 Sr/Ca ratios (mmol·mol^{-1}) in the corals' skeleton mapped with the electron microprobe using a pixel size of 10μm. The images represent experiments that were performed at temperatures 19°C (top left) 22°C, 25°C, and 28°C (bottom right). Scale on the upper left mapping indicates 200 μm for all mappings in this figure. The average pre-experiment Sr/Ca ratio is 2.3±0.8 mmol·mol^{-1} and the average experiment Sr/Ca ratio is 7.3±1.0.

Our results show very small to complete absence of axial growth on the corals' tips (Figure II.1). This may have been partly caused by damaging the skeleton's tips during sample preparation.

Nevertheless, in deeper and older parts of the skeleton we observe patches of high Sr/Ca within the low Sr/Ca areas. This observation indicates that high Sr/Ca aragonite has precipitated during the experiment in older parts of the skeleton, and does not follow the expected axial growth of corals skeleton. Previous studies have suggested an infilling process that occurs in *Acropora* spp. by observing the density increase with depth from the coral's tips in several *Acropora* species (e.g. Gladfelter 1982; Shirai et al. 2008; Roche et al. 2011), or by observing microscale heterogeneity of element composition in *Acropora nobilis* (Shirai et al., 2008). Shirai et al. (2008) claim for microscale composition heterogeneity based on EMPA and NanoSIMS measurements of Sr, Mg, Ca and S in *Acropora nobilis* skeleton. Yet, the microscale variations in chemical compositions do not necessarily indicate an infilling process. Allison et al. (2001) found microscale Sr heterogeneity in the growth bands of *Porites lobata*. They attributed the heterogeneity to calcification in disequilibrium that prevents from extending the temporal resolution of SST reconstruction. Our *Acropora* sp. branches are young and very porous. For this reason, we observe no significant density variation with depth. Nevertheless, our data support the infilling hypothesis, where calcification takes place also inside the skeleton rather than at the tips.

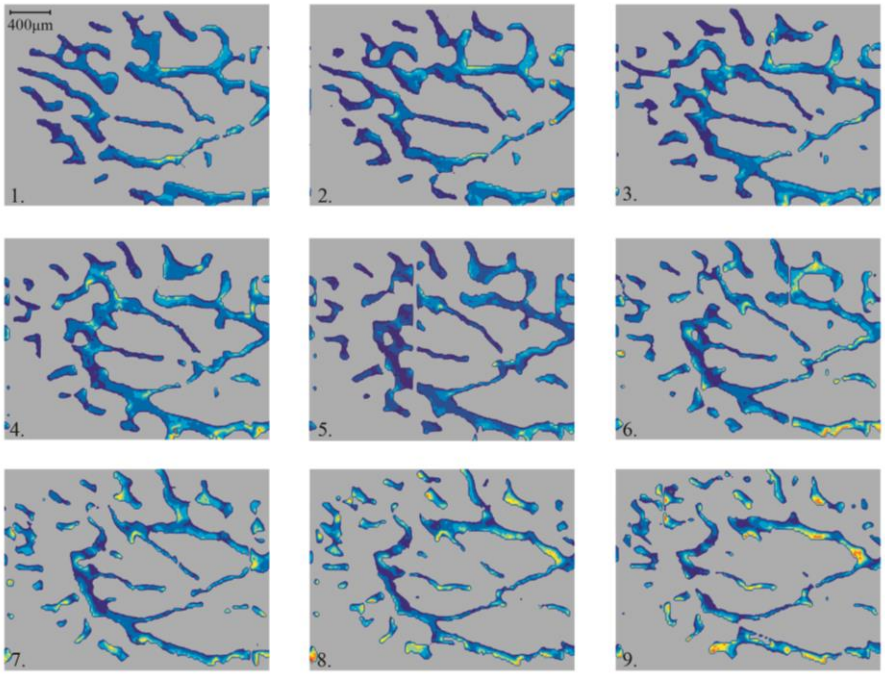

Figure II.2 Sr/Ca ratio results of 9 layers (from top left to bottom right) in the 19°C experiment as measured on µ-SXRF. Pre-experiment skeleton growth characterized by low Sr concentration is marked in blue and the experiment growth is marked in the yellow to red colors. The pictures demonstrate cross section view from the top of a new grown polyp. New growth is observed in thickening the walls and the septa of the polyp skeleton framework.

We show two distinct Sr concentrations that represents two different periods in the skeleton growth. The distribution of the second period indicates the infilling process. As proposed by Shirai et al. (2008), originally the framework of the skeleton is precipitated and the infilling precipitates on the surface of the framework and connects between components of the framework (Figures II.2, II.3). As seen on Figure II.3, the septa and the theca are thickened and the infilling connects between parts of the thin and fragile framework.

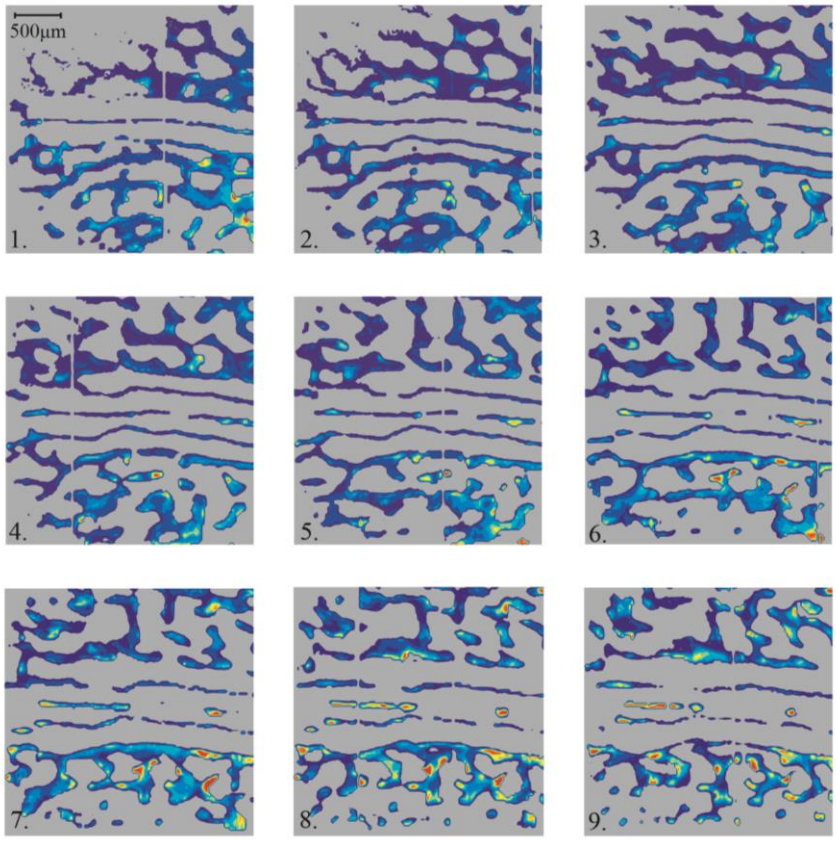

Figure II.3 Sr/Ca ratio results of 9 layers (From top left to bottom right) in the 25°C experiment as measured on µ-SXRF. Pre-experiment skeleton growth with low Sr concentration is marked in blue and the experiment growth is marked in the yellow to red colors. The pictures demonstrate a longitudinal cross section view of a polyp. New growth is observed in the entire sample (length of 2.7 mm) at all depth layers that were measured.

Differences in growth between different temperatures

The percentage of skeleton growth during the experiment was calculated from the EMPA results, as the amount of pixels with high Sr/Ca ratio (higher than 7 mmol·mol^{-1}) compared to the total amount of pixels with Sr/Ca larger than 1 mmol·mol^{-1} (Figure II.1). Small mapped skeleton areas of approximately 30 by 30 pixels that contained pre-experimental and experimental skeleton were selected to determine the range of Sr/Ca in the experimental skeleton. The Sr/Ca ratios are normally distributed, where -1SD of the experimental Sr/Ca ratio is at 7 mmol·mol^{-1} (Figure II.4). This value was determined as the minimum experimental Sr/Ca in the skeleton

growth percentage calculations. The growth percentage calculation results show good correlation with the growth calculations made by alkalinity anomaly technique (Smith and Kinsey, 1978) for each temperature experiment (Figure II.5). The experiments of the current study show that the calcification rate of *Acropora* sp. coral increase with temperature with a maximal point at 25°C and then a decrease at 28°C.

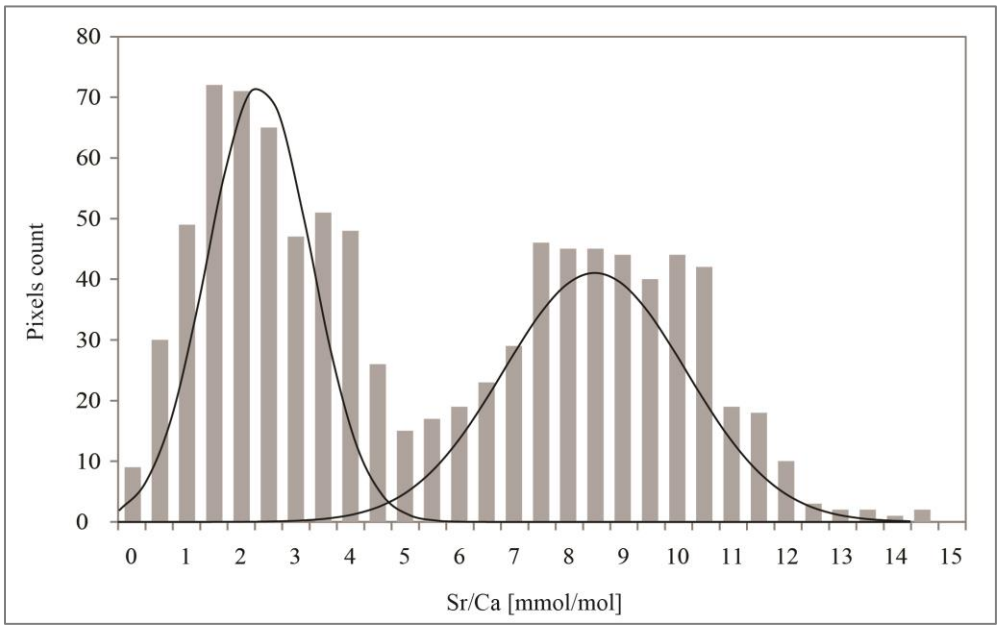

Figure II.4 Distribution of Sr/Ca in a 30 by 30 pixel area of the 25°C coral experiment as observed in EMPA. The area contains pre-experimental aragonite (low Sr/Ca values) as well as experimental aragonite (high Sr/Ca values). The two distinct Sr/Ca ratios are normally distributed, where the average low Sr/Ca ratio is 3.0 mmol·mol^{-1} and the average high Sr/Ca ratio is 8.5 mmol·mol^{-1}. We determined -1SD (7.0 mmol·mol^{-1}) from the average high Sr/Ca ratio as the minimum Sr/Ca value of the experimental skeleton.

The hypothesis that is supported in this study on irregular calcification in *Acropora* spp. was originally suggested by Gladfelter (1982) and Shirai et al. (2008) as secondary infilling precipitation. According to them, infilling precipitation is a biologically controlled precipitation that occurs in older parts of the skeleton. Shirai et al. (2008) observed different Sr/Ca ratios in older parts of the skeleton that appears as a patch-like pattern. They attributed the different Sr/Ca ratios to seasonal variations, claiming that the framework and the infilling occurred in different seasons. Other studies (Enmar et al., 2000; Lazar et al., 2004), however, associate observed secondary infilling to inorganic precipitation in *Porites lutea*. Sr/Ca is claimed to have different fractionation factors in inorganic aragonite and in biogenic aragonite (Enmar et al., 2000; Dietzel et al., 2004), as D_{Sr} in inorganic aragonite is higher in approximately 0.1 from biogenic

aragonite. It means that Sr/Ca in inorganic aragonite is approximately 1 mmol·mol^{-1} higher than in coral's aragonite.

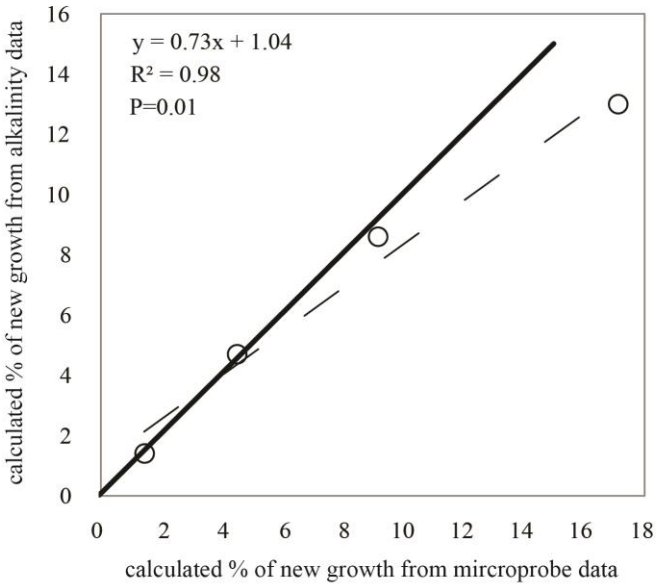

Figure II.5 Correlation between the percentages of skeleton growth during the experiment as calculated from the pixel area results in the EMPA and as calculated from the alkalinity difference measurements (alkalinity anomaly). Good correlation was found between the results of the two techniques. The dashed line is the 1:1 line of a perfect fit.

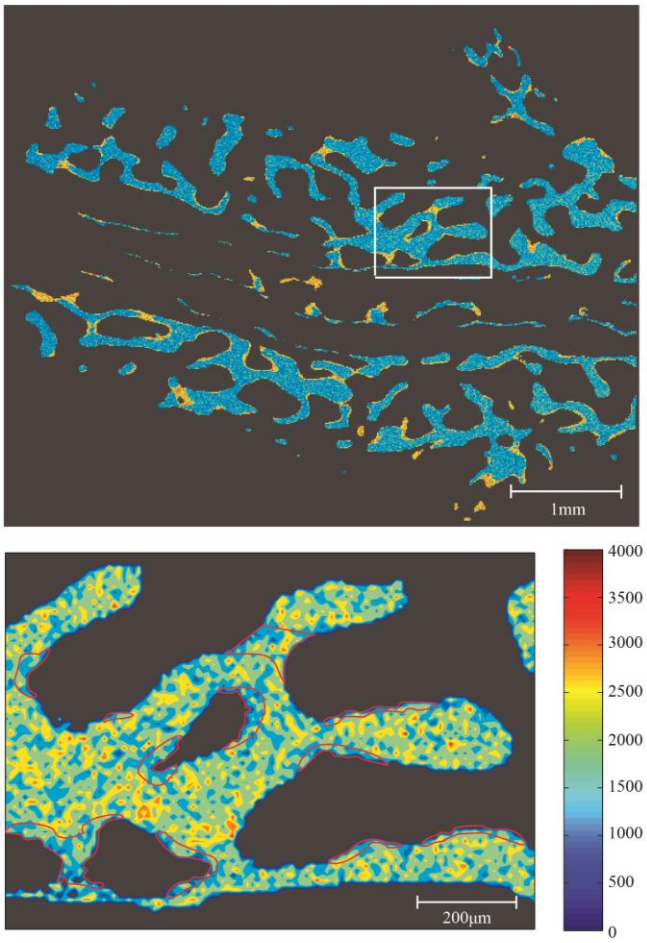

Figure II.6 A magnified image of sulfur (S) mapping in the 25°C experiment that was obtained from the EMPA (the bottom image). The S concentrations are calibrated and presented in ppm. Areas that are marked in thin red lines are the experimental calcification areas, as detected from the Sr/Ca ratio mapping (the top image). The location area of the S image is marked in the top image. The S mapping was measured in deeper part of the skeleton 3 mm bellow the tip and 0.5 mm away from the theca (outer skeleton walls), which indicates that the calcification is not part of the axial or radial growth. There are no significant differences between the average S concentrations of the experimental and the pre-experimental skeleton (2210±227ppm and 2190±76 ppm (1SD), respectively). This implies that the experimental skeleton precipitation was biologically controlled.

Due to the large variability in the Sr/Ca ratio mapping (2σ=~1 mmol·mol^{-1}), we could not calculate the Sr/Ca-temperature relation in the difference specimens nor to detect whether the infilling Sr/Ca ratio is inorganic or biogenically controlled. Nonetheless, the sulfate distribution in the samples reveals that the infilling has similar concentration to the remaining skeleton (Figure II.6). Sulfate is considered to be related to organic matrices. The concentration in corals' aragonite is 1250 to 3500 ppm of Sulfur in the skeleton's fibers and centers of calcification, respectively (Cuif and Dauphin, 1998), while in inorganic aragonite smaller concentrations of less than 100 ppm of sulfur are found (Pingitore et al., 1995). This implies that the infilling precipitation in *Acropora* sp. is biogenically controlled.

Appendix: Correction of heterogeneous samples measured in the µ-SXRF

The porous nature of corals' skeleton is not ideal for element measurements in the µ-SXRF. As the x-ray beam penetrate deeper parts of the sample, the intensity of the element signal decreases as a function of the depth and the density of the substance. When dealing with a homogenous substance, the signal attenuation can be easily calculated and then can be corrected to non-attenuated signal. However, when the substance is heterogeneous and contains many pores, the correction is not straightforward. There are two factors that can cause a Ca concentration signal reduction (that is supposed to be constant in $CaCO_3$): The first factor is 'partial pixel'; where the measured pixel is not fully composed of $CaCO_3$. The second factor is the attenuation caused by $CaCO_3$ on covering layers in the path of the secondary beam. In order to correct the data, these two factors need to be separated. The first layer at the sample's surface is free of covering layers. It means that every deviation from a maximal Ca signal (maxCa) is caused by the 'partial pixel' (pp) factor.

$$pp = \frac{signal}{maxCa} \qquad \text{Eq. II.1}$$

'Partial pixels' factor of the first layer is converted to attenuation factor for the underlying layers by multiplying it by the secondary beam distance (i.e. pixel's diagonal) this is the distance that the secondary beam needs to pass from the second layer to the detector (D).

$$amount\ of\ CaCO_3\ cover = pp \times D \qquad \text{Eq. II.2}$$

In this manner a signal in the second layer that is smaller than the expected signal is interpreted as 'partial pixel' and then added to the first layer as the attenuation factor of the third layer.

Eventually, we can correct any trace element that was measured (E') in addition to the major Ca element in order to get the true, non-attenuated value of this element. The true element value (E) is corrected to a full non-attenuated pixel value based on its depth below $CaCO_3$ cover and the emission energy of the element (SrTransmission).

$$E = \frac{E\prime}{pp \times SrTransmission} \qquad \text{Eq. II.3}$$

The bulk density of the substance is needed for the transmission calculations of the elements. Aragonite has a density of 2.95 gr·cm^{-3}, however the bulk density of a coral is much smaller due to its porosity. Transmission that was calculated with bulk density of 1.3 g·cm^{-3} fit to our data of maximum Ca values for different cover depths (Figure II.7). This density corresponds to porosity of 55% and is in agreement to the average skeletal density of 1.29±0.18 g·cm^{-3} (Lough and Barnes, 1997) and to an approximately 0.8 years old *Acropora* coral as observed by Oliver et al. (1983).

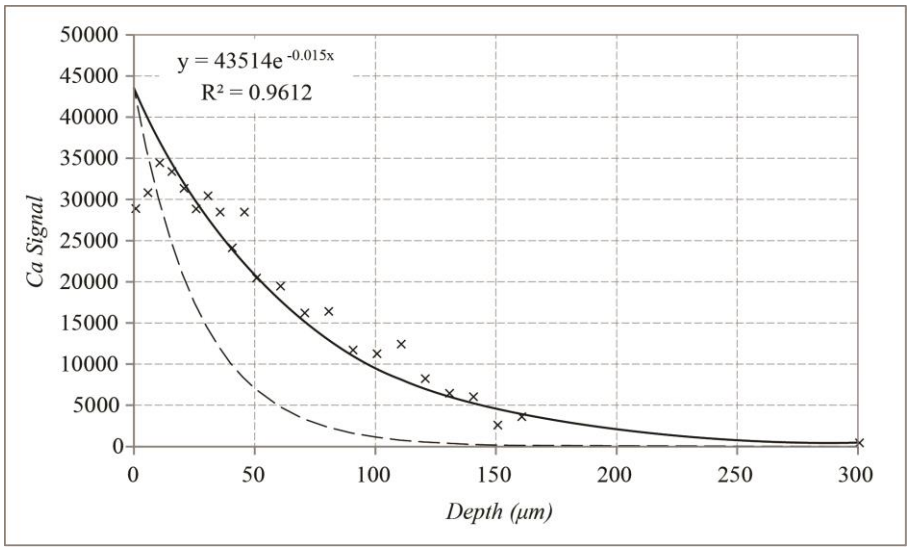

Figure II.7 Attenuation of Ca with depth. The cross signs are the results of the maximum Ca signals for each depth. The black thick line is for Aragonite 2.95 density. The thin line is the best fit to the maximum Ca values with density of 1.3. The maximum Ca signal in the first 10 μm below surface show lower Ca concentration. This may be due to focusing on the surface layer that included only half of the pixel's depth.

Acknowledgments

We would like to thank Mario Thöner from the EMPA laboratory for his help in the analyses. Funding support was provided through the European Marie Curie Initial Training Network "Calcification by Marine Organisms" (CalMarO) and the European Community's Seventh Framework Programme (FP7/2007-2013).

References

Allison N, Finch AA, Sutton S, Newville M (2001) Strontium heterogeneity and speciation in coral aragonite: implications for the strontium paleothermometer. Geochim. Cosmochim. Acta 65:2669–2676

Chisholm JRM, Gattuso JP (1991) Validation of the alkalinity anomaly technique for investigating calcification and photosynthesis in coral reef communities. Limnol. Oceanogr. 36:1232–1239

Cuif J-P, Dauphin Y (1998) Microstructural and physico-chemical characterization of "centers of calcification" in septa of some Recent scleractinian corals. Paläontologische Zeitschrift 72:257–270

Dietzel M, Gussone N, Eisenhauer A (2004) Co-precipitation of Sr^{2+} and Ba^{2+} with aragonite by membrane diffusion of CO_2 between 10 and 50°C. Chem. Geol. 203:139–151

Enmar R, Stein M, Bar-Matthews M, Sass E, Katz A, Lazar B (2000) Diagenesis in live corals from the Gulf of Aqaba. I. The effect on paleo-oceanography tracers. Geochim. Cosmochim. Acta 64:3123–3132

Gladfelter EH (1982) Skeletal development in Acropora cervicornis: I. Patterns of calcium carbonate accretion in the axial corallite. Coral Reefs 1:45–51

Huston M (1985) Variation in coral growth rates with depth at Discovery Bay, Jamaica. Coral Reefs 4:19–25

Janssens K, Proost K, Falkenberg G (2004) Confocal microscopic X-ray fluorescence at the HASYLAB microfocus beamline: characteristics and possibilities. Spectrochim. Acta Part B At. Spectrosc. 59:1637–1645

Jarosewich E, MacIntyre IG (1983) Carbonate reference samples for electron microprobe and scanning electron microscope analyses. J. Sediment. Res. 53:677–678

Jarosewich E, Nelen JA, Norbers JA (1980) Referaxe Samples for Electron Microprobe Analysis . Department of Mineral Sciences. Geostand. Newsl. 68–72

Jarosewich E, White JS (1987) Strontianite reference sample for electron microprobe and SEM analyses. J. Sediment. Res. 5:1986–1987

Lazar B, Enmar R, Schossberger M, Bar-Matthews M, Halicz L, Stein M (2004) Diagenetic effects on the distribution of uranium in live and Holocene corals from the Gulf of Aqaba. Geochim. Cosmochim. Acta 68:4583–4593

Lough JM, Barnes DJ (1997) Several centuries of variation in skeletal extension , density and calcification in massive Porites colonies from the Great Barrier Reef : A proxy for seawater temperature and a background of variability against which to identify unnatural change. J. Exp. Mar. Bio. Ecol. 211:29–67

Oliver JK, Chalker BE, Dunlap WC (1983) Bathymetric adaptations of reef-building corals at Davies Reef, Great Barrier Reef, Australia. I. Long-term growth responses of Acropora formosa (Dana 1846). J. Exp. Mar. Bio. Ecol. 73:11–35

Pingitore NE, Meitzner G, Love KM (1995) Identification of sulfate in natural carbonates by x-ray absorption spectroscopy. Geochim. Cosmochim. Acta 59:2477–2483

Reay A, Johnstone RD, Kawachi Y (1993) Anorthoclase, a second microprobe standard from Kakanui, New Zealand. Geostand. Newsl. 17:135–136

Roche RC, Abel RL, Johnson KG, Perry CT (2011) Spatial variation in porosity and skeletal element characteristics in apical tips of the branching coral Acropora pulchra (Brook 1891). Coral Reefs 30:195–201

Shirai K, Kawashima T, Sowa K, Watanabe T, Nakamori T, Takahata N, Amakawa H, Sano Y (2008) Minor and trace element incorporation into branching coral Acropora nobilis skeleton. Geochim. Cosmochim. Acta 72:5386–5400

Smith SV, Kinsey DW (1978) Calcification and organic carbon metabolism as indicated by carbon dioxide. Coral reefs Res. methods 469–484

De Villiers S, Nelson BK, Chivas AR (1995) Biological Controls on Coral Sr/Ca and d18O Reconstructions of Sea Surface Temperatures. Science 269:1247–9

CHAPTER III. $^{88}Sr/^{86}Sr$ FRACTIONATION IN INORGANIC ARAGONITE AND IN CORALS

Noa Fruchter[1*], Anton Eisenhauer[1], Martin Dietzel[2], Jan Fietzke[1], Florian Böhm[1], Paolo Montagna[3], Moti Stein[4], Boaz Lazar[5], Jonathan Erez[5]

[1] *GEOMAR, Helmholtz-Zentrum für Ozeanforschung Kiel, Wischhofstr. 1-3, 24148 Kiel, Germany*

[2] *Institute of Applied Geosciences. Graz University of Technology. 8010 Graz, Austria*

[3] *CNR - ISMAR - U.O.S. di Bologna –, Via Gobetti, 101 – 40129 Bologna, Italy*

[4,*] *Geological Survey of Israel, Malkhei Israel 30 Jerusalem, Israel*

[5] *The Hebrew University, The Edmond J. safra Campus Givat Ram Jerusalem, Israel*

In preparation, to be submitted to *Geochimica et Cosmochimica Acta*

Abstract

Major $^{88}Sr/^{86}Sr$ fractionation from bulk solution is observed in inorganic aragonite that was precipitated from natural seawater in the CO_2 diffusion technique. Similar fractionation is observed in several different coral species (*Cladocora caespitosa*, *Porites* sp. and *Acropora* sp.). Despite the large fractionation from bulk solution (~0.2‰), we found no temperature or CO_3^{-2} ion concentrations dependency on the fractionation (within 2SD). Our results implies that the Rayleigh based multi element model (Gaetani et al., 2011) cannot explain the process of corals' calcification.

Introduction

Tropical coral aragonites skeletons are one of the main archives for proxy information about past climate change. Temperature dependency was found in several elemental ratios such as Mg/Ca (e.g. Mitsuguchi et al., 1996), Sr/Ca (e.g. Beck et al., 1992) and B/Ca (e.g. Fallon et al., 1999), and recently also Li/Mg (Montagna et al., 2009). The isotope fractionation of oxygen, $\delta^{18}O$ (e.g. Weber & Woodhead, 1972) is also being used for SST reconstruction from corals' skeletons. Among all proxies, Sr/Ca and $\delta^{18}O$ are the most widely used and are the most established past sea surface temperature (SST) proxies (Corrège, 2006). However, temperature may not be the only controlling factor for trace element partitioning and isotope fractionation (c.f. Gagnon et al., 2007). For Sr/Ca ratios, for example, was shown to be significantly different in colonies from the same species growing side by side to each other (Marshall and McCulloch, 2002). Mg is incorporated together with the organic component of the skeleton (Watanabe et al., 2001), and in addition to temperature $\delta^{18}O$ is known to be influenced by seawater salinity changes (c.f. Schmidt, 1999).

Fietzke and Eisenhauer (2006) determined for the first time that $^{88}Sr/^{86}Sr$ shows a measurable fractionation in corals and in inorganic aragonites. In their study they used the bracketing standard method on an MC-ICP-MS. They showed a significant positive temperature dependency on the $^{88}Sr/^{86}Sr$ fractionation of the tropical coral *Pavona clavus*. In a following up study Rüggeberg et al. (2008) found similar trend for temperature and $\delta^{88/86}Sr$ in the cold water coral, *Lophilia pertusa*. Evidences of significantly different $\delta^{88/86}Sr$ of mineral and the bulk solution were also found in terrestrial environments by Halicz et al. (2008).

While the earlier work on $\delta^{88/86}$Sr used the bracketing standard method in MC-ICP-MS (Fietzke and Eisenhauer, 2006; Halicz et al., 2008; Rüggeberg et al., 2008), later work used the $^{87}Sr/^{84}Sr$ double spike method that was developed and applied on a TIMS by Krabbenhöft et al. (2009). Later measurements using the TIMS method could not confirm the significant positive $\delta^{88/86}$Sr-temperature trend in the tropical coral *Acropora* sp. (Krabbenhöft et al., 2010) and in the cold water coral *Lophilia pertusa* that was previously shown with temperature correlation to $\delta^{88/86}$Sr (Raddatz et al., 2013). The discrepancies between the different studies may be due to either species-related temperature dependence of $\delta^{88/86}$Sr or due to methodological bias of the two measurement techniques.

A possible model to extract the climate factor in geochemical proxies is proposed in a Rayleigh based mechanism (Gaetani and Cohen, 2006; Gaetani et al., 2011). The model defines calcification in corals as precipitation process from a renewable finite solution. Elements are depleted from the solution during precipitation according to their inorganic partitioning coefficient. Since the solution is finite, coral's apparent fractionation factor is influenced by the Rayleigh effect. Temperature is strongly correlated to the Rayleigh based mechanism (Gaetani et al., 2011), as the depletion of elements rises with the increasing precipitation rates and as a consequence also with the increasing temperatures. By combining two element ratios Gaetani et al. (2011) were able to reconstruct the remaining fraction in the bulk solution and the temperature in *Acropora* sp. samples.

In the current study we measured $\delta^{88/86}$Sr using the double spike method in natural *Porites* sp., cultured *Acropora* sp. and *Cladocora caespitosa* as well as aragonite of inorganic precipitation experiments. We found a range of $\delta^{88/86}$Sr values, which indicate a significant fractionation from the bulk solution, but did not find any significant correlation of temperature as previously claimed by Fietzke and Eisenhauer (2006) or carbonate ion concentration to Sr isotope fractionation.

Methods

Inorganic aragonite precipitation experiments

Inorganic aragonite precipitation experiments were conducted at the University of Technology in Graz, Austria using the CO_2 diffusion technique as described in detail earlier in

Dietzel et al. (2004). In this technique, CO_2 diffuses from an inner solution to an outer solution via poly-ethylene (PE) membrane (we used two different membranes thickness, 0.02 mm or 2 mm thick). The inner solution consists of 35 grams of $NaHCO_3$ in a 0.5 l solution at pH 7.5, and has a higher pCO_2 than the outer solution. In order to increase the pCO_2 in few experiments we added 10 ml of 1N HCl to the inner solution (Table III.1). The outer solution (or bulk solution), from which the precipitation occurs, is 5 l of filtered natural seawater collected from the Gulf of Aqaba (Red-Sea 19.09°N 39.49E°, salinity of 40.7 $g \cdot kg^{-1}$, from 1000 m water depth using CTD device). Filtration was done with Sartobram P. sterile MidiCap double filter of 0.45 μm and 0.2μm. The pH of the outer solution was kept constant at 8.30±0.03 using 0.5N NaOH titration and was controlled using a Schott Blueline 28 pH meter combined with automatic titration burette. The pCO_2 gradient between the inner and the outer solutions control the CO_2 diffusion rate and the saturation state for $CaCO_3$ in the outer solution.

The nine different experiments (Table III.1) varied in temperature (15°C, 25°C and 30°C) and CO_2 diffusion rates (using different PE membranes of 0.02 mm or 2 mm thick, and different PCO_2 in the inner solution). The diffusion rates regulate the saturation state for $CaCO_3$, specifically the aragonite saturation state.

Table III.1 Inorganic aragonite experiments setup conditions and elemental ratio results in the solid. Standard deviation from the mean (2SD) are presented in parentheses

Sample Label	Temp. (°C)	Diffusion membrane thickness (mm)	f [b]	$\Delta^{88/86}Sr$ [c] (‰ A-aq)	Sr/Ca (mmol/mol)	Mg/Ca (mmol/mol)	logR (mol/h)
IA-1	25	0.02	0.83	-0.172	9.80(0.48)	5.44(0.37)	3.29
IA-2	25	0.02	0.67	-0.178	9.54(0.31)	105.47(4.79)	2.95
IA-3	30	2	0.79	-0.193	9.48(0.31)	2.91(0.17)	1.84
IA-4	30	0.02	0.58	-0.205	9.10(0.13)	47.57(0.47)	3.01
IA-5	30	0.02 [a]	0.71	-0.179	9.37(0.40)	63.13(0.35)	3.20
IA-6	30	2 [a]	0.81	-0.156	9.57(0.34)	4.10(0.28)	2.55
IA-7	15	2	0.86	-0.161	10.82(0.41)	6.54(0.14)	2.33
IA-9	15	2 [a]	0.85	-0.125	11.06(0.13)	4.96(0.07)	1.71
IA-10	15	0.02 [a]	0.81	-0.174	10.72(0.40)	4.75(0.14)	2.51

[a] Addition of 10ml 1N HCl to the inner solution to increase pCO_2
[b] Remaining fraction of Sr in the solution, calculated using Eq. III.2
[c] reproducibility of 0.020‰ (2SD) according to JCP-1 measurements (n=10)

Water samples from the outer solution were collected at the beginning and at the end of the experiment for analyses of Sr/Ca and $^{88}Sr/^{86}Sr$. The precipitated solid was collected and dried at

80°C for 24 hours, and then analyzed with XRD and FTRI (PerkinElmer spectrum 100 FTIR) to determine its mineralogy and detect the poorly crystalized brucite.

Rate of precipitation is reported in $\mu mol \cdot h^{-1}$. The precipitation rate (R) was determined according to Eq. III.1 where $[Ca]_i$ and $[Ca]_f$ are the Ca concentration in the initial and the final solutions, respectively, V is the volume of the solution and Δt is the duration of the precipitation. Even though precipitation rates are influenced by the surface area and surface reactions (Wiechers et al., 1975), we could not include the surface area measurements in the calculation since in some cases brucite ($Mg(OH)_2$) precipitated in an amount of up to 7%. Brucite has a surface area of 38 $m^2 \cdot g^{-1}$ (Kaspar et al., 1991), which is much larger than the surface area of aragonite (0.81 to 2.41 $m^2 \cdot g^{-1}$). Even a small amount of brucite in the precipitated solid will result in a large excursion of the surface area measurements and a significant reduction of the calculated rate.

$$R = \left([Ca]_i - [Ca]_f\right) \cdot V/\Delta t \qquad \text{Eq. III.1}$$

Since Ca and Sr concentrations changed by up to ~28% between the initial and the final solution, the results for Sr isotopes had to be corrected for the Rayleigh effect. The calculation for the true $\Delta^{88/86}Sr$ in the aragonite samples was done using the Rayleigh process equation combined with of the measured Δ approximation described in equations 3.1.17 and page 146 from Zeebe and Wolf-Gladrow (2001).

$$f = \left(\frac{[Sr]_{fs}}{[Sr]_{is}}\right) \qquad \text{Eq. III.2}$$

$$\alpha = \frac{ln\left(\Delta^{88/86}Sr_{meas} \cdot f/_{1000} - \Delta^{88/86}Sr_{meas}/_{1000} + f\right)}{\ln(f)} \qquad \text{Eq. III.3}$$

$$\Delta^{88/86}Sr_{True} = (\alpha - 1) \cdot 1000 \qquad \text{Eq. III.4}$$

Where α is the fractionation factor, f is the remaining fraction in the fluid and $[Sr]_{fs}$ and $[Sr]_{is}$ are the Sr concentration in the final and initial solution, respectively.

Cultured corals

Acropora sp. mini colonies were cultured in the department of Earth Sciences at the Hebrew University of Jerusalem, Israel. The specimens were collected from one mother colony several weeks prior to the beginning of the experiments. They were attached to an epoxy base and were placed back in the main laboratory aquarium (i.e. holding aquarium) for recovery. Before the beginning of the experiments the specimens were stained in 15 ppm solution of Alizarin-Red S (Dodge et al., 1984) for seven hours. During the experiment each coral specimen was placed for seven weeks in a 220 ml clear chamber supplied with 19 ml of diluted Red-Sea water per hour. The experimental seawater was collected from the pier at the Interuniversity Institute for Marine Sciences in Eilat (IUI) and diluted, for the experiment, to $37 g \cdot kg^{-1}$. The flow-through system had residence time of 12 hours while constantly stirred in the chamber using a magnetic stirrer. Light was supplied at illumination of 200±10 μmol photons$\cdot m^{-2} \cdot s^{-1}$ through metal-halide lamps in 12 hours dark/light cycles. Temperature was kept constant in all tanks using heaters or a refrigerating system connected to electronic controllers with a precision of ±0.3°C. The seven different experiments varied in temperatures (19.0±0.3°C, 22.0±0.3°C, 25.0±0.3°C and 28.0±0.3°C) and CO_3^{2-} concentrations (171±13, 212±12, 279±15 and 352±28 μmole$\cdot kg^{-1}$). CO_3^{2-} concentrations were calculated from pH and alkalinity measurements using the CO_2Sys (Lewis and Wallace, 1998).

The physiology of the coral was monitored on a weekly basis through pH, alkalinity (TA) and oxygen measurements of the water source solutions (reservoirs), the reaction vessels (both at light and dark conditions) and the outflow solutions. In addition 50 ml of water samples of the reservoirs and the outflow solutions (representing the total duration of the experiments) were collected for geochemical analyses. ΔTA measurements of the reservoirs and the outflow solution were used to estimate the calcification of the specimens. Calcification rates were normalized to the buoyant weight of the micro colonies at the end of the experiment. Once in 10 days, during the experiments, the corals specimens were fed with *Artemia* sp. in an external 5 l vessel for 1 hour. While feeding, algae growth was removed from the experiment chambers.
The experiments were terminated after seven weeks. The corals skeletons were separated from their tissue using an air-brush followed by bleach in 1% NaClO and wash in double deionized water (DDW).

Cladocora caespitosa was cultured at the Scientific Centre of Monaco (CSM) at 15.00±0.05°C, 18.00±0.05°C, 21.00±0.05°C and 23.00±0.05°C in temperature experiments, and in 390±48 and 701±78 ppm pCO_2 during an atmospheric CO_2 partial pressure experiment (at temperature of 16.4±2.6°C). The corals were collected in the Gulf of La Spezia (Ligurian Sea, 44°03' N, 9°55' E) at ~25 m depth in June 2006. The corals were divided to 34 nubbins (five for each temperature experiment and seven for each pCO_2 experiment) and were acclimatized for several weeks to adapt to the new environment and to the experiment conditions. Before the initiation of the experiment, the corals were stained for 24h with a solution of 10 $mg \cdot L^{-1}$ of Alizarin Red S (Dodge et al., 1984). Alizarin Red S is incorporated into a thin layer of skeleton and provides a marker for measuring skeletal growth. Light was provided by hydrargyrum quartz iodide lamps (60 µmol photon $m^{-2} \cdot s^{-1}$; photoperiod: 12h dark/12h light). Temperature was kept constant in all tanks using heaters or a refrigerating system connected to electronic controllers with a precision of ±0.05°C. Fresh seawater (38.5$g \cdot kg^{-1}$ from 50 meters water depth) was constantly added to the experiment tanks from the local seawater in front of Monaco Scientific Center. CO_2 - free air and CO_2 - enriched air were pumped continuously to the experiment seawater of the 390 and 701 ppm pCO_2 experiments, respectively. This resulted in two different pH (8.09±0.02, 7.87±0.02) and carbonate system composition (CO_3^{2-} is 219±17, 145±15 $\mu mol \cdot mol^{-1}$), while alkalinity is similar in both experiments (Trotter et al., 2011). Corals were incubated for 87 days, during which no artificial food was supplied to the tanks, but corals were considered naturally fed since seawater supplied to the aquaria was not filtered. The linear extension rate was measured for each specimen from the Alizarin Red S marking line to the skeleton tip. The specimens in each temperature were then divided into three samples powders according to three statistical groups; average extension rates (Average±1SE), low extension rates (<Average-1SE) and high extension rates (>Average+1SE) groups. This statistic separation was not done in the pCO_2 experiments specimens.

Coral cores

Two cores from living colonies of *Porites* sp. were collected from different locations. Each core was cut to 2-3 mm thick slab, which was subsampled using a micro-drill of 0.5 mm in diameter along the growth axis of the coral for geochemical analyses. The powders were split for $\delta^{18}O$ analyses and for trace element and isotope measurements. The powders that were not designated

for $\delta^{18}O$ analysis were bleached with 1% NaClO and washed with alkaline water (at pH 9 achieved by DDW with the addition of ammonium hydroxide) prior to dissolution.

TH1: This *Porites* sp. coral core was drilled in July 1995 from a massive coral colony (TH1) located in the south-eastern part of the lagoon in Teahupoo, Tahiti French Polynesia at water depth of 2.40 meters (c.f. Cahyarini et al. (2008)). The totals of 36 samples (ca. 1 mg each) (Table III.2) were drilled along the growth axis of the slab as a 9.6 cm long transect. Similar transect was sampled on an adjacent slab from the same core by Cahyarini et al. (2008) and the $\delta^{18}O$ results from this study were compared to the current study transect results. Sampling in the current study followed the sampled transect in Cahyarini et al. (2008) by comparing the radiograph pictures of both slabs. Sea surface temperature records in Tahiti show variations between 26°C (minimum in the dry season) and 29°C (maximum in the wet season) (Cahyarini et al., 2009). The temperature record was used by Cahyarini et al. (2009) to calibrate the $\delta^{18}O$ results of the studied slab.

SOT-1: This *Porites lutea* coral core was drilled in July 2007 from the Gulf of Aqaba 29.50°N 34.92°E (coral colony SOT-1). The coral grew at 5 meters depth near the underwater observatory, south of the Nature Reserve Reef, Eilat Israel. The seawater temperature was recorded at 29.47°N 34.92°E at depths of 20 to 40 m to avoid the diurnal thermocline. Temperature measurements at these depths can be up to 2°C lower than the sea surface in the high temperature season from June to September. The total of 18 powder samples (ca. 2 mg each) (Table III.2) were drilled from SOT-1 core slab from a 3 cm long transect along the main growth axis of the coral. The clear density variations on the slab were used to estimate the period of time that is covered by the transect samples. By counting the total bands from the upper part of the core to the sampled bands, we estimate that the sampled bands cover the years 1996 to 2000.

Table III.2 $\Delta^{88/86}Sr$ results of *Porites* sp. corals. *Porites lutea* from the Gulf of Eilat and *Porites* sp. from French Polynesia

Sample Label	Sr/Ca (mmol/mol)	$\delta^{18}O$ (‰ vPDB)	Correlated[a] SST (°C)	$\Delta^{88/86}Sr$[b] (‰ A-aq)
***Porites lutea* – SOT-1**				
P07L00A	9.00	-2.977	24.1	-0.216
P07L00B	9.26	-2.716	21.0	-0.227

Sample Label	Sr/Ca (mmol/mol)	$\delta^{18}O$ (‰ vPDB)	Correlated[a] SST (°C)	$\Delta^{88/86}Sr$[b] (‰ A-aq)
P07H00A	8.97	-2.784	21.9	-0.183
P07H00B	8.86	-3.177	26.2	-0.207
P07H00C	8.96	-3.318	26.2	-0.184
P07L99A	8.91	-3.334	23.8	-0.220
P07L99B	8.96	-2.939	22.8	-0.205
P07H99A	9.23	-2.780	21.2	-0.207
P07H99B	9.15	-2.942	22.0	-0.182
P07H99c	8.75	-3.365	26.5	-0.196
P07L98A	9.07	-2.859	23.8	-0.205
P07L98B	9.32	-2.687	21.5	-0.221
P07H97A	9.23	-2.816	21.7	-0.190
P07H97B	8.96	-3.032	24.5	-0.220
P07H97C	8.92	-2.910	25.0	-0.198
P07L97A	9.09	-2.833	23.6	-0.174
P07L97B	9.33	-2.568	22.8	-0.182
P07H96A	9.14	-2.802	22.4	-0.181
***Porites* sp. – TH1**				
TH-1	8.57	-4.791	28.7	-0.154
TH-2	8.73	-4.765	28.6	-0.192
TH-3		-4.779	28.7	
TH-4		-4.439	26.9	
TH-5		-4.273	26.0	
TH-6	8.69	-4.202	25.6	-0.192
TH-7		-4.466	27.0	
TH-8		-4.652	28.0	
TH-9	8.64	-4.756	28.6	-0.156
TH-10		-4.547	27.5	
TH-11		-4.415	26.8	
TH-12		-4.444	26.9	
TH-13		-4.334	26.3	
TH-14		-4.390	26.6	
TH-15		-4.462	27.0	
TH-16		-4.609	27.8	
TH-17		-4.539	27.4	
TH-18		-4.555	27.5	
TH-19		-4.532	27.4	
TH-20		-4.448	26.9	
TH-21	8.54	-4.614	27.8	
TH-22	8.56	-4.332	26.3	
TH-23	8.70	-4.272	26.0	-0.169
TH-24	8.58	-4.445	26.9	
TH-25	8.59	-4.493	27.2	
TH-26	8.56	-4.656	28.0	
TH-27	8.72	-4.923	29.4	-0.169
TH-28	8.66	-4.812	28.9	-0.196
TH-29	8.61	-4.704	28.3	
TH-30	8.74	-4.566	27.6	-0.162
TH-31	8.68	-4.474	27.1	

Sample Label	Sr/Ca (mmol/mol)	$\delta^{18}O$ (‰ vPDB)	Correlated[a] SST (°C)	$\Delta^{88/86}Sr$[b] (‰ A-aq)
TH-32	8.93	-4.264	26.0	-0.186
TH-33	8.73	-4.487	27.1	
TH-34	8.51	-4.657	28.0	
TH-35	8.68	-4.751	28.5	-0.187
TH-36	8.62	-4.699	28.3	

[a] SST as reconstructed from Sr/Ca in SOT-1 and from $\delta^{18}O$ in TH-1
[b] reproducibility of 0.020‰ (2SD) according to JCP-1 measurements (n=10)

Analytical measurements

Part of each powder that was sampled from the two *Porites* core slabs (TH1 and SOT-1) was measured for $\delta^{18}O$ on Finnigan MAT252 at GEOMAR, Kiel. The data are presented in the usual δ-notation versus the vPDB standard. The analytical uncertainty was smaller than 0.06‰ (2SD). Powders from all coral samples and from the inorganic experiments were dissolved in 2% HNO_3 and analyzed for elemental ratios on Agilent 7500 Quadrupole ICP-MS at the mass-spectrometer facilities of GEOMAR, Kiel. The measurements were done using the bracketing standard method, with JCP-1 as the bracketing standard. The precision of the measurements was about 1-2% depending on the element measured.

Water samples were also analyzed for elemental ratios on Varian 720-ES ICP-OES at GEOMAR, Kiel. Strontium isotopes ($\delta^{88/86}Sr$) measurements of both water samples and the aragonite powders were done on the Finnigan Triton TIMS at GEOMAR in Kiel using the $^{87}Sr/^{84}Sr$ double spike method (Krabbenhöft et al., 2009). Sr was separated in the spiked and unspiked samples, using chromatographic column with BIO-RAD 650 ml columns and Eichrom Sr-SPS resin (mesh size 50–100 mm).

Sr isotopic values are presented in the usual δ-notation where $\delta^{88/86}Sr$ is the difference between the $^{88}Sr/^{86}Sr$ ratio of the aragonite sample and the isotopic ratio of the standard relative to the standard (using SRM987 value of $^{88}Sr/^{86}Sr$=8.375209 as the standard).

$$\delta^{88/86}Sr = \left(\frac{{}^{88}Sr/{}^{86}Sr_{CaCO_3}}{{}^{88}Sr/{}^{86}Sr_{SRM987}} - 1\right) \times 1000 \qquad \text{Eq. III.5}$$

In each batch of carbonate samples measurements, JCP-1 standard (0.20±0.02‰) was also measured. IAPSO standard was measured in batches of seawater sample measurements (0.39±0.02‰). No blank correction was needed since the total procedural Sr blanks were about 0.04 ng, which is insignificant compared to the amount of Sr in the measured samples (300–700 ng).

For comparison, the data is presented as the $\delta^{88/86}$Sr-difference between the sample and the solution from which it precipitated.

$$\Delta^{88/86}Sr(‰) = \delta^{88/86}Sr_{CaCO_3} - \delta^{88/86}Sr_{solution} \quad \text{Eq. III.6}$$

Data of all the analytical measurements are presented together with the statistical measurement uncertainty as two standard deviations (2SD), determined from the repeated JCP-1 measurements and not specifically for each sample. $\delta^{88/86}$Sr in JCP-1 is 0.20±0.02‰ (2SD) and was measured in 10 different measurements.

Rayleigh based model calculations

The predicted $\Delta^{88/86}$Sr values in corals that derives from the Rayleigh based model were calculated using the combined equations of Rayleigh process equation and the equation for δ notation (equations 3.1.17 from Zeebe and Wolf-gladrow, (2001) and equation 5 from the current study).

$$\Delta^{88/86}Sr_{Rayleigh} = \left(\frac{R_i \cdot \left(\frac{f^{\alpha}-1}{f-1}\right)}{R_{STD}} - 1\right) \cdot 1000 - \delta^{88/86}Sr_i \quad \text{Eq. III.7}$$

Where $\Delta^{88/86}Sr_{Rayleigh}$ is the predicted isotopic signal in corals' aragonite for a certain seawater temperature. The temperature is a variable in the remaining fraction parameter (*f*), which was determined by the Rayleigh based model (Gaetani et al., 2011). The fractionation factor α describes the isotopic difference between the bulk solution and the mineral. The model is using inorganic fractionation factors assuming that the calcification is inorganic precipitation from a finite reservoir. R_i ($^{88}Sr/^{86}Sr$: 8.37850±0.00002) and R_{STD} ($^{88}Sr/^{86}Sr$: 8.37520±0.00002) are the $^{88}Sr/^{86}Sr$ ratios in the initial bulk solution (we used seawater as the initial value) and in the

SRM987 standard, respectively. The initial value $\delta^{88/86}Sr_i$ corresponds to 0.39±0.02 being the isotopic signal in the initial bulk solution.

The remaining fraction (*f*) is the resulting parameter in the Rayleigh based model polynomial equation, which is a function of temperature (T in kelvins) (Gaetani et al., 2011).

$$f = c_1 + c_2(T)^{-1} + c_3 \cdot T + c_4 \cdot T^2 \quad \text{Eq. III.8}$$

The model manipulates *f* using c_1, c_2, c_3 and c_4 variables so that at each temperature the difference between the calculated elemental ratios ($M/Ca_{Rayleigh}$) and the measured elemental ratios ($M/Ca_{measured}$) in the coral will be the smallest possible (Eq. III.9), where M is a measured trace element. Since the model assumes that seawater is modified in the calcifying space, the multi-variables model (c_1, c_2, c_3, c_4, Ca_i and M_i) necessitate the use of several temperatures and multi element ratios.

$$\chi^2 = \sum \left(100 \cdot \left(\frac{M}{Ca_{Rayleigh}} - \frac{M}{Ca_{measured}} \right) \cdot \frac{Ca}{M_{measured}} \right) \quad \text{Eq. III.9}$$

We used *f* values obtained by modeling Sr/Ca and Mg/Ca of *Acropora* sp. specimens from Reynaud et al. (2007), and calculations based on Gaetani et al. (2011). We calculated $\Delta^{88/86}Sr_{Rayleigh}$ with the minimum and maximum inorganic aragonite α values (0.9997875 and 0.9998685) that were measured in our study.

Results

Temperature calibrations of the cores and correlation to $\Delta^{88/86}Sr$

Core TH1

We obtained good correlation of $\delta^{18}O$ between the current study results and the results of the adjacent slab that was measured by Cahyarini et al. (2008). Radiography of the slab did not show distinct density bands. Therefore, we determined the duration covered by the transect from the seasonal variations of the measured $\delta^{18}O$. However, since the definite period of the transect could not be reconstructed, we used the $\delta^{18}O$-temperature calibration that was obtained by

Cahyarini et al. (2008) to calculate temperature from $\delta^{18}O$ ($\delta^{18}O=0.67-0.19\cdot T(°C)$). We observed 4 high $\delta^{18}O$ peaks (low temperatures) and 5 low $\delta^{18}O$ peaks (high temperatures), which stand for 4.5 years of growth along the transect.

The $\delta^{88/86}Sr$ values were measured mainly on samples with high and low $\delta^{18}O$ peak values (Figure III.1). The $\delta^{88/86}Sr$ values show no correlation with $\delta^{18}O$ and temperature. The $\delta^{88/86}Sr$ results vary in a range of 0.04‰, which is within measurement uncertainty.

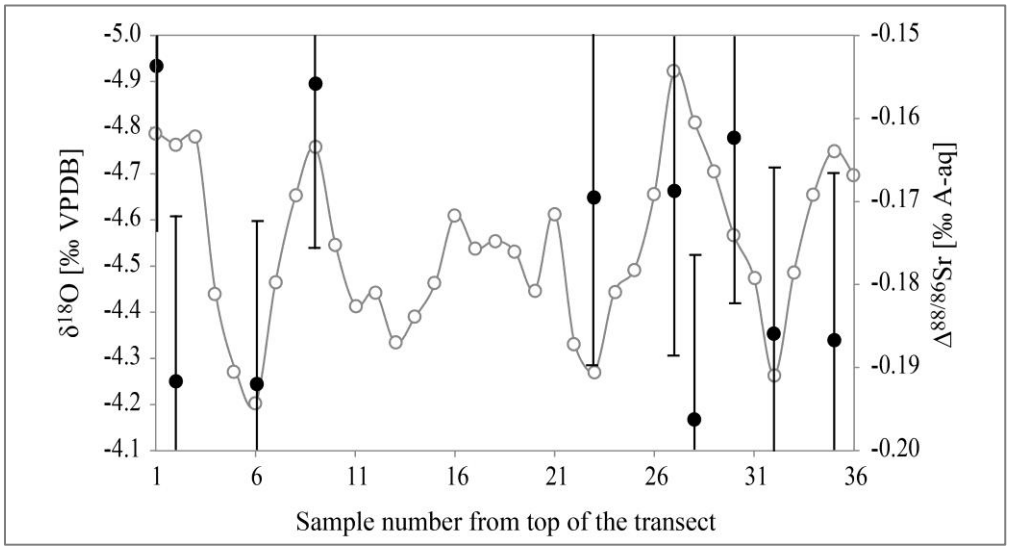

Figure III.1 Results of $\delta^{18}O$ and $\Delta^{88/86}Sr$ on a *Porites* sp. from Tahiti. The results are presented versus sample number from the top of the slab transect. The sampling was fairly equidistant. While $\delta^{18}O$ results display 4.5 annual cycles and correlate to the SST record from the area of the colony growth (Cahyarini et al., 2008), $\Delta^{88/86}Sr$ values show no seasonal cycling or systematic relationship to the $\delta^{18}O$ values.

Core SOT-1

All samples were collected along a transect following the main growth axis. The transect includes three low-density and four high-density bands showing seasonal cycles. One low-density/high-density band pair represents a full annual cycle. According to the seawater temperature data, the temperature in the Gulf of Aqaba ranges between 21°C in the winter and 27°C in the summer. The extreme values of Sr/Ca were assigned to the yearly seasonal extreme temperatures. The intermediate Sr/Ca values were added between the seasonal extremes as a linear function of their distance in the transect and the dates of the extreme temperature (Figure II.2a). The resulting correlation is $Sr/Ca=10.8\pm0.3-0.08\pm0.01\cdot T(°C)$ ($r^2=0.6$, $P=5.5\times10^{-5}$). Low Sr/Ca ratios were obtained from the samples that were taken from low density bands, and high Sr/Ca ratios were obtained from the samples that were taken from the high density bands.

Therefore low density bands were precipitated in high temperatures and the high density bands were precipitated in low temperatures corresponding to summer and winter season, respectively. This is in agreement to density bands of *Porites* sp. in this area at shallow depths (e.g. Klein and Loya, 1991; Rosenfeld et al., 2003).

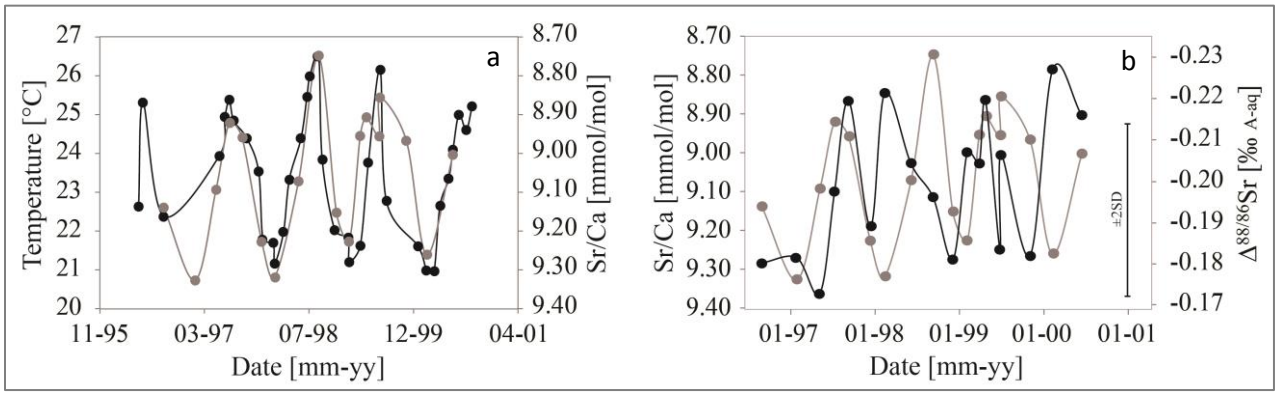

Figure III.2 Inverse correlation was found (a) between SST (black circles) and the measured Sr/Ca (gray circles), (Sr/Ca(mmol/mol)=10.8-0.8·T(°C) and R^2=0.6). No inferences can be made on the $\Delta^{88/86}$Sr-Sr/Ca relationship (b), since the measured variation of $\Delta^{88/86}$Sr values (black circles in (b)) is only slighty above reproducibility, i.e. all values are identical within statistical uncertainy.

The corresponding $\Delta^{88/86}$Sr results vary in an insignificant range of 0.05‰, and show no relationship to Sr/Ca (Figure II.2b), as the $\Delta^{88/86}$Sr-Sr/Ca relationship show a correlation coefficient in the order of about zero (R^2 ~0.001) indicating that there is no relationship of $\Delta^{88/86}$Sr to temperature at all.

Variations in $\Delta^{88/86}$Sr in cultured Acropora sp.

Sr/Ca ratio in the holding aquarium (pre-experiment conditions) was approximately two times lower than the Sr/Ca ratio of modern seawater used in the experimental chambers. This ratio difference is also reflected in the coral skeletons. The large differences between the pre-experimental Sr/Ca ratio and the experimental Sr/Ca ratio in the skeletons were used to detect the percentage of experimental skeleton in the sampled powders, i.e. to quantify mixing ratios of experimental and pre-experiment skeleton. Measured Sr/Ca results were compared to previous *Acropora* sp. studies (Gallup et al., 2006; Reynaud et al., 2007). Four of the Sr/Ca results in current study experiments fall on the Sr/Ca-temperature trend lines of previous studies, but large differences are observed in the three other experiments, which had the lowest total growths of

less than 8% (Figure III.3). The mixing ratio was calculated from a binary mixing line using the Sr/Ca-temperature relationships from previous studies (Gallup et al., 2006; Reynaud et al., 2007) as one end member and the Sr/Ca of the pre-experiment skeleton (2.99±0.02 mmol·mol^{-1}) as the second end member (Table III.3).

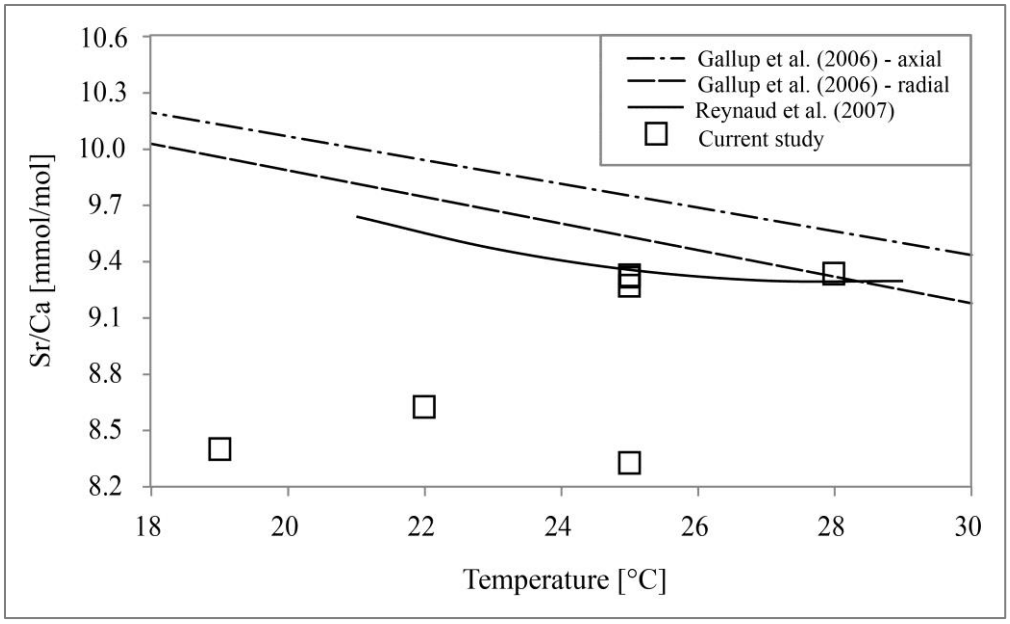

Figure III.3 Sr/Ca results of cultured *Acropora* sp. compared to the temperature of precipitation in the current study and in previous studies. Three experiments display significant differences from previous studies. The lower Sr/Ca is a result of contamination with pre-experimental skeleton, which grew in a solution that was depleted in Sr/Ca ratio

Similar to the Sr concentration, the corresponding isotope ratios in the pre-experiment skeleton were also significantly different from the expected range. The $^{87}Sr/^{86}Sr$ ratio of skeleton calcified during the experiment is expected to reflect the current $^{87}Sr/^{86}Sr$ seawater signal ($^{87}Sr/^{86}Sr$ of 0.70917(2), Krabbenhöft et al., 2009) but displayed significant variations that correlated well to the mixing ratio calculations based on Sr/Ca ratios (Figure III.4). Likewise, $\delta^{88/86}Sr$ in the pre-experiment skeleton (0.30‰±0.02) was found to be higher by 0.1‰ from the expected range of $\delta^{88/86}Sr$ values in corals that calcify from seawater (0.197±0.08‰ (2SEM) Krabbenhöft et al. (2009)). The mixing ratio values that were obtained from the Sr/Ca data calculations were used to correct the $\delta^{88/86}Sr$ in the samples. We used binaric mixing line of two end members; the pre-experiment $\delta^{88/86}Sr$ (0.30±0.02‰ of the control sample) and the experiment $\delta^{88/86}Sr$ (0.20±0.02‰ from the sample with 100% experimental skeleton in the sample powder).

Table III.3 *Acropora* sp. setup conditions and results. Standard deviation from the mean (2SD) are presented in parentheses in terms of least units cited

Sample Label	Temp. (°C)	CO_3^{-2} [a] (µmol/kg)	Meas. Sr/Ca (mmol/mol)	% of experiment skeleton from Gallup et al. (2006)[b]	% of experiment skeleton from Reynaud et al. (2007)[b]	$^{87}Sr/^{86}Sr$ normalized[c]	Corrected $\Delta^{88/86}Sr$ (‰ A-aq)[d]
N01	25	171 (13)	8.33	82 (2)	84 (2)	0.709158	-0.195
N02	25	212 (12)	9.32	97 (3)	100 (3)	0.709178	-0.159
N03	25	279 (15)	9.27	96 (3)	100 (3)	0.709199	-0.188
N04	25	352 (28)	9.33	97 (3)	100 (3)	0.709183	-0.187
N05	19	293 (25)	8.40	78 (2)	78 (2)	0.709149	-0.221
N06	22	309 (31)	8.63	83 (2)	85 (2)	0.709162	-0.202
N07	28	357 (34)	9.33	100 (3)	100 (3)	0.709165	-0.189
N08	Pre-experiment skeleton		2.99	0	0	0.708983	-0.302

[a] CO_3^{2-} was calculated from the measured TA and pH using CO_2Sys
[b] % of experiment skeleton in the sample was obtained from a mixing line calculation. Sr/Ca values from previous studies were used as the experiment Sr/Ca end member and N08 Sr/Ca as the pre-experiment end member.
[c] reproducibility of 11E-6 (2SD) according to JCP-1 measurements (n=10)
[d] reproducibility of 0.020‰ (2SD) according to JCP-1 measurements (n=10)

The corrected $\delta^{88/86}Sr$ results show a positive correlation trend of the $\Delta^{88/86}Sr$-temperature (Figure III.5a) relationship, where $\delta^{88/86}Sr = 0.004(\pm0.001)\cdot T(°C) - 0.28(\pm0.03)$ ($R^2=0.84$, P=0.084).

In the CO_3^{2-} experiments, (Figure III.5b) CO_3^{2-} varied significantly from 171±13 to 352±28 µmol·kg^{-1} (Table III.3). However, $\Delta^{88/86}Sr$ did not vary significantly, and no $\Delta^{88/86}Sr$-CO_3^{2-} relationship is observed.

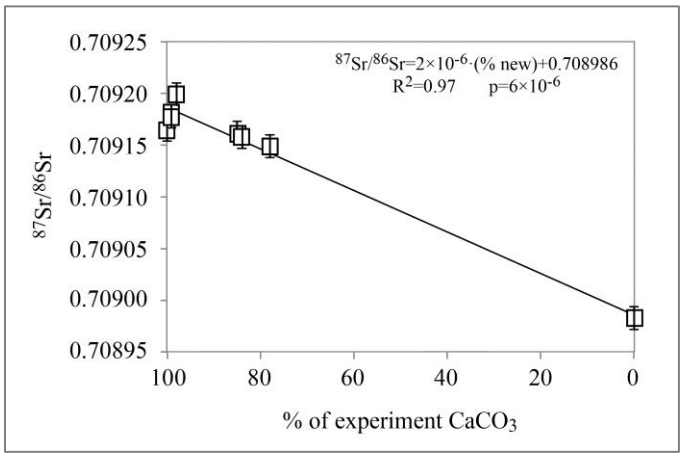

Figure III.4 $^{87}Sr/^{86}Sr$ in the *Acropora* sp. skeletons versus the amount of mixture between the pre-experiment and the experiment skeleton. The value at 0% was obtained from a sample containing only pre-experiment skeleton. Mixing ratios were calculated using Sr/Ca ratios (Table III.3). The good correlation ($R^2=0.97$) between the extent of mixing and $^{87}Sr/^{86}Sr$ is due to the significant differences in the pre-experiment and the experiment solution composition. It confirms that the mixing correction done on Sr/Ca through Reynaud et al., (2007) is accurate enough also for correcting the isotopic composition.

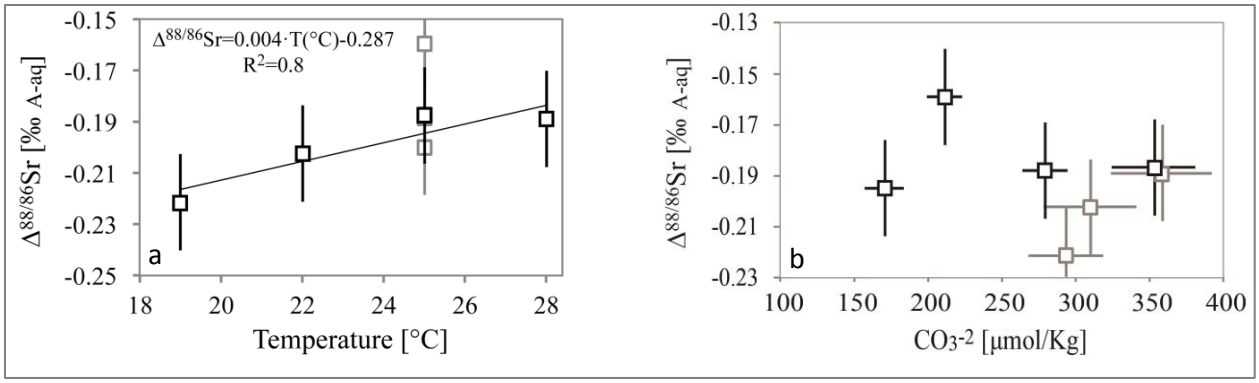

Figure III.5 $\Delta^{88/86}Sr$ variatios of cultured *Acropora* sp. with temperature (a) and with CO_3^{-2} (b). The black squares in (a) are the values of the samples from the temperature experiment and the grey squares represent the values of the samples in constant temperature but different CO_3^{2-} experiments. The black squares in (b) are the values of the samples from the CO_3^{2-} experiment and the grey squares represent the values of the samples in constant CO_3^{2-} but different temperature experiments. The $\Delta^{88/86}Sr$ shows a positive correlation with temperature, yet not significant (p=0.08). In the CO_3^{2-} concentration experiments three out of the four samples showed no significant variation, only one sample (212 µmol/mol of CO_3^{2-}) was significantly less fractionated than the other samples.

Temperature, extension rate and pCO_2 differences in Cladocora caespitosa

High extension rates samples of the 21°C and 23°C experiments have lower $^{88}Sr/^{86}Sr$ fractionation compared to the low extension rate samples from the same temperature experiment (Table III.4). Although the same observation is reoccurring in the two temperature experiments, the differences in $\Delta^{88/86}Sr$ are very small and are within the 2SD uncertainty (Figure, III.6). There is no temperature effect on $\Delta^{88/86}Sr$ as the variations between different temperatures experiments are smaller than the samples' reproducibility (2SD). Similarly, $\Delta^{88/86}Sr$ in the pCO_2 experiments we observe that both the 390 ppm experiment and the 701 ppm experiment resulted in similar $\delta^{88/86}Sr$ within the sample's reproducibility (2SD). However, comparable to the extension rates results observation in the temperature experiment, also increasing pH (and therefore increasing aragonite saturation state) causes a small decrease in $^{88}Sr/^{86}Sr$ fractionation. This may suggest on a decrease in Sr isotopes fractionation with the increasing calcification rates.

Different temperature and saturation states in inorganic aragonite

The results of $\Delta^{88/86}Sr$ in the inorganic aragonite seem to have an inverse relationship with temperature (Figure III.7a). Yet, the variations between different samples precipitated at the same temperature (but with different CO_2 diffusion rates) were as large as the variations between temperatures (Anova1 p=0.2). This observation is in contrast to a previous observation of Fietzke

and Eisenhauer (2006) of a slightly positive temperature trend (with a slope of 0.003‰·°C^{-1}) for $\Delta^{88/86}$Sr in inorganic aragonite precipitated in similar experiment using the same setup.

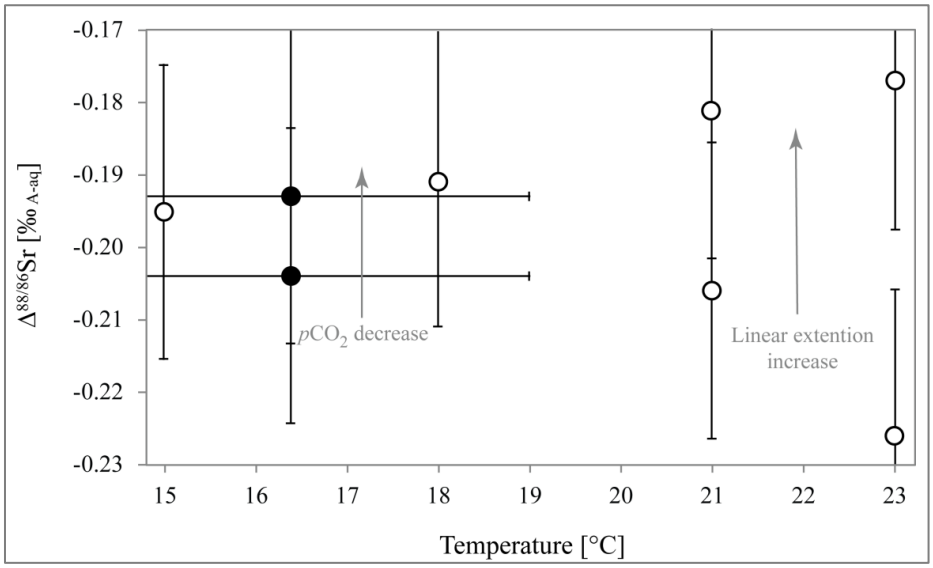

Figure III.6 $\Delta^{88/86}$Sr results of *Cladocora ceaspitosa* that was cultured at different temperatures and different pCO_2. The variations between the different experiment conditions fall within the 2SD. At 23°C we observe a significant difference between the specimens with low linear extention (more fractionated) and the specimens with high linear extention (less fractionated). Smaller fractionation is observed as the linear extention increases (in 21 and 23°C experiments). $\Delta^{88/86}$Sr in the two pCO_2 experiments (black circles) are insignificantly different. Nevertheless, the smaller $^{88}Sr/^{86}Sr$ fractionation in the ambient pCO_2 experiment compared to the fractionation in the high pCO_2 experiment is supporting the observation of less fractionation with the increasing calcification rate, as detected in the linear extention.

Table III.4 Results of *Cladocora caespitosa* experiments. Temperature and pCO2 results are reported with the standard deviation of the mean (2SD). The linear extension is reported with the standard error (1SE)

Sample Label	Temp. (°C)	pCO_2 (ppm)	Linear extension (mm)	Sr/Ca (mmol/mol)	$\Delta^{88/86}$Sr (‰ A-aq)[a]
Clad 15	15.00(0.05)	-	0.728(0.045)	9.20	-0.195
Clad 18	18.00(0.05)	-	1.305(0.060)	9.14	-0.191
Clad 21	21.00(0.05)	-	1.984(0.069)	8.90	-0.206
Clad 23	23.00(0.05)	-	1.283(0.055)	8.86	-0.226
Clad 21L	21.00(0.05)	-	>2.053	8.86	-0.181
Clad 23L	23.00(0.05)	-	>1.338	8.78	-0.177
Clad 400	16.4(2.6)	390(48)	N.A	9.08	-0.193
Clad 700	16.3(2.6)	701(78)	N.A	9.04	-0.204

[a] reproducibility of 0.020‰ (2SD) according to JCP-1 measurements (n=10)

Brucite, $Mg(OH)_2$, precipitated in some of the experiments since the inorganic aragonite precipitation was conducted using natural seawater with high Mg concentration and due to NaOH addition to the experimental solution to control the pH. We do not know the effect of brucite presence on the precipitation of aragonite and the Sr isotope fractionation that may be influenced from it. However, our measurements showed that Brucite contains approximately 5 ppm of Sr, and in the current study there was no more than a few percent of brucite from the total precipitated solid (up to 7%, according to FTIR measurements). Therefore we can assume that Sr in the solution was not reduced in significant amount due to brucite formation. Nevertheless, since the specific surface area of the brucite (40 $m^2 \cdot g^{-1}$ (Lee and Park, 2003)) is larger by 1.5 orders of magnitude from that of aragonite (0.8-2.4 $m^2 \cdot g^{-1}$ (Romanek et al., 2011)), it was not possible to determine the surface areas of the aragonite crystals. Consequently, the rate of precipitation was calculated without taking the surface area into consideration.

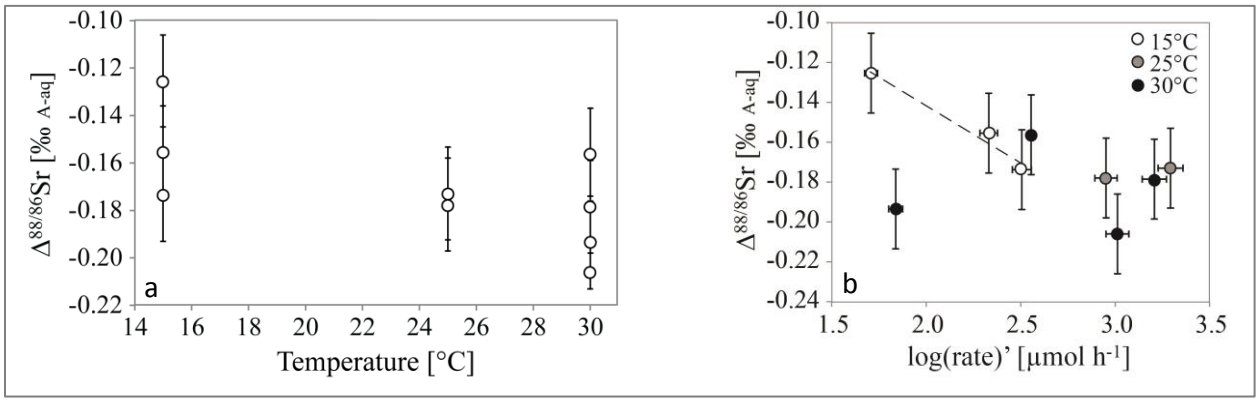

Figure III.7 $\Delta^{88/86}Sr$ in inorganic aragonite. The inverse trend with temperature (a) is insignificant compared to the variations at constant temperature (p=0.2). The variation within each temperature experiment represent different CO_2 diffusion rates, which within the conditions of the experiments, are causing different precipitation rates, as shown in plot (b). Plot (b) displays $\Delta^{88/86}Sr$ variations versus precipitation rates. The 15°C experiments (white circles) show a negative correlation to precipitation rates ($\Delta^{88/86}Sr$=-0.057(±0.010)·log(rate)-0.026(±0.022); R^2=0.97; P=0.11). At higher temperatures we did not detect a $\Delta^{88/86}Sr$-precipitation rate relationships.

The $\Delta^{88/86}Sr$-precipitation rate relationship ($\Delta^{88/86}Sr$=-0.057(±0.010)·log(rate)-0.026(±0.022); R^2=0.97; P=0.11) shows an inverse trend in the 15°C experiments (Figure III.7b), suggesting an increase in the amount of fractionation with increasing rates of precipitation. However, no trend was observed in the 30°C experiments that were more affected from the brucite formation.

Brucite formation was detected by FTIR and also in the Mg/Ca ratio in the solid, with Mg/Ca larger than ~4 mmol·mol^{-1} (Gabitov et al., 2008) indicating brucite presence in the solid. The positive correlation between Sr isotopes fractionation and precipitation rate in the 15°C experiments is in contrast to the results of *Cladocora caespitosa* experiments, in which we observed a decrease in fractionation with the increasing linear extension (that can be considered as an increase in precipitation rate).

$\Delta^{88/86}$Sr in coral aragonite predicted by to the Rayleigh based model

Our calculations on the Rayleigh based model show that $\Delta^{88/86}$Sr in corals is expected to be smaller by ~0.07‰ compared to inorganic aragonite (Table III.5). The model further predicts a slight (0.004‰·°C^{-1}) positive correlation of $\Delta^{88/86}$Sr with temperature. These model predictions are significantly different from the measured $\Delta^{88/86}$Sr in corals. While the change with temperature is very small in the model and is also not apparent in the measured corals samples, the differences between the predicted and measured ^{88}Sr/^{86}Sr fractionation values are significant (Figure III.8). The difference that we observe in ^{88}Sr/^{86}Sr fractionation between measured coral samples and the model calculations indicate a different process rather than Rayleigh fractionation that dominates coral skeleton calcification.

Table III.5 Rayleigh based model calculation for $\Delta^{88/86}$Sr in corals. Standard deviation of the mean (2SD) is reported in the parentheses in terms of least units cited

Temp. (°C)	f [a]	α=0.9997875[b] calculated $\Delta^{88/86}$Sr	α=0.99986847[b] calculated $\Delta^{88/86}$Sr	Average corals' $\Delta^{88/86}$Sr from the current study[c]
15	0.39	-0.108(10)	-0.088(10)	-0.201(20) n=1
20	0.27	-0.085(10)	-0.070(10)	-0.209(18) n=5
25	0.13	-0.052(20)	-0.042(20)	-0.191(20) n=6
30	0.06	-0.027(40)	-0.021(40)	-0.176(20) n=6

[a] molar fraction of the remaining Sr ions in the fluid (Eq. III.8)
[b] ^{88}Sr/^{86}Sr fractionation factors, α, were calculated form the inorganic aragonite experiments.
[c] Average for each temperature of all corals samples measured in the current study *Porites* sp., *Acropora* sp. and *Cladocora caespitosa*

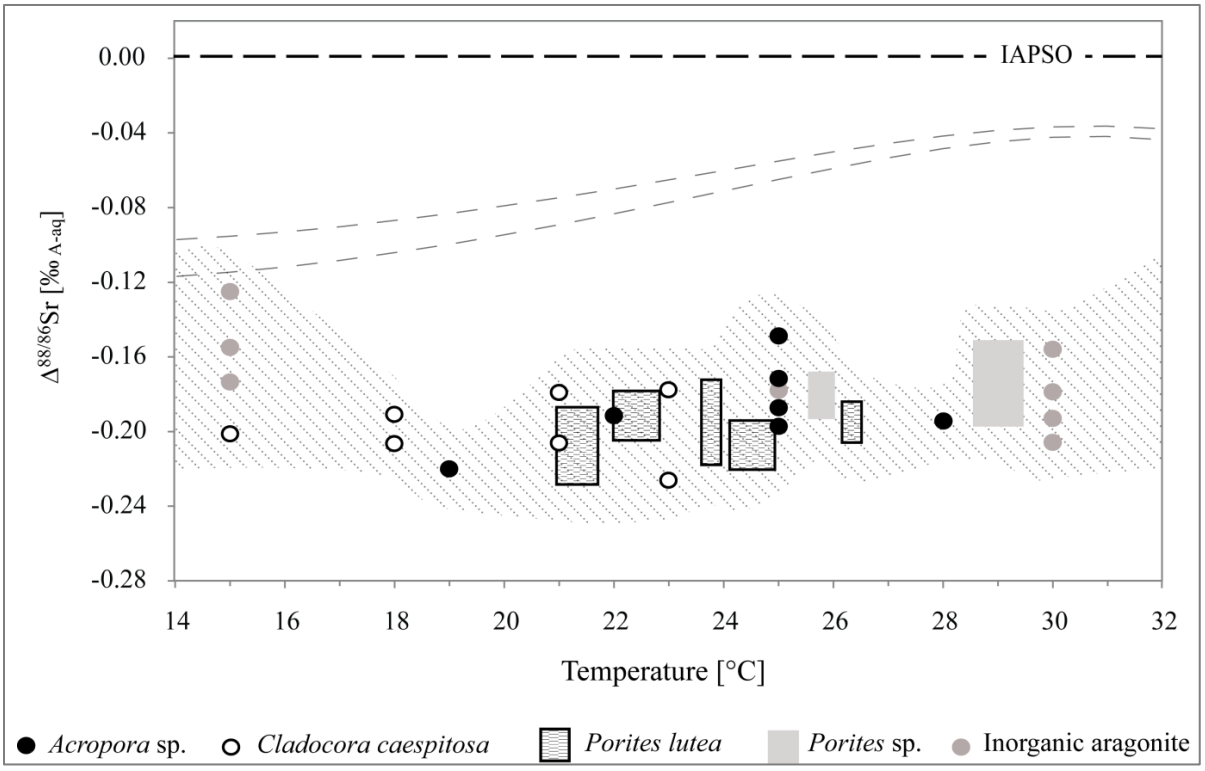

Figure III.8 $\Delta^{88/86}$Sr versus temperature in biogenic and inorganic aragonite from the current study. Fractionation from seawater compositon with preference for the light isotope is observed in both inorganic and biogenic aragonites (~0.2‰). The $\Delta^{88/86}$Sr values vary within a narrow range of 0.1‰, where different coral species and inorganic aragonite overlap. There is no observed temperature effect on $\Delta^{88/86}$Sr. The Rayleigh based model (Gaetani et al., 2011) predicts a smaller fractionation in corals compared to the inorganic aragonite (marked as two dashed grey lines). The two lines were calculated from the Rayleigh model using the maximum and minimum $^{88}Sr/^{86}Sr$ fractionation factors ($\alpha_{A/aq}$) in the inorganic aragonite experiments. Our results show that in contrast to the Rayleigh model there no significant difference between the inorganic and coral aragonite $^{88}Sr/^{86}Sr$ fractionation.

Discussion

The $^{88}Sr/^{86}Sr$ isotope ratio in aragonite shows a significant fractionation from its bulk solution; we observe this fractionation both in inorganic aragonite and coral aragonite (Figure III.8). The $^{88}Sr/^{86}Sr$ tends to incorporate the light isotope in the aragonite lattice resulting in an isotopic difference of about 0.2‰ relative to the bulk solution. The current study inorganic aragonite and the different coral species (*Acropora* sp., *Porites* sp. and *Cladocora caespitosa*) are in the same range of fractionation and do not show any significant differences between each other (Figure III.8).

In the current study we examined several different aragonite samples with temperature variations of up to 15 °C (inorganic aragonite experiments varied in temperatures between 15°C and 30°C).

The total $\delta^{88/86}$Sr variation in the inorganic aragonite samples is 0.08‰, and shows a weak inverse correlation with temperature. The $\delta^{88/86}$Sr variations within each temperature, which correspond to different precipitation rates, are almost as large as the variation in the 15°C range, resulting in obscuring the possible temperature correlation. We found a slight positive correlation between temperature and $\delta^{88/86}$Sr in *Acropora* sp. experiments. Nevertheless, the variations are very small (0.004‰·°C^{-1}) and comparable in magnitude to the analytical uncertainty (2SD of ±0.02) for the temperature range of 9°C in our experiments. The temperature trend was also not observed in the other coral samples. Fietzke & Eisenhauer (2006) found a positive correlation in both inorganic aragonite and in *Pavona clavus* corals. The change in $\delta^{88/86}$Sr with temperature in the corals was observed as 0.033‰·°C^{-1}, whereas in inorganic aragonite the slope was 0.005‰·°C^{-1} similar to our *Acropora* results. Large positive $\delta^{88/86}$Sr-temperature correlation was also observed by Rüggeberg et al. (2008) for a cold water coral, *Lophelia pertusa.* The current study as well as Krabbenhöft et al. (2010) and Raddatz et al. (2013) could not reproduce the large variations in $\delta^{88/86}$Sr in coral aragonite, nor their temperature correlation. Within the analytical uncertainty of ±0.02‰ (2SD) in $\delta^{88/86}$Sr in carbonates, a 0.005‰·°C^{-1} change over a 40°C temperature range that was observed in inorganic aragonite by Fietzke & Eisenhauer (2006), and an average 0.003‰·°C^{-1} change over 15°C from the current study are too small to detect changes in temperature within the narrow temperature range of corals' living environment (typically <10°C).

The results from the Rayleigh based model suggest that $\delta^{88/86}$Sr in corals' aragonite should be up to 0.15‰ less fractionated than open system inorganic aragonite (Figure III.8). $\Delta^{88/86}$Sr of the *Pavona clavus* (Fietzke and Eisenhauer, 2006) shows an increasing divergence from the fractionation values that are observed in the current study as the temperature increases. $^{88}Sr/^{86}Sr$ fractionation is significantly reduced in *Pavona clavus* with the increasing temperature, where in 27°C the observed $\Delta^{88/86}$Sr is -0.06‰ (Fietzke and Eisenhauer, 2006). Generally, the positive $\Delta^{88/86}$Sr – temperature correlation and the significant difference between inorganic aragonite results and the *Pavona clavus* may suggest that Rayleigh process dominates the coral's calcification process. However, the observed *Pavona clavus* $\Delta^{88/86}$Sr – temperature slope is much larger (0.033±0.005‰·°C^{-1}) than the moderate slope predicted by the Rayleigh model (approximately 0.004‰·°C^{-1}). Our data show that inorganic aragonite and corals' aragonite have

similar $\Delta^{88/86}$Sr. In our calculations we considered that the initial $\delta^{88/86}$Sr is similar to seawater composition (0.39±0.02‰). Gaetani et al. (2011), however, suggested that the initial composition of the bulk solution is slightly modified from seawater composition. In order to test the possibility that the corals' initial $\delta^{88/86}$Sr is modified from the normal seawater value, we calculated the initial $\delta^{88/86}$Sr in the bulk solution that will result in corals' aragonite with similar $\delta^{88/86}$Sr to inorganic aragonite. We obtained a range of $\delta^{88/86}$Sr in the bulk solution depending on temperature. The range between 0.317‰ in 15°C and 0.232‰ in 30°C is significant and implies that the ^{88}Sr/^{86}Sr fractionation in corals contradicts the Rayleigh based model.

A similar observation was discussed by Rollion-Bard et al. (2009) who found similar fractionation in Li isotopes between inorganic aragonite and corals' aragonite. While Li/Ca ratio follows Rayleigh based model, Li isotopes is unaffected by the Rayleigh fractionation. They explained Li isotopes disagreement with the Rayleigh fractionation model by the large reservoir of Li compared to its small incorporation in corals' skeleton. Case et al. (2010) proposed that Ca concentration variations in the calcifying fluid dominate the Rayleigh fractionation effect. For this reason, highly discriminated elements such as Mg and Li vary according to the Rayleigh fractionation of Mg/Ca and Li/Ca, but Li isotopes are not affected (Case et al., 2010). Sr, in contrast to Li, is not highly discriminated as the inorganic discrimination fractionation factor of Sr/Ca is close to unity. While Sr/Ca was shown to be strongly affected by the Rayleigh fractionation effect (Gaetani et al., 2011), Sr isotopes show similar behavior to Li isotopes and are in disagreement with the Rayleigh based model.

Conclusions

As was previously shown, both inorganic aragonite and coralline aragonite incorporate preferentially the light isotope (^{86}Sr) over the heavy isotope (^{88}Sr). We found that the fractionation of ^{88}Sr/^{86}Sr in inorganic aragonite is similar within statistical uncertainty to the fractionation in corals' aragonites. The fractionation from the bulk solution in both inorganic and corals' aragonite is 0.2‰.

Our data shows a total range of 0.08‰ in aragonite $\Delta^{88/86}$Sr values. Generally, the total range has significant variability. However, it appears that neither temperature nor precipitation rates

dominantly control these variations. This is in contrast to previous observations for temperature dependency in $\delta^{88/86}Sr$ in corals (Fietzke and Eisenhauer, 2006; Rüggeberg et al., 2008).

The $\delta^{88/86}Sr$ values from corals contradict the Rayleigh based model. The model predicts smaller $^{88}Sr/^{86}Sr$ fractionation in corals compared to open system inorganic aragonite due to the finite solution conditions. However, our data shows that inorganic aragonite precipitated in an open system conditions has similar $\Delta^{88/86}Sr$ as corals' aragonite.

Acknowledgments

We wish to thank Ana Kolevica, Regina Surberg, Andrea Wolf and Maria Hierz for supporting the lab work of this study. Funding support was provided through the European Marie Curie Initial Training Network "Calcification by Marine Organisms" (CalMarO) and the European Community's Seventh Framework Programme (FP7/2007-2013).

References

Beck J. W., Edwards R. L., Ito E., Taylor F. W., Recy J., Rougerie F., Joannot P. and Henin C. (1992) Sea-surface temperature from coral skeletal strontium/calcium ratios. *Science (80-.).* **257**, 644–7.

Cahyarini S. Y., Pfeiffer M. and Dullo W. C. (2009) Improving SST reconstructions from coral Sr/Ca records : multiple corals from Tahiti (French Polynesia). *Int. J. Earth Sci.* 31–40.

Cahyarini S. Y., Pfeiffer M., Timm O., Dullo W. C. and Schoenberg D. G. (2008) Reconstructing seawater δ18O from paired coral δ18O and Sr/Ca ratios: Methods , error analysis and problems , with examples from Tahiti (French Polynesia) and Timor (Indonesia). *Geochim. Cosmochim. Acta* **72**, 2841–2853.

Case D. H., Robinson L. F., Auro M. E. and Gagnon A. C. (2010) Environmental and biological controls on Mg and Li in deep-sea scleractinian corals. *Earth Planet. Sci. Lett.* **300**, 215–225.

Corrège T. (2006) Sea surface temperature and salinity reconstruction from coral geochemical tracers. *Palaeogeogr. Palaeoclimatol. Palaeoecol.* **232**, 408 – 428.

Dietzel M., Gussone N. and Eisenhauer A. (2004) Co-precipitation of Sr^{2+} and Ba^{2+} with aragonite by membrane diffusion of CO_2 between 10 and 50°C. *Chem. Geol.* **203**, 139–151.

Dodge R. E., Wyers S. C., Frith H. R., Knap A. H., Smith S. R., Cook C. B. and Sleeter T. D. (1984) Corals calcification rates by the buoyant weight technique: effect of alizarin staining. *J. Exp. Mar. Biol. Ecol.* **15**, 217–232.

Fallon S. J., McCulloch M. T., van Woesik R. and Sinclair D. J. (1999) Corals at their latitudinal limits: laser ablation trace element systematics in Porites from Shirigai Bay, Japan. *Earth Planet. Sci. Lett.* **172**, 221–238.

Fietzke J. and Eisenhauer A. (2006) Determination of temperature-dependent stable strontium isotope ($^{88}Sr/^{86}Sr$) fractionation via bracketing standard MC-ICP-MS. *Geochemistry Geophys. Geosystems* **7**.

Gabitov R. I., Gaetani G. A., Watson E. B., Cohen A. L. and Ehrlich H. L. (2008) Experimental determination of growth rate effect on U6+ and Mg2+ partitioning between aragonite and fluid at elevated U6+ concentration. *Geochim. Cosmochim. Acta* **72**, 4058–4068.

Gaetani G. A. and Cohen A. L. (2006) Element partitioning during precipitation of aragonite from seawater: A framework for understanding paleoproxies. *Geochim. Cosmochim. Acta* **70**, 4617–4634.

Gaetani G. A., Cohen A. L., Wang Z. and Crusius J. (2011) Rayleigh-based, multi-element coral thermometry: A biomineralization approach to developing climate proxies. *Geochim. Cosmochim. Acta* **75**, 1920–1932.

Gagnon A. C., Adkins J. F., Fernandez D. and Robinson L. (2007) Sr/Ca and Mg/Ca vital effects correlated with skeletal architecture in a scleractinian deep-sea coral and the role of Rayleigh fractionation. *Earth Planet. Sci. Lett.* **261**, 280–295.

Gallup C. D., Olson D. M., Edwards R. L., Gruhn L. M., Winter A. and Taylor F. W. (2006) Sr/Ca-Sea surface temperature calibration in the branching Caribbean coral Acropora palmata. *Geophys. Res. Lett.* **33**, 2–5.

Halicz L., Segal I., Fruchter N., Stein M. and Lazar B. (2008) Strontium stable isotopes fractionate in the soil environments? *Earth Planet. Sci. Lett.* **272**, 406–411.

Kaspar J., Trovarelli A., Zamoner F., Farnetti E. and Graziani M. (1991) Chemoselective Reduction of Enones to Allylic Alcohols, in: Studies in Surface Science and Catalysis Volume 59. p. 257.

Klein R. and Loya Y. (1991) Skeletal growth and density patterns of two Porites corals from the Gulf of Eilat , Red Sea. *Mar. Ecol. Prog. Ser.* **77**, 253–259.

Krabbenhöft A., Eisenhauer A., Böhm F., Vollstaedt H., Fietzke J., Liebetrau V., Augustin N., Peucker-Ehrenbrink B., Müller M. N., Horn C., Hansen B. T., Nolte N. and Wallmann K. (2010) Constraining the marine strontium budget with natural strontium isotope

fractionations ($^{87}Sr/^{86}Sr^*$, $\delta^{88/86}Sr$) of carbonates, hydrothermal solutions and river waters. *Geochim. Cosmochim. Acta* **74**, 4097–4109.

Krabbenhöft A., Fietzke J., Eisenhauer A., Liebetrau V., Böhm F. and Vollstaedt H. (2009) Determination of radiogenic and stable strontium isotope ratios ($^{87}Sr/^{86}Sr$; $\delta^{88/86}Sr$) by thermal ionization mass spectrometry applying an $^{87}Sr/^{84}Sr$ double spike. *J. Anal. At. Spectrom.* **24**, 1267.

Lee M. H. and Park D. G. (2003) Preparation of MgO with high surface area, and modification of its pore characteristics. *Bull. Korean Chem. Soc.* **24**, 1437–1443.

Lewis E. and Wallace D. W. R. (1998) Program Developed for CO2 System Calculations.

Marshall J. F. and McCulloch M. T. (2002) An assessment of the Sr/Ca ratio in shallow water hermatypic corals as a proxy for sea surface temperature. *Geochim. Cosmochim. Acta* **66**, 3263–3280.

Mitsuguchi T., Matsumoto E., Abe O., Uchida T. and Isdale P. J. (1996) Mg/Ca Thermometry in Coral Skeletons. *Science (80-.).* **274**, 962–963.

Montagna P., Correa López M., Rüggeberg A., McCulloch M. T., Rodolfo-Metalpa R., Ferrier-Pagès C., Freiwald A., Goldstein S. L., Henderson G. M., Mazzoli C., Russo S., Silenzi S., Taviani M. and Trotter J. (2009) Li/Mg ratios in shallow and deep-sea coral exoskeleton as a new temperature proxy. *AGU Fall Meet. 14-18 December, 2009, San Fr. USA*.

Raddatz J., Liebetrau V., Rüggeberg A., Hathorne E. C., Krabbenhöft A., Eisenhauer A., Böhm F., Vollstaedt H., Fietzke J., López Correa M., Freiwald A. and Dullo W.-C. (2013) Stable Sr-isotope, Sr/Ca, Mg/Ca, Li/Ca and Mg/Li ratios in the scleractinian cold-water coral Lophelia pertusa. *Chem. Geol.* **352**, 143–152.

Reynaud S., Ferrier-Pagès C., Meibom A., Mostefaoui S., Mortlock R., Fairbanks R. and Allemand D. (2007) Light and temperature effects on Sr/Ca and Mg/Ca ratios in the scleractinian coral Acropora sp. *Geochim. Cosmochim. Acta* **71**, 354–362.

Rollion-Bard C., Vigier N., Meibom A., Blamart D., Reynaud S., Rodolfo-Metalpa R., Martin S. and Gattuso J.-P. (2009) Effect of environmental conditions and skeletal ultrastructure on the Li isotopic composition of scleractinian corals. *Earth Planet. Sci. Lett.* **286**, 63–70.

Romanek C. S., Morse J. W. and Grossman E. L. (2011) Aragonite Kinetics in Dilute Solutions. *Aquat. Geochemistry* **17**, 339–356.

Rosenfeld M., Yam R., Shemesh A. and Loya Y. (2003) Implication of water depth on stable isotope composition and skeletal density banding patterns in a Porites lutea colony: results from a long-term translocation experiment. *Coral Reefs* **22**, 337–345.

Rüggeberg A., Fietzke J., Liebetrau V., Eisenhauer A., Dullo W. C. and Freiwald A. (2008) Stable strontium isotopes (δ88/86Sr) in cold-water corals — A new proxy for reconstruction of intermediate ocean water temperatures. *Earth Planet. Sci. Lett.* **269**, 570–575.

Schmidt G. A. (1999) Error analysis of paleosalinity calculations. *Paleoceanography* **14**, 422–429.

Trotter J., Montagna P., McCulloch M. T., Silenzi S., Reynaud S., Mortimer G., Martin S., Ferrier-Pagès C., Gattuso J.-P. and Rodolfo-Metalpa R. (2011) Quantifying the pH "vital effect" in the temperate zooxanthellate coral Cladocora caespitosa: Validation of the boron seawater pH proxy. *Earth Planet. Sci. Lett.* **303**, 163–173.

Watanabe T., Minagawa M., Oba T. and Winter A. (2001) Pretreatment of coral aragonite for Mg and Sr analysis: Implications for coral thermometers. *Geochem. J.* **35**, 265–270.

Weber J. N. and Woodhead P. M. J. (1972) Temperature dependence of oxygen-18 concentration in reef coral carbonates. *J. Geophys. Res.* **77**, 463.

Wiechers H. N. S., Sturrock P. and Marais G. V. R. (1975) Calcium carbonate crystallization kinetics. *Water Res.* **9**, 835–845.

Zeebe R. E. and Wolf-Gladrow D. A. (2001) *CO_2 in seawater: equilibrium, kinetics, isotopes*. Elsevier Oceanography Series, Elsevier.

CHAPTER IV. KINETIC CONTROL ON $^{44}Ca/^{40}Ca$ INCORPORATION IN CORALS ARAGONITE

Noa Fruchter[1*], Anton Eisenhauer[1], Martin Dietzel[2], Jan Fietzke[1], Florian Böhm[1], Andrea Niedermayr[3], and Jonathan Erez[4]

[1] *GEOMAR, Helmholtz-Zentrum für Ozeanforschung Kiel, Wischhofstr. 1-3, 24148 Kiel, Germany*

[2] *TU Graz Institute of Applied Geosciences. Graz University of Technology. 8010 Graz, Austria*

[3] *Ruhr University Bochum, Universitätsstraße 150, 44801 Bochum, Germany*

[4]*The Hebrew University, The Edmond J. safra Campus Givat Ram Jerusalem, Israel*

[*]*Current address: Geological Survey of Israel, Malkhei Israel 30 Jerusalem, Israel*

In preparation, to be submitted to *Geochimica et Cosmochimica Acta*

Abstract

We observe a strong kinetic effect on Ca incorporation in aragonite. This effect is observed in both inorganic aragonite and in corals. As the rate of precipitation increases the isotope fractionation decreases ($^{44}Ca/^{40}Ca$). At high precipitation rates above ~$10^{4.0}$ $\mu mol \cdot m^{-2} \cdot h^{-1}$ the fractionation becomes constant in a minimum fractionation point. Since corals calcify at high rates of $10^{3.9}$ $\mu mol \cdot m^{-2} \cdot h^{-1}$ and above, no rate effect on Ca isotopes fractionation is expected. Ionic strength appears to have insignificant effect on Ca incorporation of inorganic aragonite. We hypothesize that Ca isotope fractionation in corals is controlled by the saturation state in the extracellular fluid and the rate of calcification.

Introduction

Scleractinian corals are major marine calcifiers. Their aragonite skeleton calcifies from the marine solution while incorporating trace elements and isotopes to the skeleton. The elemental ratios and isotopes incorporation differences between coral and inorganic aragonite is termed "vital effect", and is attributed to the biological control of the organism on the skeleton precipitation. However, not much is known on the pathways and processes of elements and isotopes incorporation into the skeletons and the deviation of the measured ratios from the expected thermodynamic equilibrium. Several studies proposed that a significant Ca contribution to the calcification fluid in corals occurs through an active transport via the so called "transcellular pathway" (Krishnaveni et al., 1989; Tambutté et al., 1996; Clode and Marshall, 2002b). In this mechanism, ions are being transported through the cytoplasm of the calicoblastic cells to the extracellular calcifying fluid (ECF), which is located in the transition zone between cell layer and forming skeleton. This transport is active and is aided by designated enzymes that transport specific ions, such as Ca^{2+}ATPase for Ca^{2+} transport, through the cells. An additional transport mechanism called "paracellular transport" is proposed in other studies (Erez and Braun, 2007; Gagnon et al., 2012; Tambutté et al., 2012). This mechanism suggests a passive seawater transport to the ECF via diffusion that occurs due to chemical gradient between the calicoblatic cells. Although many studies have discussed the mechanisms of transport to the ECF, the role and importance of transcellular and paracellular mechanisms is still unclear. In particular, the process of Ca incorporation in the skeleton is unresolved, as it is not yet certain whether Ca

reaches the ECF through Ca^{+2}ATPase transport or by a passive transport of seawater, or rather by a combination of both possible mechanisms.

Recently, as analytical improvements were made, it became possible to detect small variations in natural fractionation processes of non-traditional stable isotopes, including the isotopes of Ca. The fractionation of Ca isotopes in coral is reported to be significantly different from fractionation in inorganic marine carbonate and aragonite specifically (Böhm et al., 2006). Ca isotope fractionation values in corals range from $\Delta^{44/40}Ca_{coral\text{-}sw}$=-0.7‰ (Halicz et al., 1999) to $\Delta^{44/40}Ca_{coral\text{-}sw}$=-1.2‰ (Böhm et al., 2006). The range of Ca isotope fractionation in inorganic marine carbonates is distinctively larger, as calcite is averagely $\Delta^{44/40}Ca_{calcite\text{-}sw}$=-0.84‰ (Tang et al., 2008), and aragonite has higher fractionation of approximately $\Delta^{44/40}Ca_{aragonite\text{-}sw}$=-1.5‰ (Gussone et al., 2003). Hence, there is a significant difference in Ca isotope values between corals and inorganic aragonite, which is commonly attributed to the so called "vital effect". A previous study suggested a positive temperature dependency on Ca isotope fractionation in corals (Böhm et al., 2006). They found a 0.020±0.015‰·°C^{-1} dependency which is very small compared to the reported uncertainty (0.1‰ 2σ), and corresponding to a temperature resolution in the order of 5°C. To our knowledge no other systematic study on the temperature dependency of $\Delta^{44/40}$Ca in corals with a sufficiently large temperature range has been published so far. The observed variation of $\Delta^{44/40}$Ca in natural and cultured corals is approximately 0.3 to 0.6‰ (Chang et al., 2004; Böhm et al., 2006; Pretet et al., 2013), which would correspond to an unreasonable temperature variation of 15 to 30°C when using the suggested temperature dependency. This clearly shows that additional factors other than temperature contribute significantly to calcium isotope variability in corals (Pretet et al., 2013). Since temperature variations cause variations in precipitation rates, it can be assumed that other factors that control the precipitation rate may control the Ca isotopes incorporation in aragonite.

Only one study was published on the relationship between Ca isotopes fractionation and precipitation rate in aragonite (Gussone et al., 2005). In calcite, however, several studies described the dependency of Ca isotopes on precipitation rates (Lemarchand et al., 2004; Tang et al., 2008; DePaolo, 2011). Lemarchand et al. (2004) observed decreasing isotope fractionation as a function of increasing precipitation rate, whereas Tang et al. (2008) demonstrate an increasing Ca isotope fractionation as a function of increasing precipitation rates. These two observations of

Lemarchand et al. (2004) and Tang et al. (2008) are discrepant and still pending an explanation. Similar to the calcite observation of Lemarchand et al. (2004), Gussone et al. (2005) observed a decrease in Ca isotopes fractionation with the increasing precipitation rate in aragonite. Böhm et al. (2006) combined the inorganic calcite data of Lemarchand et al. (2004) and inorganic aragonite data of Gussone et al. (2005) in order to explain the observed offset in $\Delta^{44/40}$Ca between corals and inorganic aragonite. Using the available data sets, they excluded precipitation rate as a significant factor controlling Ca isotope incorporation in the zooxanthellae corals *Porites, Acropora and Pavona*. Moreover, Böhm et al. (2006) and Pretet et al. (2013) compared Ca isotopes from layers of *Porites* skeletons grown with different extension rates (varying by a factor of 5) and found no significant differences.

Recent study (Niedermayr et al., in preparation) performed inorganic aragonite precipitation experiments using the CO_2 diffusion technique (Dietzel et al., 2004), similar to the method used by Tang et al., (2008) for calcite precipitation. The results show an inverse relationship between precipitation rates and Ca isotopes fractionation, similar to the observations of the earlier aragonite study (Gussone et al., 2005). The sufficiently large data set of Ca isotopes in inorganic aragonite may be helpful to understand the differences of Ca isotopes incorporation in corals compared to inorganic precipitation. In the current study we compare $\Delta^{44/40}$Ca data of natural seawater aragonite precipitation experiments with artificial solution aragonite precipitation experiments from previous, published and unpublished, studies. We compare this data with $\Delta^{44/40}$Ca of cultured *Acropora* sp. corals in order to better understand the factors controlling Ca isotopes incorporation in inorganic and biogenic aragonite.

Methods

Experimental setup

Inorganic aragonite

Inorganic aragonite precipitation experiments were conducted at the University of Technology in Graz, Austria from natural seawater using the CO_2 diffusion technique as described in detail in Dietzel et al. (2004). In this technique CO_2 diffuses from an inner solution to an outer solution via poly-ethylene (PE) membrane (we used two different membranes

thickness, 0.02 mm or 2 mm thick). The inner solution consists of 35 grams of $NaHCO_3$ in a 0.5 l solution at pH 7.5, and has a higher pCO_2 than the outer solution. In order to increase the pCO_2 in some experiments we added 10 ml of 1N HCl to the inner solution. We applied three different temperatures (15°C, 25°C and 30°C) and several precipitation rates (40-1260 $\mu mol \cdot h^{-1} \cdot m^{-2}$) in 6 experiments. Each experiment was conducted in 5 l of seawater as the outer solution, from which the $CaCO_3$ precipitates. The seawater with salinity of $40.7 g \cdot kg^{-1}$ was collected during cruise P408 in the Red Sea (19.09°N 39.49°E, 1000m) with Niskin bottles mounted onto a CTD-rosette device in February 2011. The seawater solution was filtered in Sartobram P. sterile MidiCap double filter of 0.45 μm and 0.2μm. A 'Pt 1000' temperature sensor was used to monitor the temperature of the external water bath, which was kept constant using thermostatic water bath (Julabo HC E07 F18 or Huber ministat 230 CCC2). A constant pH level of 8.30±0.03 was maintained during the experiment using 0.5 N NaOH titration (Schott Titroline alpha plus titrators), and an attached pH electrode (Blueline 28 pH) to monitor the experimental water pH. Rate of precipitation is reported in $\mu mol \cdot m^{-2} \cdot h^{-1}$.

$$R = \left([Ca]_i - [Ca]_f\right) \cdot V \cdot \Delta t^{-1} \cdot A^{-1} \qquad \text{Eq. IV.1}$$

Where $[Ca]_i$ and $[Ca]_f$ are the Ca concentration in the initial and the final solutions, respectively, V is the volume of the solution, Δt is the duration of the precipitation and A is the measured surface area of the solid. The specific surface area of the precipitates (A) was measured using Brunauer Emmett Teller (BET) gas adsorption method at the University of Bochum. Helium-nitrogen gas mixture was used in Micromeritics Flowsorb II 2300, which is designated for surface area measurements.

Since Ca concentrations decreased during the experiments by up to ~28% compared to its concentration in the initial solution, the Ca isotope fractionation values had to be corrected for this depletion. The depletion is causing a Rayleigh distillation effect of the precipitating ions. The calculation for the true $\Delta^{44/40}Ca$ in the aragonite samples was done using the Rayleigh process equation combined with of the measured Δ approximation as described in equation 3.1.17 and page 146 from Zeebe and Wolf-Gladrow (2001)

$$f = \left(\frac{[Ca]_{fs}}{[Ca]_{is}}\right)$$ Eq. IV.2

$$\alpha = \frac{ln\left(\Delta^{44/40}Ca_{meas} \cdot f/_{1000} - \Delta^{44/40}Ca_{meas}/_{1000} + f\right)}{ln(f)}$$ Eq. IV.3

$$\Delta^{44/40}Ca_{True} = (\alpha - 1) \cdot 1000$$ Eq. IV.4

f is the remaining fraction in the fluid and $[Ca]_{fs}$ and $[Ca]_{is}$ are the Ca concentration in the final and initial solution, respectively. α is the fractionation factor.

Corals experiments

Acropora sp. mini colonies were cultured in the department of Earth Sciences at the Hebrew University of Jerusalem, Israel. The specimens were collected from one mother colony several weeks prior to the beginning of the experiments. They were attached to an epoxy base and were placed back in the main laboratory aquarium for recovery. Before the beginning of the experiments the specimens were stained in 15 ppm solution of Alizarin-Red S (Dodge et al., 1984) for seven hours. During the experiment each coral specimen was placed for seven weeks in a 220 ml clear chamber supplied with 19 ml seawater per hour. Red Sea seawater was collected from the pier at the Interuniversity Institute for Marine Sciences in Eilat (IUI) and diluted, for the experiment, to 37g·kg^{-1}. The flow-through system had residence time of 12 hours while constantly stirred in the chamber using a magnetic stirrer. Light was supplied at illumination of 200±10 μmol photons·m^{-2}·s^{-1} through metal-halide lamps in 12 hours dark/light cycles. Temperature was kept constant in all tanks using heaters or a refrigerating system connected to electronic controllers with a precision of ±0.3°C. The seven different experiments varied in temperatures (19.0±0.3°C, 22.0±0.3°C, 25.0±0.3°C and 28.0±0.3°C) and aragonite saturation states, Ω (2.45±0.38, 2.99±0.33, 3.92±0.43 and 4.89±0.67). The saturation state experiments were carried out at 25±0.3°C. Different saturation states were set by adding different amounts of 1N HCl to each of the saturation experimental reservoir water. Using the pH and alkalinity measurements of the reservoir solution the saturation states of the initial condition were determined (Table IV.1) in CO_2Sys (Lewis and Wallace, 1998).

The pH and total alkalinity (TA) of the water source solutions (reservoirs) were monitored on a weekly basis. The pH was measured with 'pHM 64 Research pH meter' (Radiomter Copenhagen, Denmark) that was calibrated by pH7.000 and pH10.012 buffers (Radiometer Analytical). Alkalinity of the reservoir water was determined by Gran titration using a Metrohm DMS Titrino. The pH calibration of the titrator was done using pH7.000 and pH10.012 buffers (Radiometer Analytical), a certified reference standard was used as secondary standard for alkalinity calibration (CRM; distributed by A. Dickson, Scripps Institution of oceanography (SIO)).

Table IV.1 Parameters and $\Delta^{44/40}$Ca results of *Acropora* sp. and inorganic aragonite precipitation experiments

Sample	Temperature [°C]	pH	Alkalinity [$\mu eq \cdot l^{-1}$]	Ω	Rate [$\mu mol \cdot m^{-2} \cdot h^{-1}$]	$\Delta^{44/40}$Ca [‰ A-sw]
			***Acropora* sp.**			
Ac01	25	7.91±0.04	2038.8±22.4	2.45±0.38	$10^{3.88\pm0.01}$	-1.27±0.12
Ac02	25	8.01±0.03	2094.0±8.5	2.99±0.33	$10^{3.90\pm0.01}$	-1.48±0.02
Ac03	25	8.14±0.03	2190.0±21.9	3.92±0.43	$10^{3.94\pm0.02}$	-1.02±0.03
Ac04	25	8.26±0.05	2268.0±2.4	4.89±0.67	$10^{3.97\pm0.02}$	-1.03±0.43
Ac05	19	8.25±0.05	2271.0±2.5	4.05±0.72	$10^{3.94\pm0.02}$	-1.13±0.09
Ac06	22	8.23±0.06	2271.9±4.3	4.31±0.85	$10^{3.95\pm0.02}$	-1.17±0.18
Ac07	28	8.22±0.06	2264.8±5.2	5.02±0.90	$10^{3.98\pm0.02}$	-1.17±0.19
				Mean:	$\mathbf{10^{3.94\pm0.02}}$	**-1.18±0.15**
			Inorganic aragonite			
IA01	25	8.30±0.03	-	-	$10^{1.8\pm0.1}$	-1.54±0.01
IA02	30	8.30±0.03	-	-	$10^{2.0\pm0.1}$	-1.44±0.04
IA03	30	8.30±0.03	-	-	$10^{3.1\pm0.1}$	-1.43±0.13
IA04	15	8.30±0.03	-	-	$10^{2.3\pm0.1}$	-1.62±0.27
IA05	15	8.30±0.03	-	-	$10^{1.6\pm0.1}$	-1.61±0.07
IA06	15	8.30±0.03	-	-	$10^{2.8\pm0.1}$	-1.53±0.40
				Mean:	$\mathbf{10^{2.3\pm0.1}}$	**-1.53±0.15**

In addition, 50 ml of water samples of the reservoirs and the outflow solutions (representing the total duration of the experiments) were collected for geochemical analyses. Once in 10 days, during the experiment, the corals specimens were fed with *Artemia* sp. in an external 5 l vessel for 1 hour. While feeding, algae growth was removed from the experiment chambers.

The experiments were terminated after seven weeks. The corals skeletons were separated from their tissue using an air-brush followed by bleach in 1% NaClO and wash in double deionized water (DDW). Powder for isotopic analyses was collected from the specimens epoxy's surface, that contained only new skeleton that calcified during the experiments.

No Rayleigh effect corrections were needed for the *Acropora* sp. experiments since less than 5% of the Ca in the water was used.

Analytical measurement

Aragonite samples were dissolved in 2.25N HCl for $^{44}Ca/^{40}Ca$ measurements. A $^{43}Ca/^{48}Ca$ double spike was added to the solution of both dissolved aragonite samples and seawater samples. Seawater samples were purified with a cation-exchange- chromatography column prior the analyses following the protocol described in Heuser et al. (2002), whereas the carbonate samples were measured without the chromatograph treatment, since Böhm et al. (2007) found the chromatograph treatment unnecessary in case of carbonate samples.

The $^{44}Ca/^{40}Ca$ ratios were measured in a TRITON thermal ionization mass spectrometer (TIMS, Thermo-Fisher) at GEOMAR using the $^{43}Ca/^{48}Ca$ double spike technique (Heuser et al., 2002). The results are reported relative to the calcium carbonate reference material NIST SRM 915a. The analytical uncertainty for $\delta^{44/40}Ca$ is expressed as two standard deviations (±2σ) determined by measurements repeat from the same sample solution.

$$\delta^{44/40}Ca[‰] = \left(\frac{{}^{44}Ca/{}^{40}Ca_{CaCO_3}}{{}^{44}Ca/{}^{40}Ca_{SRM\ 915a}} - 1\right) \cdot 1000 \qquad \text{Eq. IV.5}$$

$$\Delta^{44/40}Ca[‰] = \delta^{44/40}Ca_{Sample} - \delta^{44/40}Ca_{Solution} \qquad \text{Eq. IV.6}$$

Acropora sp. $\delta^{44/40}Ca$ are reported relative to the Gulf of Eilat seawater ($\delta^{44/40}Ca_{seawater}$= 1.84±0.08‰) reported in Kısakürek et al. (2011), and are similar within 2σ to our IAPSO measurements (1.82±0.15‰). The $\delta^{44/40}Ca$ value in the inorganic aragonite samples are reported relative to the measured initial Red-Sea value (2.07±0.17‰), which is slightly higher than the reported IAPSO value but still within the reported 2σ standard deviation.

Results

We observe a general positive temperature - $\Delta^{44/40}$Ca correlation (R^2=0.78, p=0.02) in inorganic aragonite. In contrast, the coral aragonite $\Delta^{44/40}$Ca data do not show any correlation to temperature. In particular, at the same temperature the coral´s Ca isotope values tend to be higher when compared to the inorganic aragonite (Anova $p=5\times10^{-4}$; Table IV.1). From the values in Table IV.1 we can calculate a mean $\Delta^{44/40}$Ca difference of 0.4±0.2‰ between inorganic and coral aragonite. This follows the earlier general observation that Ca isotopes in corals are apparently less fractionated by about 0.4 to 0.5‰ than in inorganic aragonite at the same temperature (Böhm et al., 2006). The rates of coral aragonite precipitation are another varying parameter in the inorganic aragonite experiments. Corals calcification rates in this study ($10^{3.9}$-$10^{4.0}$ $\mu mol \cdot m^{-2} \cdot h^{-1}$) were estimated using the correlation between saturation state and calcification rate (Leclercq et al., 2000). The estimated calcification rates of the corals are ~100 times higher than the inorganic aragonite experiments (Table IV.1). From observing these two precipitation rates groups (corals and inorganic aragonite), it appears that higher precipitation rates correspond to lower Ca isotope fractionation.

Discussion

Temperature - $\Delta^{44/40}$Ca correlation in aragonite

In the current study, inorganic aragonite precipitated from seawater falls within the $\Delta^{44/40}$Ca – temperature trend line of Gussone et al. (2003) (Figure IV.1) who found a positive correlation with a slope of $0.01‰ \cdot °C^{-1}$. However, temperature is not the exclusive varying parameter in the experiments (Gussone et al., 2005). Their temperature experiments also varied in CO_3^{-2} concentration and saturation states. The CO_3^{2-} variations are reported to be independent of the temperature - CO_3^{2-} concentration relationship (Gussone et al., 2005). Therefore, $\Delta^{44/40}$Ca variation in Gussone et al. (2005) are caused by temperature and precipitation rates variations. A later study observed large $\Delta^{44/40}$Ca variations in inorganic aragonite of the same temperature (Niedermayr, 2011). The variations at constant temperature but different precipitation rates are clearly larger than the total temperature trend by Gussone et al. (2003) (Anova1 p=0.08). In addition to weakening the $\Delta^{44/40}$Ca – temperature trend in inorganic aragonite, these results (Niedermayr, 2011) overlap with $\Delta^{44/40}$Ca data of corals aragonite at the same temperature. It

was previously reported that Ca isotopes in inorganic aragonite are approximately 0.5‰ more fractionated compared to coral aragonite (Böhm et al., 2006). *Acropora* sp. $\Delta^{44/40}$Ca values of the current study are similar to the *Acropora* sp., *Pavona clavus* and *Porites* sp. from Böhm et al. (2006) study. However, when plotting the corals' $\Delta^{44/40}$Ca with inorganic aragonite $\Delta^{44/40}$Ca of Niedermayr (2011) as a function of temperature (Figure IV.1), some inorganic aragonite $\Delta^{44/40}$Ca values have similar values as the corals $\Delta^{44/40}$Ca. The similar $\Delta^{44/40}$Ca values in corals and some inorganic aragonite may imply on another parameter rather than temperature that controls fractionation.

Böhm et al., (2006) reported $\Delta^{44/40}$Ca – temperature correlation in corals with a small slope of 0.02‰/°C, which is significant only in temperature variations exceeding 5°C (as the current precision is 0.1‰ (2σ). Even though the *Acropora* sp. experiments have a 9°C temperature differences, and correspond to a significant 0.18‰ $\Delta^{44/40}$Ca differences, the results do not indicate a significant $\Delta^{44/40}$Ca variation (within the 2σ) in the different temperatures.

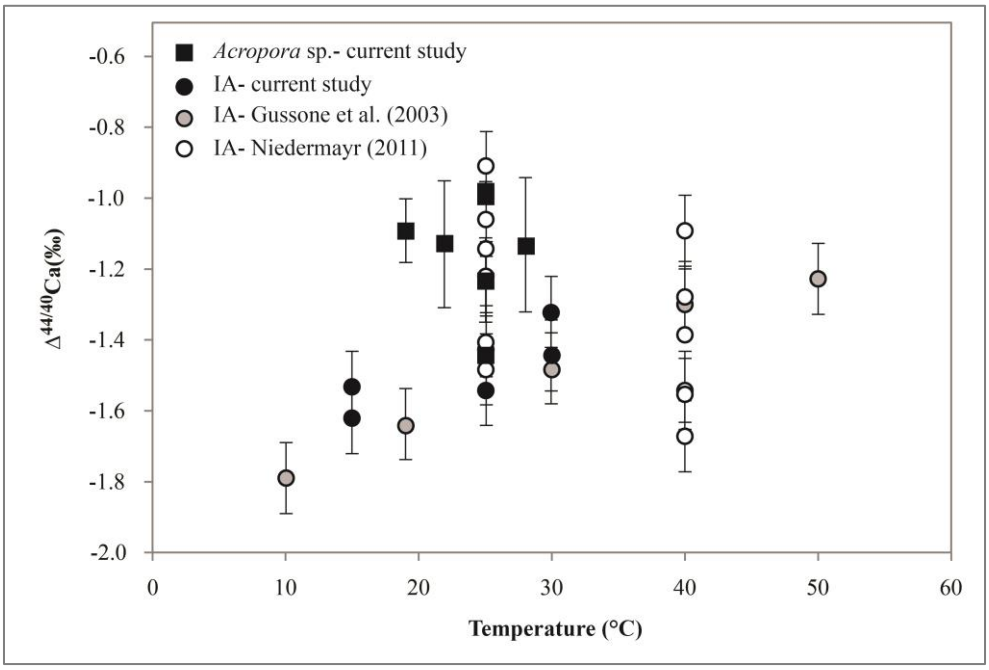

Figure IV.1 Graph of temperature versus $\Delta^{44/40}$Ca in aragonite. The data show positive correlation between temperature and $\Delta^{44/40}$Ca in inorganic aragonite (0.02‰·°C^{-1}). However the correlation is insignificant in the 90% confidence level (R^2=0.1 p=0.11). Corals' aragonite seem to have smaller Ca isotopes fractionation (in ~0.4‰) than inorganic aragonite in the same temperature.

Ionic strength and salinity effect on $\Delta^{44/40}Ca$

The solution used in the inorganic experiments of the current study differ significantly from the solution used in the experiments of Gussone et al. (2003) and Niedermayr et al. (2013) (Table IV.2). The current inorganic aragonite experiments were performed from natural seawater of 40.7g·kg^{-1}. Previous studies of 3g·kg^{-1} solution that are presented in Figures IV.1 and IV.2 (Gussone et al., 2005; Niedermayr, 2011) shows similar results with no detectable $\Delta^{44/40}$Ca differences from the high salinity aragonites.

In our experiments the salinity of the solution is thirteen times higher than in Gussone et al. (2003) and Niedermayr et al. (2013) studies, and the ionic strength of the solution in our study is eight times higher than in Gussone et al. (2003) and Niedermayr et al. (2013) studies.

Table IV.2 Inorganic aragonite experimental conditions

Solution parameter	**(Gussone et al., 2003)**	**(Niedermayr et al., 2013)**	**This Study**
Ionic Strength	0.1	0.1	0.8
salinity	Ca-Mg-Cl solution; 3PSU	Ca-Mg-Cl solution; 3PSU	Red-Sea seawater; 40.7PSU
Ca (mol·kg)	0.01	0.01	0.01
Mg/Ca (mol·mol)	2.0	0.8-5.2	5.4
Temperatures (°C)	10,20,30,40,50	25,40	15,25,30
pH	9.0	8.30±0.03	8.3±0.03
Precipitation rate (μmole·h^{-1}·m^{-2})	60-600	50-20000	40-1260

The influence of salinity and ionic strength on calcium carbonate precipitation was discussed in previous studies for calcite. Zuddas and Mucci (1998) determined that an increase of two-folds in the ionic strength would cause two orders of magnitude increase in the calcite precipitation rate. Tang et al. (2012) demonstrate that calcite precipitation rates dominate variations in $\Delta^{44/40}$Ca, but they showed that when using different ionic strength at similar precipitation rates $\Delta^{44/40}$Ca in calcite remains constant within the measurements uncertainty. Lemarchand et al. (2004) made a calculation model and suggested that the salinity parameter will have a small positive effect of 0.01 on $\delta^{44/40}$Ca in the calcite lattice. The large salinity differences inorganic aragonite (and as a consequence, also large ionic strength difference) between the current study and the study of Gussone et al. (2003) would create, according to the estimation of Lemarchand et al. (2004), a shift in $\Delta^{44/40}$Ca of ~ 0.15‰ in the $\Delta^{44/40}$Ca - temperature trend line. However,

this shift is rather close to the uncertainty of $\Delta^{44/40}$Ca measurement (± 0.1‰), and hence insignificant (Figure IV.1). This may imply that the $\Delta^{44/40}$Ca differences observed between inorganic aragonite and corals' aragonite (Figure IV.1) are not caused due to increasing ionic strength of the solution in the ECF. Thus, we observe a significant difference in $\Delta^{44/40}$Ca between corals' aragonite and inorganic aragonite, which is not caused by ionic strength differences. Besides ionic strength, the different experiments varied in saturation states for aragonite, which may be another factor for the $\Delta^{44/40}$Ca variations between inorganic aragonite and corals' aragonite.

Rate Effect on $\Delta^{44/40}$Ca Incorporation in Inorganic and Coral Aragonite

The inorganic aragonite data showed here varied in precipitation rates that were controlled through diffusion of CO_2 into the bulk solution while keeping a constant pH. Therefore the changes in precipitation rate are related to changes in the carbonate ion concentration and saturation states in the bulk solution. The inorganic aragonite data from the current study supported by data of previous studies (Gussone et al., 2005; Niedermayr et al., 2013) show a positive relationship ($\Delta^{44/40}Ca=\log R\cdot 0.28\pm0.04-2.14\pm0.11$, $R^2=0.7$, $P=3\times10^{-7}$) between the rates of precipitation and their corresponding $\Delta^{44/40}$Ca (Figure IV.2a). This means that as the saturation state increases, and causes higher precipitation rate, the fractionation of Ca isotopes decreases. As already mentioned above, it was pointed out that large $\Delta^{44/40}$Ca variations are observed in inorganic aragonite of the same temperature (Figure IV.1). The precipitation rate in the 25°C experiments, for example, varies from $10^{1.8}$ to $10^{3.7}$ $\mu mol\cdot m^{-2}\cdot h^{-1}$ and $\Delta^{44/40}$Ca varies between -1.54 to 0.91‰, respectively. This can be explained by the effect of aragonite saturation state on Ca incorporation (Figure IV.2a), causing large fractionation during low saturation state and a small fractionation during high saturation state of the bulk solution. Tang et al. (2008) found slope variations in the $\Delta^{44/40}$Ca -precipitation rate relationship in inorganic calcite. They found that as the temperature grows the slope of $\Delta^{44/40}$Ca vs. rate decreases. This observation is supported by the theoretical prediction of the SEMO model (Watson, 2004). However, in inorganic aragonite we did not find a temperature control on the $\Delta^{44/40}$Ca- precipitation rates slope (Figure IV.2b).

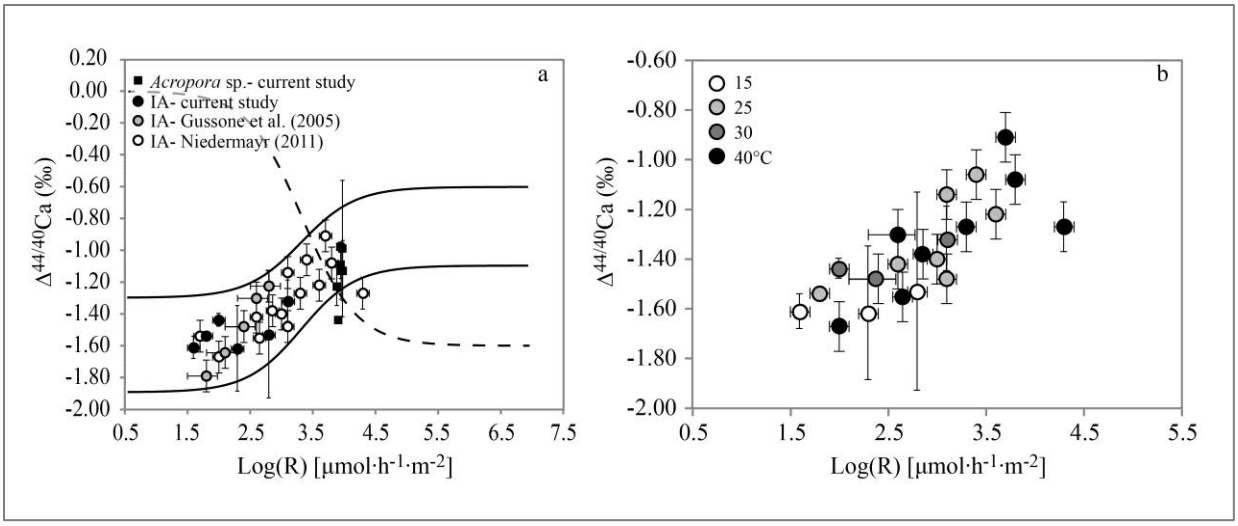

Figure IV.2 Precipitation rate in aragonite is positively correlated to $\Delta^{44/40}$Ca. (a) Inorganic aragonite precipitated in different salinities (40.7 PSU in the current study and 3 PSU in Gossone et al. (2005) and Niedermayr (2011)) do not show any difference in $\Delta^{44/40}$Ca. DePaolo (2011) model for rate dependency on Ca isotope incorporation fits the inorganic aragonite data (solid lines) as the equilibrium fractionation is between -1.8 and -1.3‰, and as the fractionation is the smallest (-0.6 to -1.1‰) at high precipitation rates (above 10^4 μmol·m^{-2}·h^{-1}). Corals fit the high precipitation rate zone, where the fractionation is expected to remain constant. Rate dependency on $\Delta^{44/40}$Ca in inorganic aragonite is opposite to the dependency in inorganic calcite (dashed line from De Paolo (2011)) (b) When plotting $\Delta^{44/40}$Ca in inorganic aragonite versus precipitation rates at different temperatures we do not observe temperature dependent slopes. This is in contrast to the different slopes observed in calcite at different temperatures (Tang et al., 2008).

According to previous studies the precipitation rate of corals is higher than the precipitation rate of inorganic aragonite (Cohen and McConnaughey, 2003). Calcification rates determination in corals has been a subject of several studies, and is subjected to a lot of uncertainty due to the difficulty to estimate the active surface area of the coral (e.g. Hoegh-guldberg, 1988; Laforsch et al., 2008; Veal et al., 2010). The corals calcification rates in this study ($10^{3.9}$-$10^{4.0}$ μmol·m^{-2}·h^{-1}) were estimated using the correlation between saturation state and calcification rate (Leclercq et al., 2000). Whereas other studies reported corals calcification rates in *Porites* sp. of approximately $10^{4.3\pm0.2}$ μmol·m^{-2}·h^{-1} (Lough and Barnes, 1997). While the precipitation rates of the inorganic aragonite experiments show large range of values, the corals estimated calcification rates have very small range of variation (Figure IV.3). Latter observation may indicate the strong control of the corals' physiology onto the calcification process. The corals' calcification rates are very close to the highest precipitation rates obtained by Niedermayr et al. (2013). Respectively, the $\Delta^{44/40}$Ca of these highest precipitation rates is similar to the corals' $\Delta^{44/40}$Ca values. According to the model proposed by DePaolo (2011) for the relationship between $\Delta^{44/40}$Ca and precipitation rate in calcite, Ca isotope fractionation is increasing as the precipitation rate increases. At high precipitation rates, however, Ca isotope fractionation becomes constant, and

remains at its highest value (Figure IV.2a). In the current study this model was applied to aragonite using the inorganic aragonite data. The model follows the data that shows an opposite behavior of aragonite with precipitation rate compared to calcite. Based on the model, at a precipitation rate of ~$10^{4.0}$ $\mu mol \cdot m^{-2} \cdot h^{-1}$ the fractionation of Ca isotopes becomes constant on a minimum fractionation value (Figure IV.2a). The $\Delta^{44/40}Ca$ of Corals is following DePaolo (2011) model, where the fractionation is small and the precipitation rates are high. According to the rates of corals' calcification, the model predicts insignificant $\Delta^{44/40}Ca$ variations in the current corals experiments (Figure IV.3).

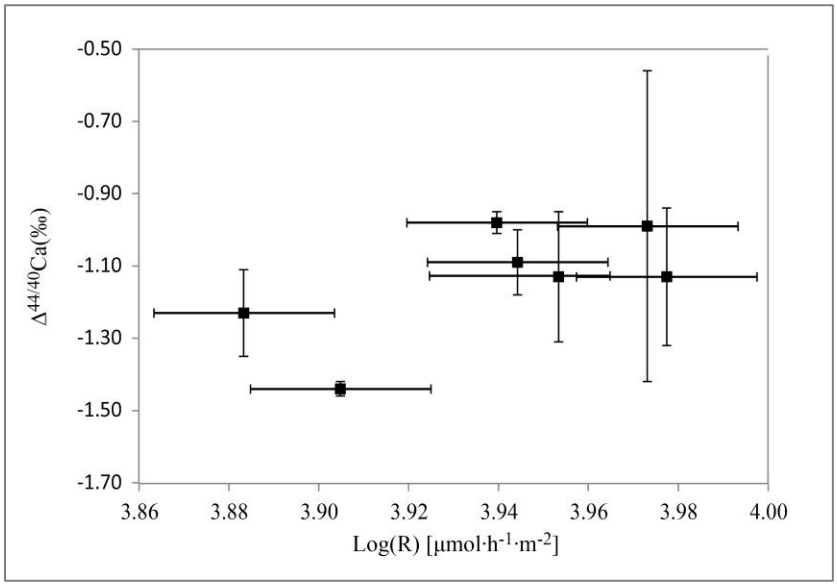

Figure IV.3 $\Delta^{44/40}Ca$ in *Acropora* sp. skeleton is independent of calcification rates. The calcification rates were calculated by the measured saturation state of the solution from Lerlercq et al. (2000). Minimum Ca isotopes fractionation at precipitation rates of 10^4 $\mu mol \cdot m^{-2} \cdot h^{-1}$ and above was determined from to the surface kinetic model for Ca isotopes incorporation (DePaolo, 2011). The high calcification rates of corals are within the expected range of minimum fractionation in aragonite.

The data with high precipitation rates (Niedermayr, 2011) is reported to have Ω>12. This saturation state is more than double the saturation state that we calculated in the bulk solution of the corals experiments (Table IV.1). Al-Horani et al. (2003) already reported that aragonite saturation in corals is elevated in the calcification site compared to the bulk solution. They reported Ω=25 during light calcification, and Ω=3.2 during dark calcification. The mechanism of increasing the saturation state in the calcification site (ECF) was suggested as an active transcellular pathway in which Ca is actively pumped into the ECF and in return protons are transported to the cell. As a result, the pH of the ECF rises and the concentration of both Ca^{2+}

and CO_3^{2-} ions rise. An elevated saturation state in the ECF can explain the high calcification rates in corals. Given that the physiologically raised calcification rate of corals are larger than the usual experimental inorganic precipitation rates, the less fractionated Ca isotope values observed in the corals' skeleton reflect the increased pH, saturation state and precipitation rate.

Conclusions

- Corals and inorganic aragonite show different Ca isotope fractionation. $\Delta^{44/40}$Ca in corals is ~0.4‰ less fractionated than inorganic aragonite that precipitated at same temperature. Low ionic strength that is usually used in inorganic experiments cannot explain the Ca fractionation difference between inorganic aragonite and corals aragonite, since our inorganic aragonite experiments were done from natural seawater that is similar to the corals' experiments solutions.
- Precipitation rates and Ca isotopes fractionation are strongly related. High precipitation rates correspond to a relative small fractionation, and low precipitation rates corresponds to a relative large isotope fractionation value.
- We found that at precipitation rates above ~$10^{4.0}$ $\mu mol \cdot m^{-2} \cdot h^{-1}$ $\Delta^{44/40}$Ca in aragonite is constant at a minimum fractionation value. This finding is in accordance with the $\Delta^{44/40}$Ca of corals in the current study; Corals, which have estimated calcification rates of ~10^4 $\mu mol \cdot m^{-2} \cdot h^{-1}$, show in the current study relatively constant $\Delta^{44/40}$Ca.
- Ca incorporation in corals aragonite is kinetically controlled and reflects a direct control of the corals physiology. Corals enhance the calcification causing higher precipitation rates which corresponds to low Ca isotope fractionation.

Acknowledgments

We wish to thank Ana Kolevica, Regina Surberg, Andrea Wolf and Maria Hierz for supporting the lab work of this study. Funding support was provided through the European Marie Curie Initial Training Network "Calcification by Marine Organisms" (CalMarO) and the European Community's Seventh Framework Programme (FP7/2007-2013).

References

Al-Horani, F.A., Al-Moghrabi, S.M., De Beer, D., 2003. The mechanism of calcification and its relation to photosynthesis and respiration in the scleractinian coral Galaxea fascicularis. Mar. Biol. 142, 419–426.

Böhm, F., Gussone, N., Eisenhauer, A., Dullo, W.C., Reynaud, S., Paytan, A., 2006. Calcium isotope fractionation in modern scleractinian corals. Geochim. Cosmochim. Acta 70, 4452–4462.

Chang, V.T.-C., Williams, R.J.P., Makishima, A., Belshawl, N.S., O'Nions, R.K., 2004. Mg and Ca isotope fractionation during $CaCO_3$ biomineralisation. Biochem. Biophys. Res. Commun. 323, 79–85.

Clode, P.L., Marshall, A.T., 2002. Low temperature X-ray microanalysis of calcium in a scleractinian coral: evidence of active transport mechanisms. J. Exp. Biol. 3552, 3543–3552.

Cohen, A.L., McConnaughey, T.A., 2003. Geochemical perspectives on coral mineralization. Rev. Mineral. Geochemistry 54, 151–187.

DePaolo, D.J., 2011. Surface kinetic model for isotopic and trace element fractionation during precipitation of calcite from aqueous solutions. Geochim. Cosmochim. Acta 75, 1039–1056.

Dietzel, M., Gussone, N., Eisenhauer, A., 2004. Co-precipitation of Sr^{2+} and Ba^{2+} with aragonite by membrane diffusion of CO_2 between 10 and 50°C. Chem. Geol. 203, 139–151.

Dodge, R.E., Wyers, S.C., Frith, H.R., Knap, A.H., Smith, S.R., Cook, C.B., Sleeter, T.D., 1984. Corals calcification rates by the buoyant weight technique: effect of alizarin staining. J. Exp. Mar. Biol. Ecol. 15, 217–232.

Erez, J., Braun, A., 2007. Calcification in hermatypic corals is based on direct seawater supply to the biomineralization site. Geochim. Cosmochim. Acta 71, SA260.

Farkaš, J., Böhm, F., Wallmann, K., Blenkinsop, J., Eisenhauer, A., Geldern, R. Van, Munnecke, A., Voigt, S., Veizer, J., 2007. Calcium isotope record of Phanerozoic oceans: Implications for chemical evolution of seawater and its causative mechanisms. Geochim. Cosmochim. Acta 71, 5117–5134.

Gagnon, A.C., Adkins, J.F., Erez, J., 2012. Seawater transport during coral biomineralization. Earth Planet. Sci. Lett. 329-330, 150–161.

Gussone, N., Böhm, F., Eisenhauer, A., Dietzel, M., Heuser, A., Teichert, B.M.A., Reitner, J., Dullo, W.C., 2005. Calcium isotope fractionation in calcite and aragonite. Geochim. Cosmochim. Acta 69, 4485– 4494.

Gussone, N., Eisenhauer, A., Heuser, A., Dietzel, M., Bock, B., Böhm, F., Spero, H.J., Lea, D.W., Bijma, J., Nägler, T.F., 2003. Model for kineticeffects on calciumisotopefractionation ($\delta^{44}Ca$) in inorganic aragonite and cultured planktonic foraminifera. Geochim. Cosmochim. Acta 67, 1375–1382.

Halicz, L., Galy, A., Belshaw, N.S., O'Nions, R.K., 1999. High-precision measurement of calcium isotopes in carbonates and related materials by multiple collector inductively coupled plasma mass spectrometry (MC-ICP-MS. J. Anal. At. Spectrom. 14, 1835–1838.

Heuser, A., Eisenhauer, A., Gussone, N., Bock, B., Hansen, B.T., Nägler, T.F., 2002. Measurement of calcium isotopes ($\delta^{44}Ca$) using a multicollector TIMS technique. Int. J. Mass Spectrom. 220, 385–397.

Hoegh-guldberg, O., 1988. A method for determining the surface area of corals. Coral Reefs 113–116.

Kısakürek, B., Eisenhauer, A., Böhm, F., Hathorne, E.C., Erez, J., 2011. Controls on calcium isotope fractionation in cultured planktic foraminifera, Globigerinoides ruber and Globigerinella siphonifera. Geochim. Cosmochim. Acta 75, 427–443.

Krishnaveni, P., Chou, L., Ip, Y.K., 1989. Deposition of calcium ($^{45}Ca^{2+}$) in the coral, Galaxea fascicularis. Comp. Biochem. Physiol. Part A Physiol. 94, 509–513.

Laforsch, C., Christoph, E., Glaser, C., Naumann, M., Wild, C., Niggl, W., 2008. A precise and non-destructive method to calculate the surface area in living scleractinian corals using X-ray computed tomography and 3D modeling. Coral Reefs 27, 811–820.

Leclercq, N., Gattuso, J.-P., Jaubert, J., 2000. CO_2 partial pressure controls the calcification rate of a coral community. Glob. Chang. Biol. 6, 329–334.

Lemarchand, D., Wasserburg, G.J., Papanastassiou, D.A., 2004. Rate-controlled calcium isotope fractionation in synthetic calcite. Geochim. Cosmochim. Acta 68, 4665–4678.

Lewis, E., Wallace, D.W.R., 1998. Program Developed for CO2 System Calculations.

Lough, J.M., Barnes, D.J., 1997. Several centuries of variation in skeletal extension , density and calcification in massive Porites colonies from the Great Barrier Reef : A proxy for seawater temperature and a background of variability against which to identify unnatural change. J. Exp. Mar. Bio. Ecol. 211, 29–67.

Niedermayr, A., 2011. Effects of magnesium , polyaspartic acid , carbonate accumulation rate and temperature on the crystallization , morphology , elemental incorporation and isotopic fractionation of calcium carbonate phases.

Niedermayr, A., Köhler, S.J., Dietzel, M., 2013. Impacts of aqueous carbonate accumulation rate, magnesium and polyaspartic acid on calcium carbonate formation (6–40°C). Chem. Geol. 340, 105–120.

Pretet, C., Samankassou, E., Felis, T., Reynaud, S., Böhm, F., Eisenhauer, A., Ferrier-Pagès, C., Gattuso, J.-P., Camoin, G., 2013. Constraining calcium isotope fractionation ($\delta^{44/40}Ca$) in modern and fossil scleractinian coral skeleton. Chem. Geol. 340, 49–58.

Tambutté, É., Allemand, D., Müller, E., Juabert, J., 1996. A compartmental approach to the mechanism of calcification in hermatypic corals. J. Exp. Biol. 1041, 1029–1041.

Tambutté, É., Tambutté, S., Segonds, N., Zoccola, D., Venn, A., Erez, J., Allemand, D., 2012. Calcein labelling and electrophysiology: insights on coral tissue permeability and calcification. Proc. R. Soc. B Biol. Sci. 279, 19–27.

Tang, J., Dietzel, M., Böhm, F., Köhler, S.J., Eisenhauer, A., 2008. Sr^{2+}/Ca^{2+} and $^{44}Ca/^{40}Ca$ fractionation during inorganic calcite formation: II. Ca isotopes. Geochim. Cosmochim. Acta 72, 3733–3745.

Tang, J., Niedermayr, A., Köhler, S.J., Böhm, F., Kısakürek, B., Eisenhauer, A., Dietzel, M., 2012. Sr^{2+}/Ca^{2+} and $^{44}Ca/^{40}Ca$ fractionation during inorganic calcite formation : III . Impact of salinity/ionic strength. Geochim. Cosmochim. Acta 77, 432–443.

Veal, C.J., Carmi, M., Fine, M., Hoegh-guldberg, O., 2010. Increasing the accuracy of surface area estimation using single wax dipping of coral fragments. Coral Reefs 29, 893–897.

Watson, E.B., 2004. A conceptual model for near-surface kinetic controls on the trace-element and stable isotope composition of abiogenic calcite crystals1. Geochim. Cosmochim. Acta 68, 1473–1488.

Zeebe, R.E., Wolf-Gladrow, D.A., 2001. CO_2 in seawater: equilibrium, kinetics, isotopes. Elsevier Oceanography Series, Elsevier.

Zuddas, P., Mucci, A., 1998. Kinetics of calcite precipitation from seawater : II . The influence of the ionic strength. Geochim. Cosmochim. Acta 62, 757–766.

SUMMARY

This study focused on the incorporation of Sr/Ca and their isotopes in corals' skeletons. Both $^{88}Sr/^{86}Sr$ and $^{44}Ca/^{40}Ca$ in aragonite have significant large fractionation from the bulk solution. However, while similar $\Delta^{88/86}Sr$ values are observed in all samples, corals and inorganic aragonite, $\Delta^{44/40}Ca$ values display significant variations between inorganic and corals aragonite. A kinetic model that was suggested to explain Ca incorporation in inorganic calcite (DePaolo, 2011) can explain also the behavior of Ca isotopes fractionation in inorganic aragonite. According to the aragonite model, as the rate of precipitation increases Ca isotopes are less fractionated. Ca isotope data of corals from the current study corresponds to the inorganic aragonite model curve. At the high calcification rate of corals (~$10^{3.9}$ $\mu mol \cdot m^{-2} \cdot h^{-1}$ in this work) the 'S curve' shaped model (*sigmoid curve*) is at the minimum fractionation value. Provided that this model predicts the behavior of Ca in corals as well as inorganic aragonite, no change in $\Delta^{44/40}Ca$ in corals at different calcification rates of ~10^{4} $\mu mol \cdot m^{-2} \cdot h^{-1}$ and above is expected.

As opposed to Ca, Sr does not show any significant variation in aragonite. Inorganic aragonite and corals aragonite are 0.2‰ more depleted in the light ^{86}Sr isotope than their bulk solution. The observed variations in $\Delta^{88/86}Sr$ between different samples are not controlled by saturation state or by temperature. The similarity in $^{88}Sr/^{86}Sr$ fractionation between inorganic and corals' aragonite challenges the Rayleigh Based Multi Element model (Gaetani and Cohen, 2006; Gaetani et al., 2011) that predicts significant differences between inorganic and corals' aragonite. The Rayleigh based model that was previously suggested to explain the trace elements incorporation in corals cannot explain the $^{88}Sr/^{86}Sr$ isotope incorporation in terms of Rayleigh distillation effect.

The experiments that were conducted on *Acropora* sp. corals revealed an irregular pattern of calcification. Since the Sr concentration in the pre-experimental solution differed significantly from the concentration in experimental solutions, mixing between pre-experimental and experimental skeleton were detectable through Sr concentration measurements. Using these two different Sr concentrations, it was possible to sample experimental skeleton for isotopes geochemical analyses and correct for possible mixing with pre-experimental skeleton. In addition, it was possible to use the skeleton for Sr element mapping and distinguish between pre-experimental and experimental skeleton regions. The mapping results showed a patchy pattern of

calcification, where the experimental skeleton appeared not only as axial and radial growth but also in patches within the pre-experimental skeleton. This observation confirms a previous assumption of secondary infilling in *Acropora* sp. skeleton that was based on the increasing density of the skeleton with the increasing distance from the skeleton tip (Gladfelter, 1982; Roche et al., 2011). Due to the irregular calcification pattern shown in this study, *Acropora* sp. skeleton may not be a suitable coral for paleo-proxy reconstruction. Nevertheless, this calcification pattern is an important observation for the study of calcification mechanisms.

References

DePaolo D. J. (2011) Surface kinetic model for isotopic and trace element fractionation during precipitation of calcite from aqueous solutions. *Geochim. Cosmochim. Acta* **75**, 1039–1056.

Gaetani G. A. and Cohen A. L. (2006) Element partitioning during precipitation of aragonite from seawater: A framework for understanding paleoproxies. *Geochim. Cosmochim. Acta* **70**, 4617–4634.

Gaetani G. A., Cohen A. L., Wang Z. and Crusius J. (2011) Rayleigh-based, multi-element coral thermometry: A biomineralization approach to developing climate proxies. *Geochim. Cosmochim. Acta* **75**, 1920–1932.

Gladfelter E. H. (1982) Skeletal development in Acropora cervicornis: I. Patterns of calcium carbonate accretion in the axial corallite. *Coral Reefs* **1**, 45–51.

Roche R. C., Abel R. L., Johnson K. G. and Perry C. T. (2011) Spatial variation in porosity and skeletal element characteristics in apical tips of the branching coral Acropora pulchra (Brook 1891). *Coral Reefs* **30**, 195–201.

ACKNOWLEDGMENTS

This thesis is the result of few years of research and hard work that could not have been accomplished without the help of many people.

I would like to express my special appreciation and thanks to my advisor, Prof. Dr. Anton Eisenhauer, for his guidance, support, trust and for the fruitful discussions we had. I would also like to thank Dr. Florian Böhm and Dr. Jan Fietzke for mentoring me and helping me whenever I needed and for the good discussions and ideas that came up during our many conversations. I owe a special thanks to Prof. Dr. Jonathan Erez who taught me with enthusiasm the fascinating nature of corals and for helping me with my corals experiments in his laboratory. My sincere thanks also go to Prof. Dr. Martin Diezel who guided me and hosted me in his laboratory during the inorganic experiments and to Dr. Andrea Niedermayr for her helpful suggestions and assistance. Sincere thanks to Prof. Dr. Thor Hansteen who had always an open door for me, and helped me with the SynXRF analyses and data processing, I thank also Dr. Karen Appel from the Deutsches Electronen Synchrotron for allowing me to work and operate DORIS. I am grateful to Prof. Dr. Boaz Lazar, Prof. Dr. Moti Stein and Dr. Paolo Montagna for their support and advices.

I would also like to thank the people who helped me with the laboratory work: Ana Kolovica, Andrea Wolf, Dr. Folkmar Hauf, Franziska Wilsky, Maria Hierz, Mario Thöner and Regina Surberg.

I am obliged to my colleagues and friends in GEOMAR and HUJI: Dr. Andre Krabbenhöft, Dr. Basak Kisakurek, Dr. Christian Hörn, Dr. Ed Hathhorn, Eyal Wurgaft, Dr. Federica Ragazzola, Dr. Hauke Vollstaedt, Dr. Isabelle Taubner, Dr. Jacek Raddaz, Dr. Marlene Wall, Dr. Nicolaas Glock, Stephanie Schurigt, Rashid Rashid, Dr. Volker Liebetrau, Yael Levinson and Yona Geller. I also greatly appreciate the help of the secretaries in GEOMAR and in HUJI: Anne Völsch, Batya Moshe, Christine Utecht, Isabel Patzwald and Magi Perkin.

Lastly I want to thank to my family and especially to Adi for his endless love and patience.

This work was funded through the European Marie Curie ITN386 "Calcification by Marine Organisms" project (CalMarO SP7/2008-2012) and through Sonderforschungsbereich 754 (SFB754/ B7).

APPENDIX 1

The following algorithm was used to correct the attenuation of the Sr signal obtained by the micro-SXRF. The correction was done using 'Matlab'.

```
clear
% Load and arrange the data
cd('D:\Documents\PhD\Acropora\Desy Calculations\DeSY');
importdata('N04_14Lay.txt');
Xpixels=109;
Ypixels=109;
Surf=Xpixels*Ypixels;
PixelSize=[25 25 25];
angleDepth=sqrt(PixelSize(2)^2+PixelSize(3)^2);
n04=ans.textdata(98:2:end, : );
n04( :, 9:16)=ans.textdata(99:2:end, : );
SrData=str2double(n04(:,10));
CaData=str2double(n04(:,14));
Layers=floor(length(SrData)/Surf); % get complete layers
for i=1:Layers;
    tempSr{i}=reshape(SrData(1+(Surf*(i-1)):i*Surf),Xpixels,Ypixels);
    tempCa{i}=reshape(CaData(1+(Surf*(i-1)):i*Surf),Xpixels,Ypixels);
    D(:,:,i)=cat(3,tempSr{i}); % '3' for 3D array- all layers Sr
    DC(:,:,i)=cat(3,tempCa{i}); % '3' for 3D array- all layers Ca
    MaxCa(1,i)=max(max(DC(:,:,i)));
end

%%
% create a matrix ('UpCover') that includes the amount of CaCO3 covering
% each Pixel.
UpCover(Xpixels,Ypixels,Layers)=cat(3, zeros); % 3D array
int=5;
LM(:,1)=0:int:350; % Create a local max for pixels with different covering
depth.
LM(:,2)=48315*exp(-0.016*LM(:,1)); % The expected transmission from each
depth. Parameters fit to Ca (3692eV) in aragonite with bulk density of 2.95
g*cm-3. -just for a start
```

```
% Now we check how much layer 1 covers each pixel in layer 2
for y=2:(Xpixels)
     UpCover(y,:,2)=DC(y-1,:,1)./LM(1,2)*angleDepth; % Layer 1 is not
covered. Layer 2 is simply covered by layer 1.
 end

% Coverage of the overtopping layers for each layer.
 for L=2:(Layers-1)
 for s=1:length(LM)
 for y=1:(Xpixels-1) % 1 pixel backward due to the 45° beam angle
     for x=1:Ypixels
         if
(UpCover(y,x,L)<LM(s,1)||UpCover(y,x,L)==LM(s,1))&&UpCover(y,x,L)>(LM(s,1)-
int)&&LM(s,2)>0&&L<14
             Caf(y+1,x,L+1)=DC(y+1,x,L+1)/LM(s,2)*angleDepth;
         end
     end
 end
 end
     for y=2:Xpixels
         if L<14
             UpCover(y,:,L+1)=UpCover(y-1,:,L)+Caf(y,:,L+1);
         end
     end
 end

  for l=(1:Layers)
     RelCa(:,:,l)=reshape(CaData(1+(Surf*(l-
1)):l*Surf),Xpixels,Ypixels)./LM(1,2);
 end


% The real transmission based on the real density (from max Ca at each depth)
Transmition=1.000*exp(-0.015.*UpCover); % 3.692 KeV
TransmitionSr=1.0002*exp(-0.002.*UpCover); %14.165 KeV
```

```
Residuals=Transmition-RelCa; % Residuals are partial pixels parameter (how
much CaCO3 is missing in each pixel)
Residuals=round(Residuals.*1000)/1000;

%%
Sr(Ypixels,Xpixels,Layers)=cat(3,zeros);
Sr=D./(1-Residuals);
T=Residuals>0.85;  % binaric matrix for high and low Residuals
Sr(T)=0;  % High Residuals are becoming zero to avoid inf Sr values
Sr=Sr./TransmitionSr;

Hist(:,1)=0:50:5000;
for L=1:Layers
    Hist(:,L+1)=0;
for i=1:(length(Hist)-1)
[a b]=find((Sr(:,:,L)>Hist(i,1)|Sr(:,:,L)==Hist(i,1))&Sr(:,:,L)<Hist(i+1,1));
Hist(i,L+1)=Hist(i,L+1)+length(a);
end
end

% Values above 1900 counts are outliers, artifacts. Sr is the corrected Sr
counts (i.e. the result)

Sr(Sr>1900)=1900;
```

APPENDIX 2

True isotope fractionation in a Rayleigh distillation process

This appendix explains the Δ correction equation development in a Rayleigh distillation effect:

1. When a process undergoes a Rayleigh distillation process, the change in the solution composition is described as the remaining fraction in the solution (*f*) at a certain point of the process $[Ca]_{fs}$ compared to its initial composition $[Ca]_{is}$

$$f = \left(\frac{[Ca]_{fs}}{[Ca]_{is}}\right)$$

2. The basic Rayleigh equation describes the isotopic ratio between the final solid (R_{sam}) and the initial solution (R_{sol}^{0}). This equation equals the apparent fractionation (α'), as obtained from the ratios between the isotopic ratios.

$$\alpha' = \frac{R_{sam}}{R_{sol^0}} = \frac{f^{\alpha} - 1}{f - 1}$$

3. By definition ε is described as the 'enrichment factor' and can be used as an approximation for Δ

$$\Delta{\sim}\varepsilon = (\alpha - 1) \cdot 1000$$

4. Then, using equation 2 the approximation of equation 3 we can combine Δ in the Rayleigh distillation equation. Where α of equation 3 is replacing the apparent α (α') of equation 2.

$$\frac{\Delta}{1000} + 1 = \frac{f^{\alpha} - 1}{f - 1}$$

5. In order to extract the true α from the previous equation we apply 'ln' on it.

$$\alpha = \frac{ln(f \cdot \Delta/1000 - \Delta/1000 + f)}{ln(f)}$$

6. Using equation 3 again, this time with α as the true α, will extract the true isotopic fractionation (Δ) of the process.

$$\Delta{=}\ (\alpha - 1) \cdot 1000$$